Escola de Camins
Escola Tècnica Superior d'Enginyeria de Camins, Canals i Ports
UPC BARCELONATECH

FINAL MASTER THESIS

Protecting sensitive constructions from tunnelling by means of lateral walls.

Thesis written by:
Joan Fraile Diana

Directed by:
Alberto Ledesma Villalba

Master in Science in:
MSc in Civil Engineering
Specialized in Geotechnical Engineering

Barcelona, September 30th 2019

Department of Civil and Environmental Engineering

ETSECCPB

Barcelona School of Civil Engineering

Department of Civil and Environmental Engineering

Protecting sensitive constructions from tunnelling by means of lateral walls

Joan Fraile Diana

Barcelona, September 30th 2019

"On account of the fact that there is no glory attached to the foundations and that the sources of success or failure are hidden deep in the ground, building foundations have always been treated as stepchildren and their acts of revenge for lack of attention can be very embarrassing."

Terzaghi, 1951



Bertha Tunnelling Boring Machine, 17.5-meter diameter
Alaskan Way viaduct replacement Tunnel

0.1. Acknowledgements

It is not easy to thank all the people involved in this Thesis because my feeling of gratitude goes far beyond the effort put in this document.

First of all, I would like to express my gratitude to the Director and Coordinator of this Thesis. Thanks Professor Alberto Ledesma Villalba for turning the difficult into easy, for meeting me almost each Thursday afternoon and for providing me the knowledge to understand and apply in the correct manner the basic theory involved throughout this Final Master Thesis.

Secondly I would like to thank the opportunity that Ángel Garcia-Fontanet Molina and all PRO-Geo crew has given to me. My passion for Geotechnical Engineering has come true by becoming a member of their team. Thanks to that opportunity I am in a constant learning process that is helping me not only for writing this Thesis but also for my future as a professional Engineer.

Obviously I cannot end this section without expressing my infinite gratitude to the main pillars that have sustained me not only in this last chapter of my university stage but also throughout my life. Thanks Dolors, Joan, Victor and all my family for being beside me in my ups and downs, you mean a lot to me.

One last time I want to express my endless gratitude to those who shared with me the last seven years of my university stage. Seven years plenty of emotions, uncertainty, progress, more than a hundred exams, family feeling, respect, non-rivalry, cries and laughter but above all, friendship. Each one of you knows the meaning you have in my life and I will just say thanks for being there in the right moment, in the right place.

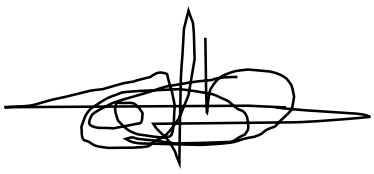

Joan Fraile Diana

September 30th 2019

0.2. Abstract

Title: Protecting sensitive constructions from tunnelling by means of lateral walls

Author: Joan Fraile Diana

Director: Alberto Ledesma Villalba

During the past decades, due to city expansion and the fact that some of the current transportation system has become obsolete and demands of improvements, the increase of underground transportation has become an evidence leading to more tunnelling works in urban areas. Tunnel designing works goes far beyond the tunnel itself. It is important to carry out a deep study about the current structural situation of the surrounding buildings in order to assess and quantify the potential damage that buildings can suffer due to the induced settlements.

In some cases, due to location facts, ground conditions, presence of utilities and other underground facilities, the tunnel alignment cannot be deflected and the final layout may pass near old or historical buildings which do not have resistant foundations. Usually these type of buildings are supported on shallow foundations or rafts leading to be more prone to suffer from ground displacements.

During the past years several structural approaches such as lateral walls, located between the tunnel axis and the building, have been studied by means of both empirical methods and finite-element simulations in order to analyse its efficiency in terms of reducing the ground displacements far beyond the wall with the aim of protecting the building. The technical approach to solve this kind of geotechnical problems in general is by means of empirical methods due to the lack of field data and observations that can lead the creation and calibration of different models.

This document analyses and quantifies the efficiency of lateral walls as a measure of protecting sensitive constructions from tunnelling. This structural solution is deeply studied in this document by means of analysing the main parameters governing both the ground displacements and the tunnel-wall interaction problem. The analysis is carried out by means of applying both empirical methods and finite-element simulations.

Keywords

Tunnelling, displacements trough, lateral wall, wall stiffness, ground surface settlement, vertical settlements, horizontal displacements, structural damage

0.3. Resum

Títol: Murs laterals com estructures de protecció en edificacions sensibles a l'excavació de túnels

Autor: Joan Fraile Diana

Director: Alberto Ledesma Villalba

En les darreres dècades, degut a la constant expansió de les ciutats i que alguns dels sistemes de transport del moment es trobàvem obsolets i requerien d'actuacions de millora, l'augment de l'ús de les infraestructures subterrànies es fa evident i com a conseqüència, l'increment en la construcció de túnels. El disseny d'un túnel va molt més enllà del túnel en si mateix. És necessari dur a terme un estudi d'anàlisi de la situació estructural actual dels edificis que envolten l'àrea d'influència del túnel per tal de poder quantificar els danys que aquests puguin arribar a patir degut a les obres d'excavació del túnel.

En determinats casos, degut a factors de localització, característiques del terreny, presència de serveis i d'altres infraestructures de transport, l'alineació del túnel no pot ser modificada en el disseny final pot passar molt proper d'edificacions antigues o històriques. Aquest tipus d'edificació no es caracteritzen per estar suportades en cimentacions profundes i normalment són poc resistents.

Amb el pas dels anys, diferents solucions estructurals com per exemple murs pantalla laterals, situats entre l'eix del túnel i l'edifici, s'han estudiat tant a partir de metodologies empíriques com utilitzant elements finits per tal d'analitzar i determinar l'eficiència d'aquest tipus de murs com a solució per reduir i mitigar els assentaments en superfície més enllà del mur amb l'objectiu final de protegir l'edifici. Normalment aquests problemes geotècnics es solucionen mitjanant mètodes empírics degut a les poques dades de camp i a la falta de casos reals d'estudi que puguin conduir a la realització de models concrets i al seu calibratge.

Aquest document analitza i quantifica l'eficiència de murs laterals com a mesura de protecció d'edificacions sensibles a l'excavació de túnels. Aquesta solució estructural s'analitza en profunditat mitjançant tot el desenvolupament analític pertinent i determinant els paràmetres que governen els assentaments del terreny així com els de la interacció túnel-mur. L'anàlisi es desenvolupa tant mitjançant tècniques analítiques com simulacions numèriques.

Paraules clau

Excavació de túnels, camps de desplaçament, pantalles laterals, rigidesa del mur, assentaments en superfície, moviments verticals, moviments horitzontals, dany estructural

0.4. Resumen

Título: Muros laterales como estructuras de protección en edificaciones sensibles a la excavación de túneles

Autor: Joan Fraile Diana

Director: Alberto Ledesma Villalba

En las últimas décadas, debido a la constante expansión de las ciudades y que algunos de los sistemas de transporte actuales se encontraban obsoletos y requerían de actuaciones de mejora, el aumento del uso de las infraestructuras subterráneas ha sido evidente y como consecuencia, el auge de la construcción de túneles. El diseño de un túnel va mucho más allá del túnel en si mismo. Es necesario llevar a cabo un análisis de la situación estructural actual de los edificios que rodean el área de influencia del túnel para poder cuantificar los daños que estos puedan llegar a sufrir debidos a la excavación del túnel.

En determinados casos, debido a factores de localización, características del terreno, presencia de servidumbres y demás infraestructuras subterráneas, hacen que la alineación final del túnel no se pueda ver alterada y pase cerca de las cimentaciones de edificios antiguos. Estos edificios no se caracterizan precisamente por estar apoyadas en cimentaciones profundas y normalmente son poco resistentes.

Con el paso del tiempo, diferentes soluciones estructurales como por ejemplo muros pantalla laterales, ubicados entre el eje del túnel y el edificio, se han estudiado a partir de metodologías empíricas y elementos finitos con el fin de analizar la eficiencia de los mismos como solución para reducir o mitigar los asientos en superficie más allá del muro con el objetivo final de proteger el edificio. Normalmente este tipo de problemas se soluciona mediante métodos empíricos debido a la falta de datos de campo y de la experiencia que permitan llevar a cabo el desarrollo de modelos concretos y su calibración.

Este documento analiza y cuantifica la eficiencia de muros laterales como medida de protección de edificios sensibles a la excavación de túneles. Esta solución estructural se analiza en profundidad mediante todo el desarrollo analítico pertinente determinando los parámetros que gobiernan los movimientos del terreno, así como los de la interacción túnel-muro. El análisis se desarrolla mediante técnicas analíticas, así como mediante simulaciones numéricas.

Palabras clave

Excavación de túneles, campos de desplazamiento, pantallas laterales, rigidez del muro, asientos en superficie, movimientos verticales, movimientos horizontales, daño estructural

TABLE OF CONTENTS

CHAPTER 1 – Introduction

CHAPTER 2 – State of the Art

CHAPTER 4 – Analysis of horizontal displacements

CHAPTER 5 – Finite Element Analysis

CHAPTER 6 – Sensitivity analysis of the results

LIST OF FIGURES

LIST OF TABLES

CHAPTER 1

Introduction

FINAL MASTER THESIS

1.1. Introduction

During the last decades, the necessity of building tunnels beneath urban areas has increased due to city expansions and new infrastructure projects. Hence, the necessity of controlling the induced damage to neighbouring buildings due to tunnelling works has become a matter of special interest. With that aim, tunnelling design needs of an accurate analysis of the ground displacements induced by the excavation works in order to assess and quantify the possible effects to other buildings.

Damage mitigation due to ground displacements is one of the key parameters when designing underground works. With the goal of reducing the impact of tunnelling works to neighbour buildings several measures have been implemented in the past years in order to reduce, in one hand, the threat that ground movements may suppose and in the other hand, the building vulnerability associated to its construction type and elements. It is important to analyse the quality of the foundations in case of existing and the overall structural system of the building.

One of the most used measure is the implementation of a diaphragm wall or lateral wall parallel to the tunnel axis with the aim of achieving a double goal; in one hand, the reduction of soil displacements at ground surface and in the other hand, avoiding any structural damage to the building. As it will be developed throughout the thesis, the general approach of this type of geotechnical problems is carried out by means of empirical methods. This is basically due to the lack of data gathered from experience and case studies that allow the validation or calibration of the models used in order to analyse the problem.

As it will be presented in the State of the Art, there are few cases in which the efficiency of lateral walls as a measure of soil displacements at ground surface mitigation is analysed. However, many geotechnical authors have put in a great effort to develop physical models, such as the centrifuge model, combined with finite-element analysis for the evaluation of tunnel excavation for both sands and clays.

Bilotta (2004, 2008), studied with both physical and numerical analysis, the efficiency of diaphragm walls used to mitigate displacements due to tunnel excavation in clays. As will be provided in the State of the Art, his conclusions reported that for specific cases, as opposite as can be thought, the implementation of a lateral wall to reduce ground displacements due to tunnel excavation may end up harmful for the settlement control at ground surface. These conclusions are contrary to some real cases which performed well. (Gens, Di Mariano, & Gesto et al., 2006)

1.2. Scope of the works

As stated before, tunnelling in urban areas constitutes a challenge due to the impact of ground settlements on existing sensitive buildings. A procedure to mitigate that impact consists of constructing a diaphragm wall or a

row of piles, separating the sensitive building from the tunnel, prior to the excavation of the tunnel itself. This document considers this geometry and analyses the mechanical problem, first by means of classical elastic solutions and after that, by means of a Finite Element Code, as Plaxis 2D.

The motivation of this thesis is based in evaluate and quantify the efficiency of lateral walls as measures to protect sensitive constructions from tunnelling. These measure is deeply studied throughout the chapters of this thesis with both empirical and numerical methods.

The main tasks that are going to be considered in this thesis are the ones presented as follows:

- Analysis of previous works and case histories. In particular, the experience from the AVE tunnel in Barcelona and its impact on the Sagrada Familia Temple.
- Analysis of the pattern of vertical displacements using elastic solutions.
- Extending the formulation to take into account the horizontal displacement field.
- Use of PLAXIS for checking purposes.
- Sensitivity analysis in order to reveal the main parameters that govern the settlement troughs.
- Conclusions. Relative importance of vertical and horizontal displacements.

In order to achieve the goals presented above, this Final Master Thesis is structured in seven chapter which the main topics threated at each one are presented as follow.

In the State of the Art the main information presented by Geotechnical authors is analysed as well as the conclusions of the most important documents. In the third and fourth chapter, both the vertical and horizontal displacement troughs are analysed by means of analytical solutions using the superposition principle of displacements. Firstly, it is obtained the displacements trough suffered by the ground due to the tunnelling works by means of classic solutions from Loganathan & Poulos (1998). Secondly, it is solved the problem of a load applied to an inner point in the 2D elastic half-space also known as Melan 2D problem. These loads will be the interaction forces between soil and wall. Finally, adding the effects of greenfield conditions, the final soil displacements are obtained.

In order to validate the analytical results, in the fifth chapter of the Thesis a finite-element code is used in which the geometry used in the previous calculations is implemented and the results obtained by the simulations are compared with those obtained from the calculations. The software used is Plaxis 2D, a widely used program in terms of underground design works with high levels of accuracy in the results.

In the sixth chapter of the Thesis a sensitivity analysis of the results will be developed. As the goal of this document is to analyse the effect in ground displacements when a structural wall is constructed between the tunnel axis and a building, it is important to quantify the efficiency of this wall as well as to analyse different parameters governing this displacements, such as the stiffness of it and the distance between the tunnel axis and the lateral wall.

Finally, in the seventh chapter, the overall conclusions are presented and discussed.

CHAPTER 2

State of the Art

FINAL MASTER THESIS

2.1. Introduction

Ground deformations generated during tunnelling works, may induce in general, surface settlements. For the past years, The International Tunnelling Association Working Group has analysed and assessed the impact of tunnelling works beneath urban areas. A wide range of conclusions have been reported during different meetings which are going to be exposed in the following points and chapters of this Final Master Thesis. (Leca & New, 2007)

It is obvious that nowadays Tunnelling Boring Machines are provided with the newest technological advances which help them to cope with different ground conditions hence, reducing ground deformations and surface settlements. Despite that, empirical methods discovered by the main important geotechnical authors remain much the same although they are in a constant evolution as more experience of case studies are developed and built providing valuable data.

It is not easy to understand the evolution of the mobility in some of the main important cities of the world. Nowadays one is in search of areas free of traffic and pollution leading to an increase of underground traffic. However, it is important to pay attention to the existing underground facilities and utilities which can generate problems and interferences to new projects. Also, another factor to take into account is the population growth of the cities and also its consequent transport expansion leading to more underground projects.

One main factor to be highlighted is that an underground infrastructure must be constructed within the soil, hence uncertainties such as, presence of different or difficult ground conditions, appearance of water table and old utilities…, are difficult to predict in design stage and will eventually be found during construction stage. If the project is developed in urban areas residents and business located in the influence area of the building activities may be affected by such works.

In this thesis, the main focus is the analysis of a procedure to protect existing buildings from ground displacements due to tunnelling. There are different factors governing this response such as geometry of the tunnel, building's foundations, tunnelling construction process and ground conditions which are going to be analysed and developed throughout this chapter and thesis.

This section will be finished highlighting one major unknown when assessing the current impact of underground works beneath or close to existing buildings. This happens because there is a lack of knowledge of the history of deformations suffered by existing buildings previously from ground displacements, and even less when considering building foundations.

In the following sections of this document the State of the Art of tunnelling induced ground movements is presented and developed highlighting the main points and factors to be considered.

2.2. Tunnelling-induced ground movements

As stated before, there are quite a lot factors governing ground displacements in the context of tunnelling. In general, these factors can be grouped in four groups namely geological factors, hydro-geological and geotechnical factors, tunnel geometry and depth, excavation and construction process and finally quality of the workmanship and management. (Leca & New, 2007)

Based on experience and field measurements, it has been noticed that the geometry of the displacements troughs, as will be explained later, can be directly represented by the Gaussian curve. In Figure 2.1, both the longitudinal settlement profile and the transverse settlement profile are presented.

Figure 2. 1.- Typical cross-sections of the displacements troughs *(Leca & New, 2007)*

As will be explained in following sections of this thesis it is important to differ when granular or cohesive soil is encountered during ground investigations or design stages. That is important because, due to the pore pressure changes during tunnelling works, for cohesive soils longer term deformations are expected than in granular soils.

As stated before, there are different factors governing the appearance of ground movements such as: geotechnical conditions encountered on site, surface loads, hydro-geological conditions on site and both methods of tunnel excavation and ground support. It is trivial to understand that when the soil resistance is exceeded, ground displacements are generated. (Leca & New, 2007)

In the following points of this section, different factors contributing to ground movements due to tunnel excavation are presented developing the main ideas of the failure mechanism generated as well as possible consequences of the failure.

2.2.1. Tunnel face stability

It is important to analyse the tunnel face stability in order to proceed with an optimal characterization of the geotechnical parameters involved. That characterization is of vital importance in order to identify the main failure mechanisms that can occur in the tunnel face. In Figure 2.2 the main mechanisms are presented and identified.

As stated in the previous paragraph, in Figure 2.2 the typical failure mechanisms for both cohesive (left) and granular (right) soils are presented. As can be seen having a deeper look to the figure, failure in cohesive soils involve a greater volume of ground when failure generating a sinkhole at ground surface which its width can be larger than one tunnel diameter in some cases.

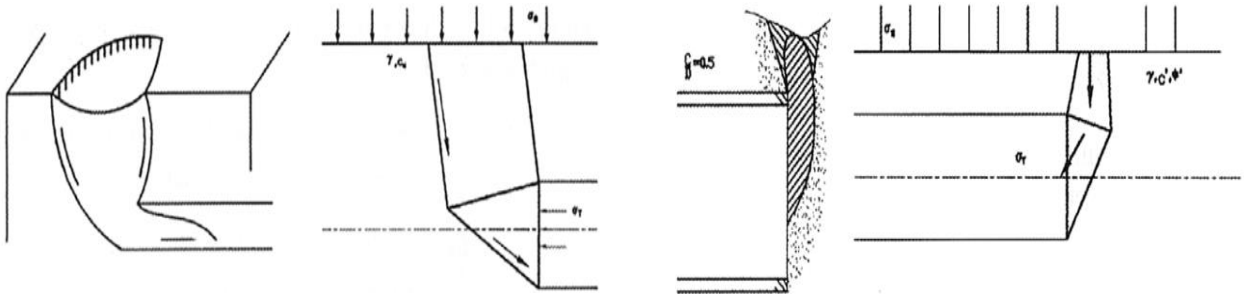

Figure 2. 2.- Failure mechanisms for both cohesive and granular soils *(Leca & New, 2007)*

When talking about granular soils (cohesionless soils) the failure mechanism tends to generate a chimney along which the failure is propagated above the tunnel face as it is shown in the previous Figure 2.2.

First of all, it is widely known that the failure mechanisms presented above are based on experience, ground investigations and field measurements but also on some centrifuge tests have been carried out in order to verify the geometries presented.

Although these geometries are validated with theses centrifuge tests, it is important to highlight that ideal conditions are assumed and they need to be adjusted to the real conditions of soil and hydro-geology encountered during the ground investigations.

Finally, it is important to remark that the figures presented above do not represent the ground displacements troughs induced by tunnelling but, the failure conditions and ground movements at the tunnel face.

2.2.2. Propagation of movements towards the surface

In general, when an instability of the tunnel face occurs and ground movements are generated, they tend to be propagated towards the surface. Different factors govern the extent and time scale of this phenomenon which are the geotechnical conditions and the geometrical conditions of the failure. Also a key aspect is the tunnel excavation method used. In this thesis only tunnelling boring machines are considered when talking about tunnelling induced ground movements. (Leca & New, 2007)

There are two basic modes of propagation namely primary and secondary mode which are going to be described as follows. These modes have been identified thanks to field measurements and in situ observations.

- *Primary mode of propagation*: this mode occurs when the release of stress happens in the tunnel front. This release generates an area of loosened ground above the excavation. The geometry of this area is usually between 1 – 1.5 times the tunnel diameter and 1 diameter width. Based on experience and field measurements, for tunnels in which the relation coverage over diameter (C/D) is greater to 2.5 namely as deep tunnels the observed tunnelling induced ground movements are limited. (Leca & New, 2007)

- *Secondary mode of propagation*: for shallow tunnels in which the relation coverage over diameter is smaller than 2.5 (C/D < 2.5) what happens is that there is not enough confining support hence, the formation of rigid ground blocks occurs. These rigid blocks are usually bounded by multiple shear planes which goes from the tunnel front to the ground surface generating the failure mechanism. In general, it has been observed that displacements generated at ground surface coincide with those measured at the tunnel front. (Leca & New, 2007)

In Figure 2.3 both primary and secondary mode of propagation are shown in a basic tunnel transverse cross section.

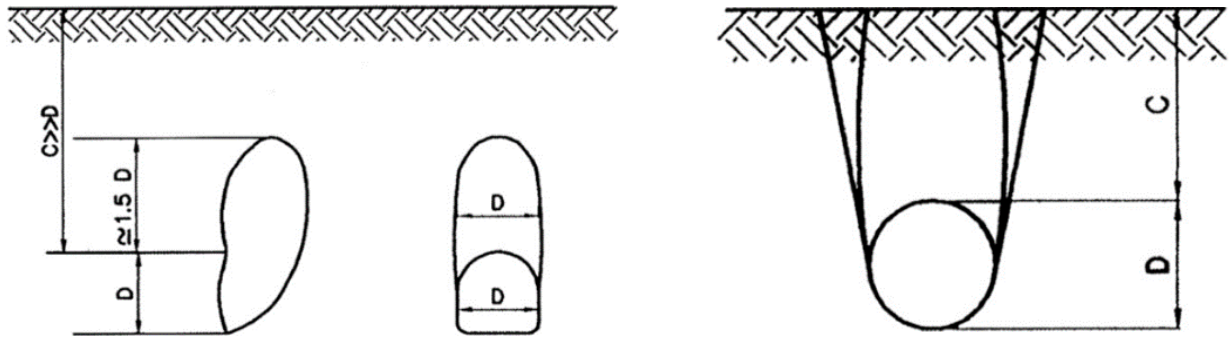

Figure 2. 3.- Primary and secondary mode of failure for a basic transverse cross-section *(Leca & New, 2007)*

For both mechanisms, the experience indicated that both vertical and lateral displacements are generated. These ground movements are experienced in ground surface while the tunnel is being excavated. In Figure 2.4 the so called three-dimension settlement trough is presented.

Although in design stage only transverse cross-section with Gaussian distribution is analysed, in reality its shape has three dimensions. This settlement trough is usually characterized by means of a longitudinal trough along the tunnel centre line and a transverse plane.

2.2.3. Parameters governing the stability of the tunnel front during construction

There are many factors, governing the stability of the tunnel front in construction stage. The main ones are presented below: (Leca & New, 2007)

- *Ground layering:* it is important because of the heterogeneity that the layers may present which can lead to difficulties during the excavation process as well as different geotechnical parameters in the ground units.

- *Nature of the ground:* the nature of the ground present at the tunnel front is important because of its geotechnical parameters. The better the ground is, the less support may be required.

- *Deformability:* The deformability of the ground is important for both short and long term because of the ground displacements that may induce and the consequences that may have at ground surface.

- *Anisotropy of the ground*: Anisotropy is important in terms of strength and deformability of the ground.

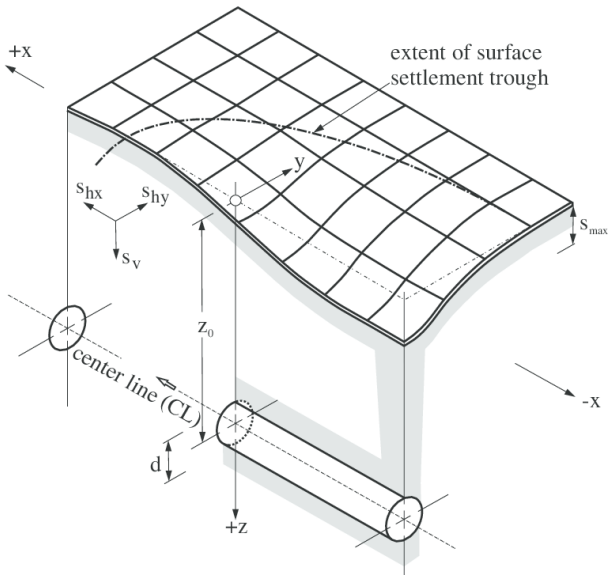

Figure 2. 4.- Three-dimension settlement trough. *(Leca & New, 2007)*

There are other important parameters governing the stability of the tunnel front such as the hydro-geological conditions of site. For all that reasons, it is vital to achieve good understanding levels of the site's geological and geotechnical conditions in order to proceed to a good geotechnical parameter estimation of the different units.

Experimental works and different case studies have led to the conclusions that there are limited factors that applied together can be used to characterize the stability of the tunnel front. A difference between cohesive and granular soils is going to be presented in the following point of this sections. It is important to differ between these types of soils due to the different failure mechanisms and also the different resistant parameters they usually have. Also its deformation moduli are different.

2.2.3.1. Cohesive soils

Fort the case of cohesive soils, when it is necessary to estimate the stability of the tunnel front, the overload factor "**N**" is used, which is defined as: (Leca & New, 2007)

$$\mathbf{N} = \frac{\gamma H}{S_u} \tag{2.1}$$

where **H** is the depth of the tunnel centre line, $\boldsymbol{\gamma}$ is the unit weight of the soil and $\mathbf{S_u}$ is defined as the undrained shear strength of the ground layer. It has been noticed that this last parameter, is one of the most important ones when studying the stability of the tunnel front for the case of cohesive soils.

There are two more parameters which are important to take into consideration which are the cover-to-diameter ratio (C/D) and the ratio $\frac{\gamma D}{S_u}$. The first one is important because it controls the effect of depth on the stability condition while the second one take into account possible instabilities at the tunnel front. However, the expression presented in equation 2.1 can be written in a more general way when considering a surcharge load applied at the ground surface. In Equation 2.2, the general equation is presented: (Leca & New, 2007)

$$\mathbf{N} = \frac{\gamma H + \sigma_s - \sigma_T}{S_u} \tag{2.2}$$

where $\boldsymbol{\sigma_s}$ is defined as the ground surface surcharge and $\boldsymbol{\sigma_T}$ is the support pressure applied at the tunnel front. This pressure usually comes from tunnelling boring machines. As in the previous case, $\mathbf{S_u}$ is defined as the undrained shear strength of the cohesive material and $\boldsymbol{\gamma}$ is the unit weight of the soil. As a result of experience and some field observations of real cases it can be concluded that for cohesive soils, there are some limiting values for the overload factor, N that need to be taken into account for the overall stability. These values are presented in Table 2.1.

VALUES OF N (dimensionless)	CASE DESCRIPTION
$N \leq 3$	Tunnel face stability is ensured. No need for extra support
$3 < N \leq 6$	Deeper study of the settlement risk is required. Large ground loss expected
$6 < N$	Tunnel face is in general, unstable

Table 2. 1.- Typical limiting values for the stability number, N. *(Leca & New, 2007)*

PARAMETER	LIMITING VALUES	DESCRIPTION OF THE CASE
C/D	< 2	Detailed analysis is required to ensure stability
$\gamma D/S_u$	< 4	Local failures may happen at the tunnel front

Table 2. 2.- Typical limiting values for the two parameters controlling the influence of depth and local instabilities *(Leca & New, 2007)*

In section 2.2.3.2, the case for granular or cohesionless materials is going to be studied.

2.2.3.2. Granular soils (Cohesionless soils)

When analysing the stability conditions of tunnels in cohesionless soils, due to their poor cohesion it is obvious that no stability will be achieved at the tunnel face when excavating a tunnel. Despite that, in granular soils there is usually a remaining cohesion providing resistance to the soil during a limited amount of time. Usually analysing the stability of a tunnel face it is not as easy as for the case of cohesive soils. For that case some other parameters such as the ground deformability and the anisotropy play a main role when assessing the displacements.

While for the case of cohesive soils the ratio cover to diameter is relevant, for the case of cohesionless soils is not that important. For the case concerning this section the parameter $\frac{\gamma D}{S_u}$ is modified because granular soils do not have undrained shear strength. Instead, the important parameter is the stabilizing pressure applied to the tunnel front. Hence, the ratio is $\frac{\gamma D}{\sigma_T}$. Also the effective friction angle is another parameter governing the displacements troughs for granular soils (ϕ'). (Leca & New, 2007)

2.2.3.3. Cohesive frictional grounds

There are granular soils that present both effective cohesion and friction angles. These soils are called cohesive frictional grounds. The strength of that types of soil hence, is defined for the addition of a cohesive controlled by the cohesion (c') and the frictional part governed by the friction angle (ϕ'). There are four parameters to analyse the stability of the tunnel front for this type of soils: (Leca & New, 2007)

$$\frac{\gamma H}{\sigma_c}, \frac{\gamma D}{\sigma_c}, \frac{\sigma_T}{\sigma_c} \text{ and } \phi' \tag{2.3}$$

where $\sigma_c = \frac{2c'cos\varphi'}{1-sin\varphi'}$

2.2.3.4. Rock

When shallow tunnels are excavated in rock, it is not usual to reach the rock strength as a consequence of the stress changes due to the excavation process. It is important to remember that in case of tunnels being excavated in hard rock a good characterization of the materials is necessary. There are many parameters controlling the strength of a rock material such as rock stratification, joint orientation, discontinuities, RQD, RMR, GSI, water table, etc.

2.2.3.5. Convergence of the excavation

It is important to analyse the convergence of the excavation as another key parameter governing displacements induced by tunnelling.

An important factor controlling the convergence of the excavation is the moment in which the tunnel support is installed behind the tunnel face. As illustrated in Figure 2.5, it is important to install it as early as possible in order to avoid excessive displacements after excavation.

The right part of Figure 2.5 shows that when the lining is installed early, the ground deformations are limited, but if the lining is installed late, the deformations are larger and maybe excessive compromising the stability of the tunnel itself. (Leca & New, 2007)

The left side of Figure 2.5 shows an illustration of the key parameters controlling the stability of the tunnel front that have been explained above.

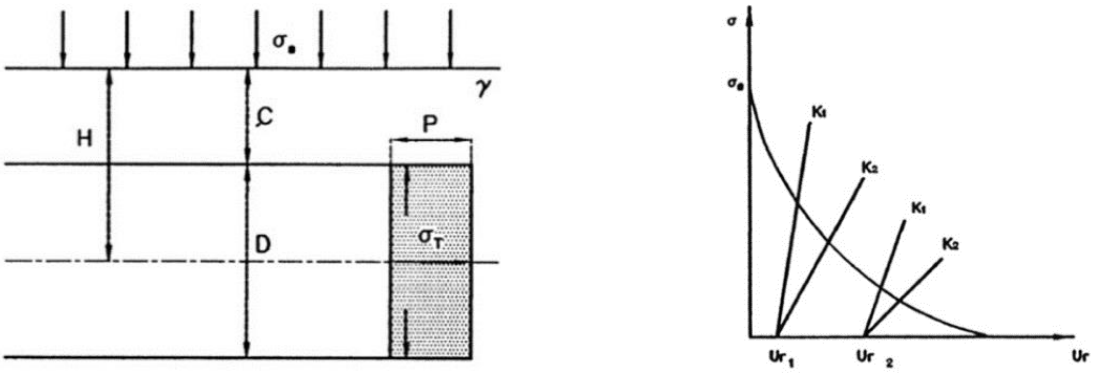

Figure 2. 5.- In the left side, the main stability parameters. In the right side, the influence of support conditions. *(Leca & New, 2007)*

2.3. Causes for construction induced settlements

Before analysing the different approaches that currently exist in order to mitigate or reduce the ground displacements induced by tunnelling it is important to deeply know the causes of these displacements and understand the way these displacements are propagated or extended towards the surface. In later paragraphs of this chapter different structural approaches to mitigate ground displacements are going to be presented and analysed.

When talking about tunnelling induced ground movements it is important to state the origin of these displacements. They are originated at some distance ahead of the tunnel front and then they are propagated until they find a stiffer element that prevents a larger propagation of them. It is important to differentiate between two types of displacements. On the one hand there are the settlements induced by the excavation method and on the other hand settlements that occur behind the tunnel face. (Leca & New, 2007)

Before talking about settlements induced by the excavation method, it is obvious that nowadays the tunnel excavation methods have improved a lot. The shield technology has developed to the point that settlements induced by these machines are almost imperceptible. However, some displacements exist and the main factors that influence them are going to be presented in the following points.

The opposite term of Tunnelling boring machines is what is called the "*sequential method*" or "*conventional method*". These methods refer to traditional methods when the tunnelling activities were developed by means of ribs and wood and do not reflect the technological advances that nowadays present the Tunnelling boring machines.

2.3.1. Sequential method

As stated before, the sequential method is referred to those traditional methods in which the tunnelling activities were developed by means of ribs and wood and as it is obvious, there is no settlement control implemented in the method. Different types of settlements are associated to this methodology which are presented in the following points.

2.3.1.1. Settlements associated to the tunnel face stability

As has been noticed in previous paragraphs, ensuring the face stability of the tunnel is of vital importance. It can be concluded from field measurements and experience observations that there is a correlation between the stability at the tunnel face and the settlements induced ahead of the tunnel face. (Leca & New, 2007)

2.3.1.2. Settlements associated to the installation of temporary support

During design stage and prior to the tunnel excavation and based on ground investigations and laboratory testing, it is important to select the appropriate temporary ground support. That implies to reach a balance between simulation models and calculation requirements and the construction requirements. Hence, the main parameters need to be deeply studied. (Leca & New, 2007)

- The first key factor is the nominal stiffness of the temporary support. It is important to verify by means of tests that this resistance is achieved analysing its mechanical characteristics.
- The other factor is the time necessary to proceed with the installation of the temporary support. This factor is mainly governed by the installation distance to the face.

These two parameters explained above it are enough to evaluate the overall resistance of the temporary support. Once analytical calculations of the resistance are validated it is important to ensure that this resistance is enough given the conditions at worksite. If not, a recalculation may be needed.

2.3.1.3. Settlements associated to the staging of the excavation works

Construction staging is closely related to the ground deformations around the opening. Three areas of ground deformations may be described: (Leca & New, 2007)

- *At the tunnel front*: it has been noticed based on observation and field measurements that the ground deformations at the tunnel front are related to the size and shape of the front section.

- *At some distance to the tunnel front*: it is observed that this type of settlement depends basically on the ability to the quick installation of the stiffer support, the excavation staging of the tunnel front and finally the length of unsupported ground behind the excavation front.

- *At some distance behind the tunnel front*: it is important to highlight that the quick installation of the tunnel lining may contribute to a uniform distribution of the tunnel induced ground movements in the longitudinal plane.

2.3.1.4. Settlements associated with the final lining installation and response

For shallow tunnels in which there is limited coverage and large excavated distance without stiffer support, it is important to take into account the ground displacements influenced by the liner deformations.

2.3.2. Case of shield-driven tunnels

This is an important section to cover for this thesis because all the calculations presented in later chapters will be referred to settlements induced by tunnelling boring machines. Four different type of settlements can be detected for the case of shield-driven tunnels which are presented in the following points. (Leca & New, 2007)

Figure 2.6 presents an illustrative vision of the evolution of settlements along the shield.

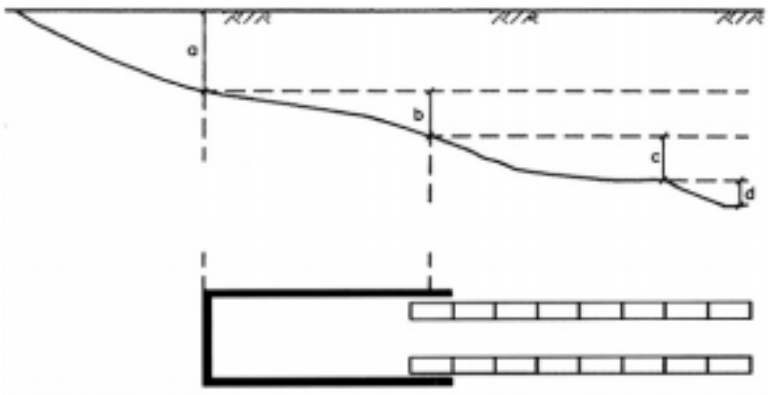

Figure 2. 6.- Evolution of the settlements along the tunnelling boring machine. *(Leca & New, 2007)*

2.3.2.1. Settlements ahead and above the face

The cause of these settlements usually is because of ground deformations that occur ahead and above the shield. These displacements are propagated in some cases towards the opening. The key parameter governing this

type of ground movements is the level of confining support at the tunnel front which is usually achieved by means of pressurized chambers behind the cutting wheel of the machine.

2.3.2.2. Settlements along the shield

The settlement profile along the shield is not constant. It is usual to experience more settlement at the tail of the tunneling boring machine rather than the tunnel front. Furthermore, based on field measurements this effect is clearly accentuated as the tunnel coverage increases.

Other observations have revealed that, settlements along the shield of the machine propagates to the ground surface at a constant pace for a specific ground. The following causes for settlements along the shield machines may be the basic ones: (Leca & New, 2007)

- *Overcutting*: that happens when the cutters of the cutting wheel are installed in the periphery of it which excavate a larger tunnel diameter than the shield has. This is in order to reduce the skin friction.
- *Tapering*: of the shield.
- *Roughness of the cutting wheel*: the roughness of the cutting wheel can generate soil displacements ahead of the tunnelling boring machine shield. These settlements are namely as crown settlements and are generated by friction and ground shear.

2.3.2.3. Settlements at the shield tail

As stated in the previous paragraph, the settlements at the tail of the shield machine are the most unfavorable ones because are expected to be the greatest. The main causes of these settlements may be the ones presented as follow: (Leca & New, 2007)

- Gap produced along the shield machine generated due to the overcutting.
- Thickness of the tail-skin that can be very thick due to the type of shield necessary to excavate the tunnel (single shield or double shield)
- The space between the inner face of the tail-skin and the outer face of the lining.

A factor controlling the amount of this settlement is the grout provided at the tail gap. If the tail gap is properly grouted, then this settlement would be reduced.

2.3.2.4. Settlements due to lining deformation

The reinforced concrete rings that constitute the liner segments must have enough resistance to sustain the thrust generated by the shield jacks and also the ground pressure that can eventually generate settlements along the liner. The shield jacks are the responsible of tunnelling machine movement. Notice that if the tail gap is well grouted then the resulting deformations will result as acceptable ones. (Leca & New, 2007)

2.3.3. Effect of worksite conditions

Settlements induced by the effect of worksite conditions refers to those generated by the vibrations caused by both sequential method or shield and also muck removal operations. This type of settlements has been observed in both soft and good ground conditions.

2.4. Incidence of ground displacements on existing structures

As stated before the displacements generated in the tunnel opening may be propagated by means of the modes explained above towards the surface generating movements in current structures. The displacements will vary depending on the type of soil encountered and the excavation methods used to excavate the tunnel.

In case of urban areas in which the tunnel goes beneath a street very close to existing buildings and utilities, these buildings may suffer from the ground displacements induced by the tunnelling machine. It is important to notice that the building stiffness is an important parameter in this case. (Leca & New, 2007)

2.4.1. Movements induced on existing structures

In case of dealing with constructions supported by shallow foundations such as rafts or footings, the displacements that will suffer the structure will be the same displacement suffered by the ground. Examples of this buildings are the typical old masonry buildings.

As today most of the structures are heavily reinforced, it has been noticed that the lateral displacements are dramatically reduced in comparison with the lateral displacements that the ground will experience. The parameter governing this is the flexural stiffness which allows lower values of distortion in comparison with the ground distortion values. These stiffer structures present also high shear strength capacity.

When assessing the damage that a structure may have as a consequence of tunneling induced ground movements it is important to locate the structure with respect to the settlement trough. This location of the settlement trough will influence the movements the structure will experience. In Figures 2.7 to 2.9, some idealized patterns are presented. (Leca & New, 2007)

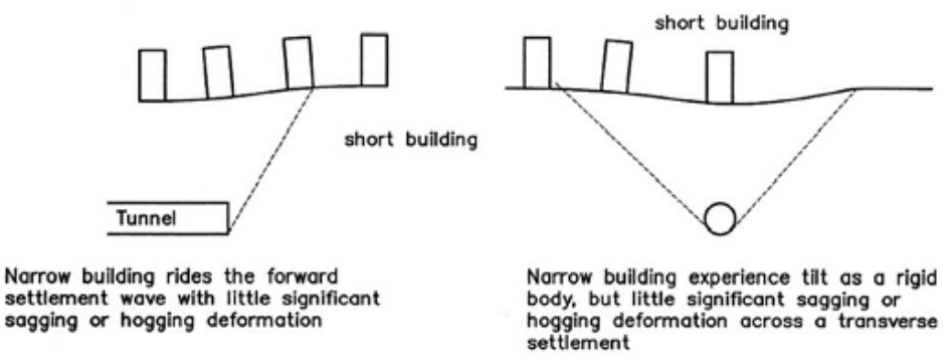

Figure 2. 7.- Building response to tunnelling works (I). *(Leca & New, 2007)*

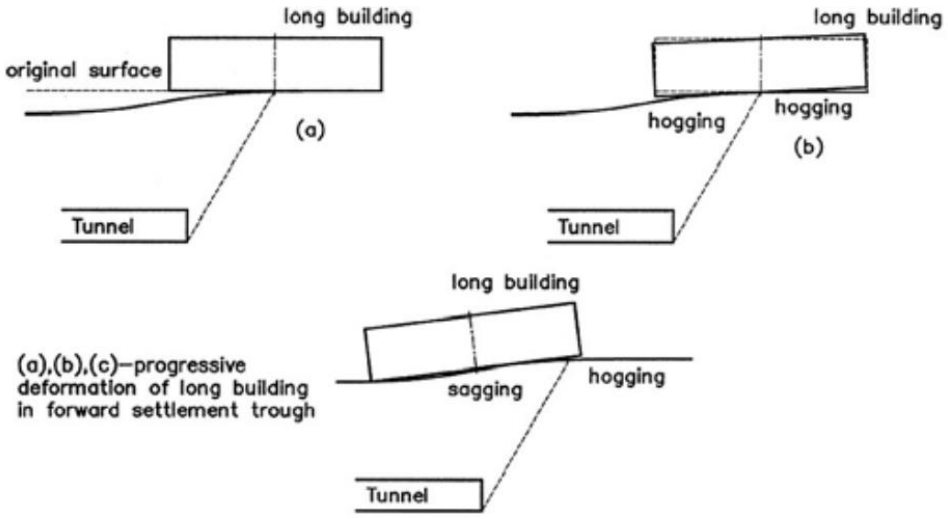

Figure 2. 8.- Building response to tunnelling works (II). *(Leca & New, 2007)*

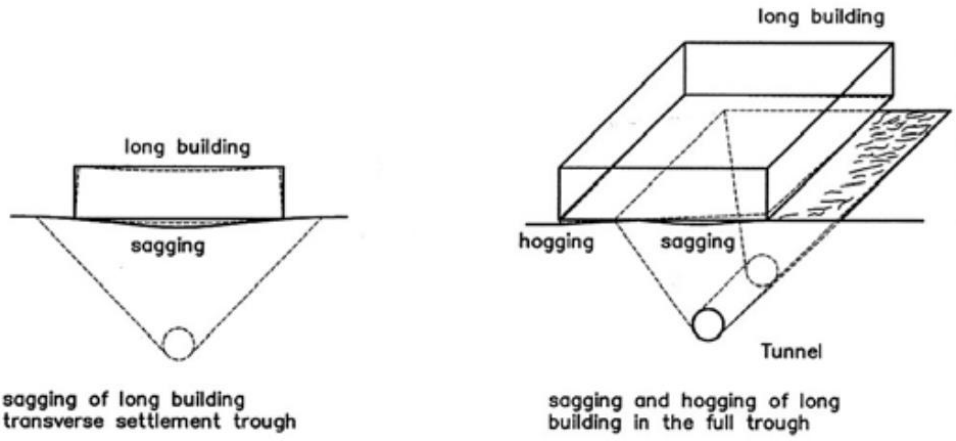

Figure 2. 9.- Building response to tunnelling works (III). *(Leca & New, 2007)*

A structure located in the influence area of a tunnel under construction may experience the following movements: Uniform settlement, differential settlements between supports, overall or differential rotation, horizontal displacements and differential horizontal displacements depending on the case. (Leca & New, 2007)

2.4.2. Classification of damage into existing structures

In general, structural damage suffered by structures can be divided into three categories:

- Architectural damages that affect the external and visual appearance of the structure.
- Functional damages that may difficult the daily routine operations in the structure
- Structural damages that affect the overall stability of the building.

The main factor causing damage into buildings is cracking. Cracking is created in materials of poor tensile strength such as concrete, mortar, plaster and coating. Failure occurs when there is excessive cracking or a great amount of load is transferred onto the reinforcements. As a consequence of cracking, corrosion may appear.

When assessing the structure damage due to excessive deformations, the main parameter studied is the crack width. In Table 2.3, a general criteria followed in order to assess the damage of a structure is presented.

DAMAGE TYPE	DEGREE	DESCRIPTION	CRACK WIDTH [mm]
Type 0	Negligible damage	Micro-cracks	< 0.1
Type 1	Very slight damage	Architectural	< 1.0
Type 2	Slight damage	Architectural to be treated	< 5.0
Type 3	Moderate damage	Functional	5 – 15, or several cracks > 3 mm
Type 4	Severe damage	Structural	15 – 25
Type 5	Very severe damage	Structural	> 25

Table 2. 3.- Classification of structural damage from crack width. *(Leca & New, 2007)*

In the following points the different types of damage presented in the previous table are going to be detailed. As one can imagine, the purpose of this criteria is purely practical in order to develop an easy repair guide of the different types of damages. (Leca & New, 2007)

- *Type 1*: As there is no structural damage, these crack can be easily treated by means of a reparation process.
- *Type 2:* As in the previous case, the structure itself is not damage and its stability is not an important problem but it need rehabilitation. Cracks may be filled with material. Wood elements such as doors and windows may suffer affections from ground movements.
- *Type 3:* This damage is more serious than the previous ones. Both internal and external cracks appear during ground movements. For type 3 the Serviceability Limit State of the structure may not be satisfied and the residents may suffer the inconveniences.

- *Type 4:* For type 4, the Ultimate Limit State of the structure may not be satisfied compromising the overall stability of the building. Large cracks may appear that will need significant repairing works. The reinforcement may be damaged too and may need replacements.

- *Type 5:* Type 5 is the worst one. The structure is 100% unstable and it needs to be partially or totally rebuilt.

As stated before, these classifications may not be applied to new structures that are built nowadays because of they have enough reinforcement in the concrete to ensure long term stability. These classifications are more applicable to those structure with no foundations or shallow foundations such as shafts or rafts. This type of foundations are more prone to suffer from structural damage. (Leca & New, 2007)

This can be the case also of World Heritage Buildings which have been constructed a long time ago an now are dealing with the design and construction of new utilities beneath their foundations that may compromise the overall stability of the building itself. In following sections of this document and thesis lateral walls made of rows of piles will be considered to protect sensitive constructions from tunnelling.

2.5. Settlement control

When designing a new infrastructure such as a tunnel, one must be conscious about the impact that the new structure may have to existing structures. So, in order to minimize that impact is necessary to plan, before construction stage starts, all the measures to reduce or mitigate the damage due to tunnelling works. However, that is not 100% possible due to the technical difficulties and the lack of knowledge of both the real worksite and ground conditions. Prior to tunnel excavation is necessary to analyse the structural state of the current buildings surrounding the tunnel area. (Leca & New, 2007)

With all the available information during design stage, is important to plan the set of measures that will be applied at the beginning of the excavation works. Also a set of extra measures need to be planned in case of unexpected difficulties during tunnelling works. It is important to ensure safety of all workers and safety of neighbouring structures.

In the following points a set of techniques developed in order to mitigate and reduce the settlements on the ground are presented. For each solution the main advantages as well as the limitations will be described.

2.5.1. Improvement of the overall project conditions

When referring to the initial design stages, all the alternative alignments for the new tunnel must be deeply studied and selected the one that offers the most favourable conditions for settlement control. (Leca & New, 2007)

To achieve that the most important key factors to study are the ones presented in the following points:

- As much coverage as possible. The designer must be ensured that providing depth to the tunnel axis, does not affect in terms of encountering ground layers of insufficient geotechnical characteristics. To achieve that goal is of vital importance to define an accurate geotechnical ground investigation.

- The designer also must ensure that the tunnel alignment coincides with a ground layer of good mechanical properties. This layer should have the desirable thickness which is usually one tunnel diameter above the crown. It is obvious that there will be cases in which that condition may not be satisfied so the designer must keep in mind to excavate the tunnel underneath a stiffer layer. By doing that, later on, the bridging effect will provide the soil the temporary resistance necessary to avoid failure while the final tunnel liner is installed.

- Another point to take into account is to optimise the excavated cross section to the smallest one. At that point is when the designer needs to choose between a single or twin-tube tunnel. The final decision will be made according to ground conditions in which the tunnel will be placed. In case of choosing the twin-tube tunnel it is important to determine well the distance between tubes because that zone will be the one that will accumulate more stresses and hence, more ground displacements.

- Regarding the construction process, if tunnelling boring machines are selected one must try to design the more straightest alignment possible and avoid curves that can generate difficulties to operate the machine.

2.6. Structural solutions to mitigate damages

As stated in previous chapters of this document, tunnelling in urban areas may affect those structures which are mainly founded in shaft foundations or rafts. These affections can be both structural damages or the appearance of cracks due to the tunnelling induced ground movements. In previous lines, the main geotechnical theoretical basis in order to understand the main soil parameters governing these movements have been presented.

Nowadays before planning a new tunnel beneath an urban area, a deep study of the affections that this tunnel may create to surroundings structures is developed and in case needed sometimes a structural solution to mitigate theses damages is studied and implemented. In order to mitigate and reduce ground displacements there are different solutions such as diaphragm walls, row of piles or also jet grouting columns may be solutions widely used in order to protect current buildings from excessive ground displacements. (Leca & New, 2007)

In the following lines of the document, different documentation of important geotechnical authors presenting their conclusions about structural solutions to prevent and mitigate ground displacements due to tunnelling are presented and analysed.

2.6.1. Diaphragm walls to mitigate ground movements induced by tunnelling. (Bilotta, 2008)

2.6.1.1. Diaphragm wall as a solution to mitigate ground movements

As explained in previous sections of this document, old buildings which are not sufficient well supported, are the most prone to suffer from ground displacements due to tunnelling works. Some techniques have been studied during the last few years which are going to be presented in the following lines. A diaphragm wall constructed between the tunnel and the area were the ground displacements are desired to be prevented can act as a barrier preventing the propagation of the ground displacements beyond the diaphragm wall. The efficiency of the wall depends basically on its geometry but also there are few key parameters such as its stiffness and inertia and parameters related to the interface between soil and reinforce concrete. (Bilotta, 2008)

Results of field measurements and experience observations have revealed that this measure performed well in the cases that it has been implemented. In the following sections the main ideas and analysis of the document are going to be provided.

2.6.1.2. Previous definitions

As explained in few sections above, the settlement trough in reality is a three-dimension phenomenon but for the case concerning this document only transverse cross-sections are going to be analysed due to the simplification of plane-strain that can be applied to tunnelling problems. (Bilotta, 2008)

As defined above in previous sections, Peck (1969) based on field experiences defined the transverse cross-section of the settlement trough as a Gaussian distribution. The settlement caused due to a single tunnel excavation is what is called “greenfield conditions” and can be estimated applying the equation presented as follows:

$$\mathbf{S_y[m]} = \frac{0.31V'D^2}{i}\exp\left[\frac{-x^2}{2i^2}\right] \tag{2.4}$$

In where $\mathbf{V'}$ parameter represents the area of the settlement trough. These area represents a percentage of the total are of the cross-section of the tunnel. It can be assumed that in undrained conditions that parameter is equal to the ground loss. The ground loss parameter as will be explained in following chapters of the thesis, depends mainly on the excavation method chosen in order to execute the tunnel. The typical values for the ground loss usually varies between 0.5% and 2%. These typical values are based on experience observations. (Bilotta, 2008)

D is defined as the tunnel diameter and **x** is defined as the transverse position of the studied point. The **i** parameter represents the distance between the infection point of the settlement trough and the tunnel centre line. This parameter is the main one governing the width of the settlement trough which typical values vary between 2.5i – 3i. The mathematical expression presented in Equation 2.5, represents the **i** parameter. (Bilotta, 2008)

$$\mathbf{i}[\mathbf{m}] = \mathrm{K}\left[\mathrm{C} + \frac{\mathrm{D}}{2}\right] \tag{2.5}$$

The **K** parameter is a constant that basically depends on the nature of the ground. Its typical values vary between 0.25 for granular soils and 0.6 for purely cohesive soils.

2.6.1.3. Experimental analysis and test procedure

The goal of this test by Bilotta was to prove the efficiency of a diaphragm wall embedded between the tunnel axis and existing buildings in order to reduce and mitigate ground displacements due to tunnelling works. The test was carried out by means of the centrifuge apparatus which is one of the best tools to test reduced-scale models. The original geometry of the prototype was a tunnel with a diameter of 8 meters with a relation coverage over diameter equal to one. For that geometry features de model was set with a diameter of 50 mm hence, the centrifuge acceleration of the test was 160g. (Bilotta, 2008)

In order to validate the results obtained by this author both centrifuge and finite-element method models were developed. In Figure 2.10 and Table 2.4, the main geometry of the models is presented as well as the geometric characteristics of the centrifuge models developed by Bilotta.

The diaphragm walls were built up in the model by means of aluminium which has a specific weight of $\gamma_{\mathrm{al}}\left[\frac{\mathrm{kN}}{\mathrm{m}^3}\right] = 27$ and it is quite similar to the concrete unit weight although its elasticity moduli is higher. Once the wall is built with aluminum in some models is covered with different materials in order to simulate the roughness and different conditions of the interface (smooth or rough). The summarized procedure of the centrifuge test is the one explained in the following points: (Bilotta, 2008)

- Preparations of the different geometries and tunnel construction. Also the lateral wall is built and the instrumentation apparatus for the displacements is introduced.
- Sample consolidation to a vertical effective stress of $\sigma'_{\mathrm{V}} = 350\ \mathrm{kPa}$ and unloading to a pressure of 150 kPa.
- Acceleration of the model of 160g, increasing manually the air pressure in the tunnel cavity in order to equilibrate stresses.

- The pressure inside the tunnel reaches a value of $p_0 = 190$ kPa where the equilibrium of stresses is reached. That value corresponds to the total vertical stress evaluated in a mid-point between the centre of the tunnel and the crown.

- The acceleration of the model remains constant (160g) until the pore pressure equilibrium is reached, normally 6 hours after the beginning of the test.

- Now the simulation of the excavation is carried out by means of reducing the air pressure inside the tunnel cavity to a rate of 100 kPa/min, in order to achieve a drained condition behaviour of the soil.

- The air pressure reduction is maintained in the tunnel cavity until reaching collapse of the tunnel.

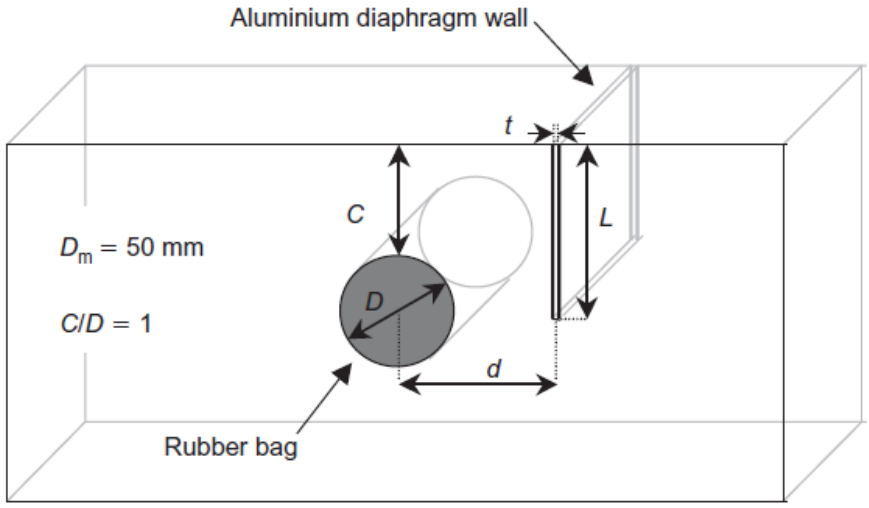

Figure 2. 10.- Scheme of the geometry of the different models (Bilotta, 2008)

TEST ID	L: mm [m]	t: mm [m]	d: mm [m]	Interface wall – clay
EB5	70 – [11.2]	9.5 – [1.52]	50 – [8]	Rough
EB6	Reference test without lateral wall			
EB7	70 – [11.2]	9.5 – [1.52]	75 – [12]	Rough
EB8	120 – [19.2]	9.5 – [1.52]	50 – [8]	Smooth
EB8	120 – [19.2]	9.5 – [1.52]	75 – [12]	Smooth
EB10	120 – [19.2]	9.5 – [1.52]	50 – [8]	Rough
EB11	120 – [19.2]	9.5 – [1.52]	75 – [12]	Rough
EB12	70 – [11.2]	9.5 – [1.52]	50 – [8]	Smooth
EB13	120 – [19.2]	0.8 – [0.128]	50 – [8]	Smooth
EB16	70 – [11.2]	7.2 – [1.15]	50 – [8]	Rough (toothed)

Table 2. 4.- Description of centrifuge model tests. (Bilotta, 2008)

While the tests are being carried out both variation of the air pressure and settlement troughs are registered. This last is done with the virtual imaging processing technique. Later on, the volume loss is calculated for different levels of support pressure by means of numerical integration of the settlement trough assuming undrained conditions.

Finally, for each of the models developed for the analysis the displacements ground field is obtained considering values for the ground loss (V_{loss}) of 1.3% and 10% approximately. (Bilotta, 2008)

2.6.1.4. Experimental results

In Figure 2.11, both horizontal and vertical surface displacements are presented for the tests EB5 to EB13 from table 2.4 considering a tunnel front support pressure of 40% of the initial value of p_0.

In the reference test without lateral wall, that support pressure is equal to a volume loss of 1.35% approximately. The results are presented in two groups making a differentiation between rough walls (left) and smooth walls (right)

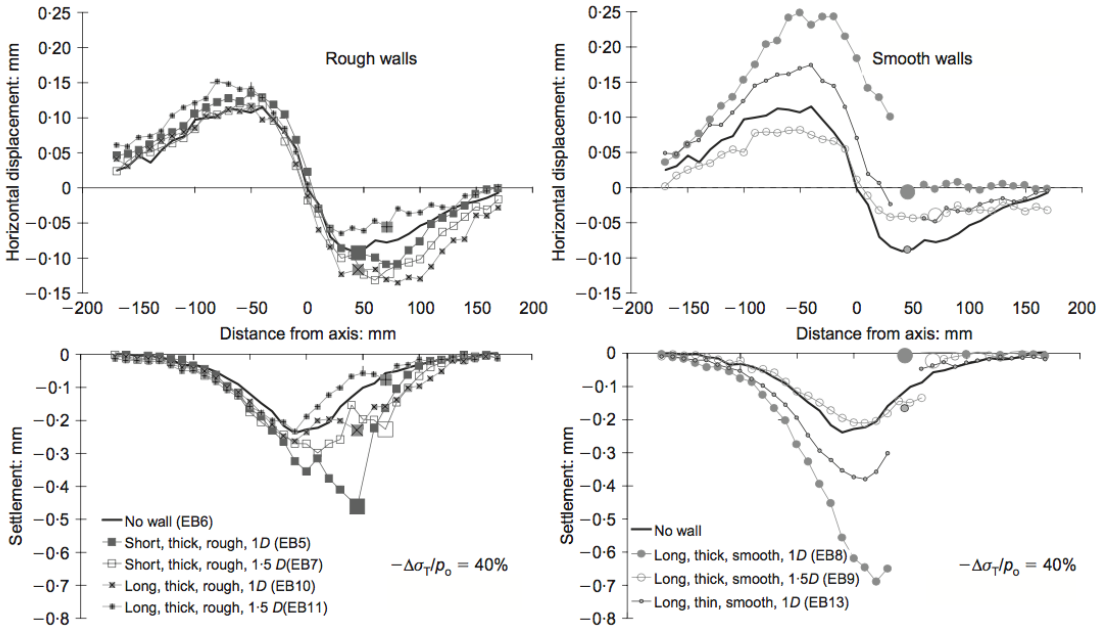

Figure 2. 11.- Horizontal displacements (upside) vertical displacements (downside), measured in surface for a support pressure of 40% (Bilotta, 2008)

As can be observed, in general terms the volume of the vertical settlement troughs for those models in which the lateral wall is implemented, the volume is higher than greenfield conditions for the same support pressure. Hence, the results show that the concept of building a diaphragm wall instead of mitigating and reducing the settlements induced by tunneling, these are increased. Some of the possible reasons of increasing the displacement field may be the ones that follow: (Bilotta, 2008)

- The lack of length for the lateral walls in some cases with the tip near the tunnel gables which cannot reduce the displacement trough. More length should be needed.

- The unit weight of the aluminium as stated before is equal to $\gamma_{al}\left[\frac{kN}{m^3}\right] = 27$ which means a 50% more than the soil used for the centrifuge test. The volume of the lateral walls is between 30% (for the short cases) and 60% (for the long cases) of the total tunnel volume. The effect of the huge amount of weight instead of stabilizing the displacement field contributes to generate instabilities of it.

- Another factor is the roughness of the interface wall-clay. For the smooth interface there is an evident discontinuity in the displacement field while for the rough interface this effect is not perceptible. In one of the models, the smooth interface achieves the settlement control in an efficient way.

In Figure 2.12, both the horizontal and vertical surface displacement troughs are presented in surface for tests EB5 to EB13 from table 2.4 assuming a constant volume loss of 1.35% in all the studied cases. The results are presented in two groups making a differentiation between rough walls (left) and smooth walls (right)

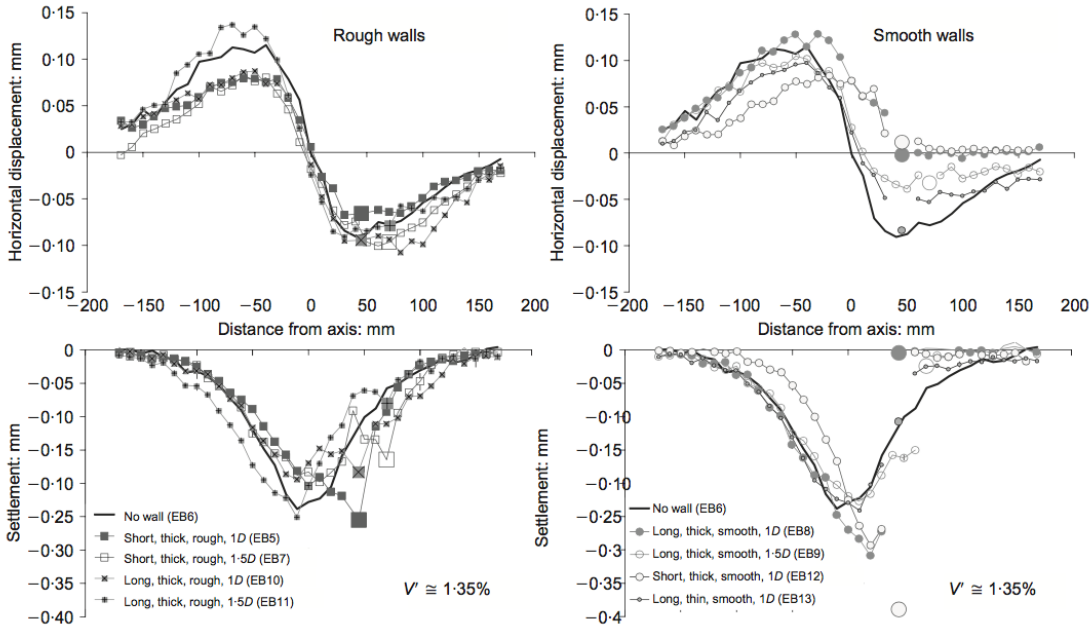

Figure 2. 12.- Horizontal displacements (upside) vertical displacements (downside), measured in surface for a volume loss of 1.35 % (Bilotta, 2008)

Having a deeper look to the figure presented above, it can be seen the following aspects; The presence of rough diaphragm walls does not control in an efficient way the displacement troughs beyond the wall. Furthermore, it changes its distribution creating a displacement concentration in the influence area of the diaphragm wall.

In the opposite side, the settlements and horizontal displacements are reduced for the points located near the tunnel centre line in comparison with those in the greenfield case. Now some finite-element models were run in order to validate the conclusions the author obtained with the centrifuge tests.

2.6.1.5. Numerical Analysis

In order to validate the physical results gathered from the centrifuge tests, Bilotta (2008), carried out a set of Finite-element simulations with the goal to reproduce the same geometrical conditions of the centrifuge analysis presented in table 2.4. Some other analyses were developed in order to study different variables and parameters that could not be studied with the centrifuge tests. (Bilotta, 2008)

In Bilotta's analysis the Hardening Soil model was used considering three cinematic surfaces (Stallebrass, 1990) in order to model well the soil behavior. The structural walls were assumed to be elastic with interfaces that were modeled with slip elements. The results for some of the analysis are provided in Figures 2.13 to 2.15.

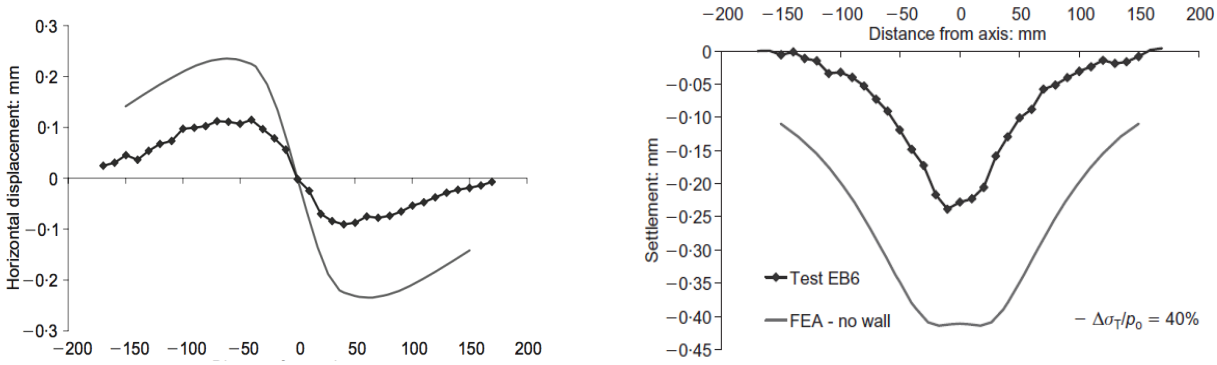

Figure 2. 13.- Comparison between the surface settlements between the centrifuge model and the finite-element one for the case without lateral Wall. (Bilotta, 2008)

As can be seen, the maximum displacements obtained with the finite-element simulation are almost two times the ones measured in the centrifuge model for the case of greenfield conditions. In Figure 2.14, the results of a short diaphragm wall and rough interface are presented.

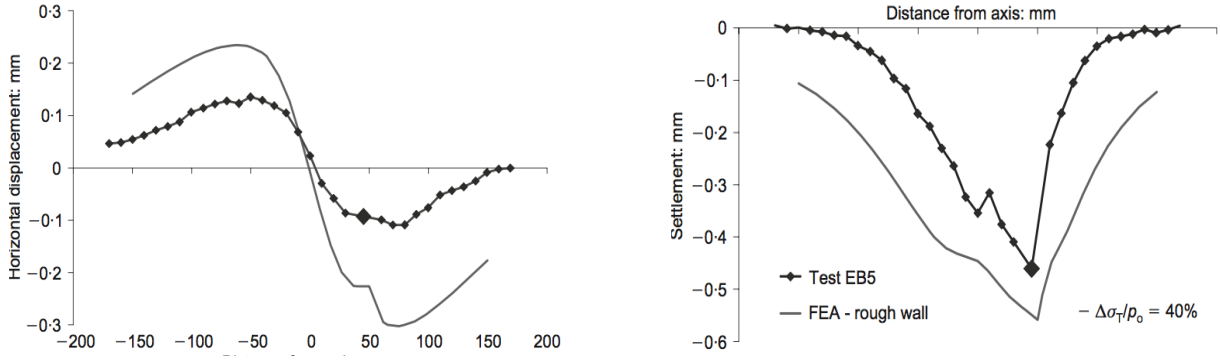

Figure 2. 14.- Comparison between surface settlements for the model EB5 and the corresponding finite-element model for the case of short diaphragm wall with rough interface. (Bilotta, 2008)

In Figure 2.15, the results for the short diaphragm wall and the smooth interface are presented. In these results a clear difference is observed between the centrifuge test results and the ones obtained from the finite-element simulations. Both horizontal and vertical displacement troughs are smaller for the case of the finite-element simulation.

Another aspect to notice, is the presence of a discontinuity in the settlement troughs due to the smooth interface between the soil and the structural wall which can be well reproduced by the model. However, the displacement beyond the lateral wall for the case of the numerical analysis are higher than the centrifuge model.

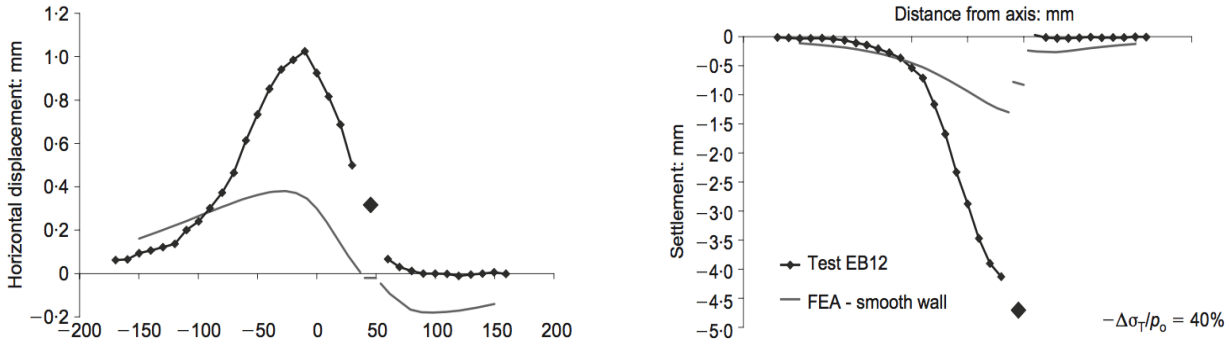

Figure 2. 15.- Comparison between the surface settlements for the model EB5 and the corresponding finite-element model for the case of the case of short diaphragm wall with smooth interface. (Bilotta, 2008)

2.6.1.6. Efficiency of the measure

The efficiency of a structural element to reduce the settlements induced by tunnelling is calculated with the expression presented in Equation 2.6 which is a dimensionless ratio that quantifies the potential of a vertical diaphragm wall to reduce ground movements. (Bilotta, 2008)

$$\boldsymbol{\eta}^{\mathbf{v}}_{\mathbf{bw}}[-] = \frac{[\mathrm{S_{ref}} - \mathrm{S_{bw}}]}{\mathrm{S_{ref}}} \tag{2.6}$$

Where $\mathbf{S_{ref}}$ is the settlement trough in greenfield conditions and $\mathbf{S_{bw}}$ is the settlement of the ground surface immediately beyond the diaphragm wall. When $\boldsymbol{\eta}^{\mathbf{v}}_{\mathbf{bw}}$ is equal to 1 it means that the solution of a diaphragm wall is totally effective whereas when $\boldsymbol{\eta}^{\mathbf{v}}_{\mathbf{bw}}$ present a value of 0, means that the wall has no positive effect when reducing the settlement trough. In Figures 2.16 to 2.18, the efficiency plots for both rough and smooth walls is provided.

The following figure shows the variation of the efficiency of diaphragm walls with rough interface as a function of their length for a constant value of Volume loss of 1%.

As can be seen analyzing the figure, the rough diaphragm walls can present negative values of efficiency for almost cases analyzed. However, it can be noticed an increase of the efficiency when the diaphragm wall length is also increased.

In addition to that, the values of efficiency obtained from the finite-element simulations are higher than the values obtained from the centrifuge tests excepting the model EB16 in which the rough interface almost is the same as the finite-element model. That reveals that the way in which the interface is created has a strong influence in the final results. (Bilotta, 2008)

As a practical conclusion of the efficiency, the results show that when the roughness is improved in the interface soil-structural wall it can be increased also the efficiency of the lateral wall with the aim of reducing the settlements.

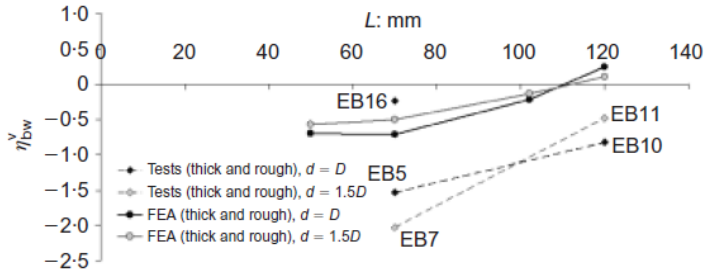

Figure 2. 16.- Efficiency of the structural walls with rough interface with a constant volume loss of 1%. (Bilotta, 2008)

In Figure 2.17, the results for the smooth interface are presented. The values of efficiency for the models EB8, EB9 and EB12 present values of efficiency near one independently of the wall length and its distance to the tunnel centre line. Furthermore, the results for the finite-element simulation present positive values however, these values are smaller than in the centrifuge tests.

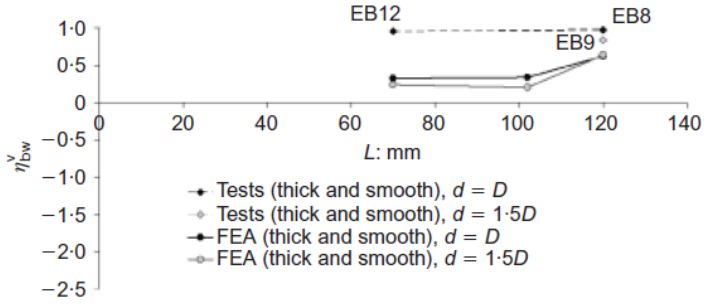

Figure 2. 17.- Efficiency of the structural walls with smooth interface with a constant volume loss of 1%. (Bilotta, 2008)

As a final stage of the calculation process, Bilotta (2008), calculated the efficiency of the overall system modifying the unit weight of the structural walls with similar geometries to the centrifuge models. The results are presented in Figure 2.18.

In the figure presented, it is compared the efficiency of heavy diaphragm walls with rough interface with lighter diaphragm walls with similar unit weight as the soil. It can be seen that lighter walls achieve positive values of efficiency at smaller lengths than heavy diaphragm walls. That is due to the fact that lighter walls do not introduce extra weight which can generate an additional settlement.

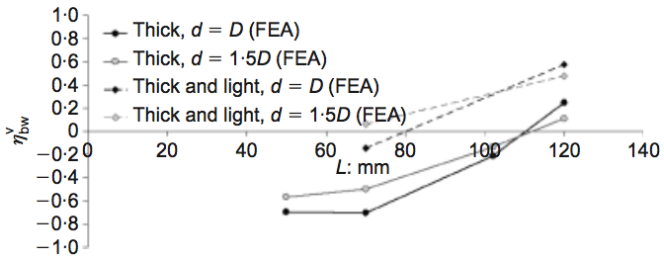

Figure 2. 18.- Efficiency of light and heavy diaphragm walls with a constant volume of 1%. (Bilotta, 2008)

As it has been observed in the centrifuge models, heavy walls tend to introduce extra weight and as a consequence of that, an increase of the settlements. Hence in order to reduce the settlement a reduction of the extra weight induced by the wall is an option to take into account. That would lead to positive values of efficiency also for those cases of rough interface.

2.6.2. Line of piles to prevent damages Induced by tunnelling excavation. Emilio Bilotta and Gianpiero Russo (2011)

2.6.2.1. Introduction

During the past few years, different techniques have been studied in order to reduce and mitigate ground movements induced by tunnelling works. While in previous document a diaphragm wall was studied, now the case of a row of piles is analysed. Some studies have been carried out by important authors in the geotechnical field and some factors have been remarked such as the length of the pile as well as its location. In some cases, it has been noticed that when the pile tip is beneath the tunnel, the pile-head settlement is not as high as when the pile tip is above the tunnel.

The idea is that the row of piles is installed prior to the tunnel excavation in order to protect neighbouring structures and foundations from excessive ground movements when the tunnel is being excavated. The level of damage explained in previous sections of this chapter governed by the crack width is a key factor when designing a protecting measure to current buildings.

In the case concerning this article, some three-dimensional finite-element analysis have been carried out in order to analyse the performance of a row of piles when a tunnel is being excavated. As will be noticed, rows of piles constructed between the tunnels to be excavated and existing buildings to be protected, have been performed well and effectively to reduce ground movements. As in the previous section when talking about the greenfield conditions as reference, in this analysis again, greenfield conditions will be assumed as reference when evaluating the efficiency of the piles. That's because in many studies all the results of deformations and settlements are compared with the basic case which is greenfield conditions. (Bilotta & Russo, 2011)

The basic purpose of this three-dimensional analysis is to take into consideration effects that cannot be evaluated in a single two-dimensional analysis and also asses the level of damage induced by tunnelling to current structures. In the following sections, the purposes of this analysis are going to be deeply developed and analysed.

2.6.2.2. Numerical analysis and model geometry

The goal is to carry out the three-dimension analysis on the same case studied with the centrifuge test. Hence, an 8-meter tunnel diameter is considered with a relation cover over diameter equal to one. In order to obtain the spring line of the tunnel it is enough to apply Equation 2.7: (Bilotta & Russo, 2011)

$$\mathbf{z_0[m]} = \mathrm{C} + \frac{\mathrm{D}}{2} \tag{2.7}$$

For the studied case, $\mathbf{z_0}$**=** 12 m. The cover-to-diameter ratio (C/D) is equal to 1, hence, the cover is equal to the diameter, so C= 8 m. The distance between the pile axis and the tunnel spring line is set as a value of 8 meter.

An important fact to be highlighted is that when talking in terms of efficiency of the piles one must be aware that when using rows of piles instead of diaphragm walls, the values of efficiency will be slightly lower due to the separation between piles. For the studied model, the length of the piles implemented to the Plaxis model was calculated by means of Equation 2.8: (Bilotta & Russo, 2011)

$$\mathbf{L[m]} \cong \mathrm{C} + \frac{3\mathrm{D}}{2} \tag{2.8}$$

That expression was used for what is called long piles but what is interesting in most articles is to have a set of results in order to proceed with comparisons between them. Another expression was used to obtain the length of what was called short piles and is the one presented below: (Bilotta & Russo, 2011)

$$\mathbf{L[m]} \cong \mathrm{C} + \frac{\mathrm{D}}{2} \tag{2.9}$$

As stated before, the software used in order to develop the simulations is Plaxis 3D, a widely used software nowadays in its lately versions in terms of designing underground works. Plaxis software has been developed exclusively for the analysis of boundary value problems in the geotechnical field.

For the case concerning this section, a mesh of 80-meter-wide and 30-meter-deep was used for calculation and the constitutive model implemented was Hardening Soil Model which is a nonlinear elastic-plastic constitutive law with volumetric and deviatory hardening. In Table 2.5, the main inputs parameter for this constitutive model have been presented. (Bilotta & Russo, 2011)

PARAMETER	VALUE	UNIT
Unit weight [γ]	17.5	kN/m^3
$E_{50,ref}$ [for p_{ref} = 100 kPa]	8 to 25	MPa
$E_{ur,ref}$ [for p_{ref} = 100 kPa]	2.8·$E_{50,ref}$	MPa
$E_{oed,ref}$ [for p_{ref} = 100 kPa]	$E_{50,ref}$	MPa
Cohesion [c]	0.001	kPa
Friction angle [ϕ]	20 to 30	º
Dilatancy angle [ψ]	0	º
Poisson ratio [υ]	0.2	-
Power [m]	1	-
Tensile strength	0	kPa
Failure ratio $q_{failure}/q_{asymptote}$	0.9	-

Table 2. 5.- Soil parameters implemented for the Hardening Soil Model in Plaxis 3D. (Bilotta & Russo, 2011)

The groundwater table has been set to be at ground level. Plaxis software in order to calculate the effective stress state uses the earth pressure coefficient which is obtained from the friction angle (ϕ).

$$\mathbf{k_0}[-] = 1 - \sin\phi \tag{2.10}$$

The tunnel was modeled as a cavity and the tunnel excavation was simulated with several steps in which each of them a percentage of stress reduction was applied until failure is reached. Piles were simulated as structural elements with the same unit weight as the soil. The structural elements were plates assumed elastic and isotropic. Different spacing length between piles have been studied in order to analyze the results provided by the simulation. (Bilotta &Russo, 2011)

In Figures 2.19 to 2.21, different views of the mesh are presented as well as a table with the mechanical properties of the structural elements. It is important to notice that in terms of comparison, the same simulation has been carried out with a diaphragm wall in order to compare the displacements troughs between piles and the diaphragm wall.

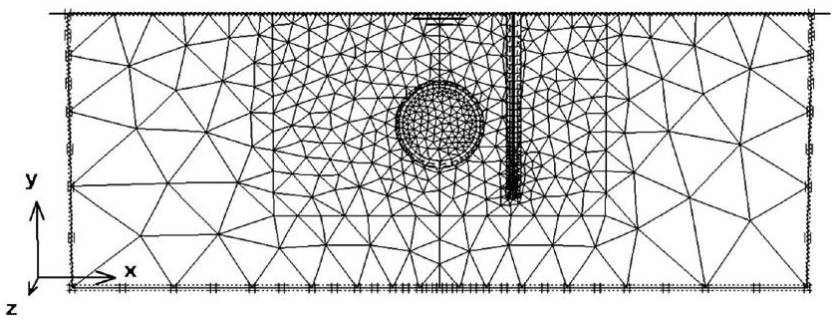

Figure 2. 19.- Front view of the mesh. Pile length calculated as L ≅ C+1.5D. (Bilotta & Russo, 2011)

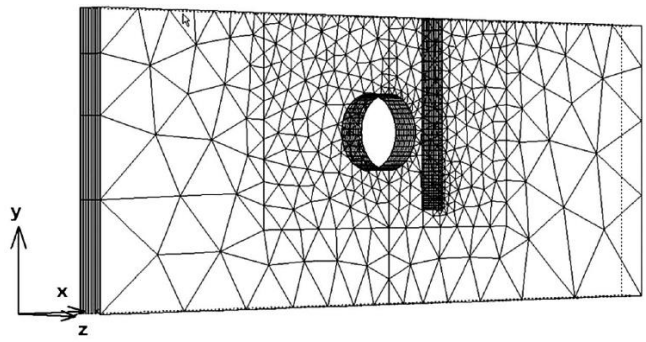

Figure 2. 20.- Elevation view of the mesh. Pile length calculated as L ≅ C+1.5D. (Bilotta & Russo, 2011)

ELEMENT	L [m]	b [m]	EI [kNm²/m]	EA [kN/m]	υ [-]	s/b [–]
Piles	11.2 to 19.2	0.25	5.9E+04 – 3.4E+06	1.43E+07 – 5.46E+07	0.25	2, 3, 4, 6 and 12
Wall	11.2 to 19.2	3	5.9E+04 – 3.4E+06	1.43E+07 – 5.46E+07	0.25	

Table 2. 6.- Mechanical properties of the structural elements. (Bilotta & Russo, 2011)

As it can be seen in the mechanical properties table, five different geometries have been considered for the pile row analysis each one with the corresponding spacing between piles. The last geometry corresponds to the 3-meter width diaphragm wall used in terms of comparison as explained above. In Figure 2.21, a draft of the geometries explained is presented.

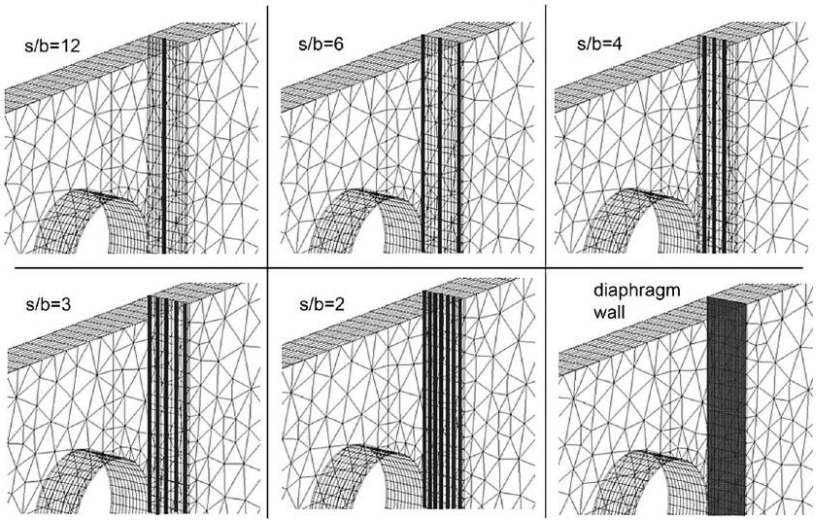

Figure 2. 21.- Configuration of the different structural elements presented in table 2.6. (Bilotta & Russo, 2011)

2.6.2.3. Results

In Figure 2.22, the settlement trough computed as a result of the simulation for the different spacing values of the piles is presented being compared with the greenfield case. Also a Gaussian curve is being plotted (Peck, 1969) in order to compare it to the greenfield case. Finally, the results for the diaphragm wall are plotted in order to be compared with those piles.

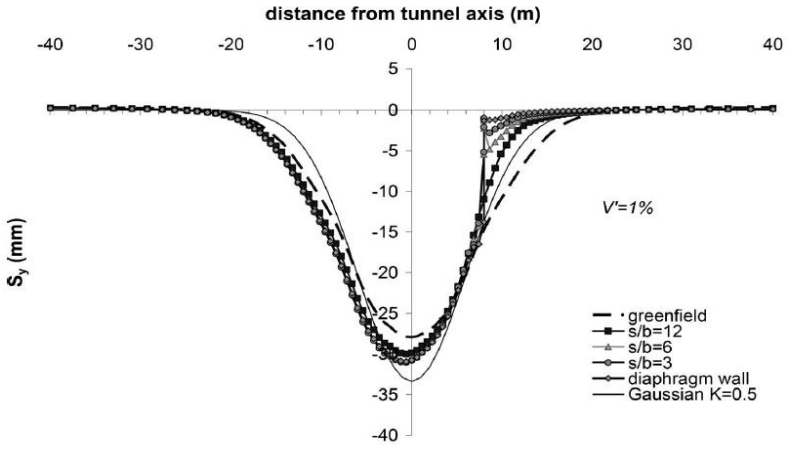

Figure 2. 22.- Vertical settlement trough for pile lengths of L ≅ C+1.5D and different configurations for the value of pile spacing at V'=1% and $E_{50,ref}$ = 25 MPa. (Bilotta & Russo, 2011)

Having a deeper look to the presented figure, it can be seen that the piles act as a barrier absorbing a great part of the displacements. As a consequence, far beyond the wall the settlement is very limited. That is not the case for the both Gaussian distribution and the settlement in greenfield conditions. In Figure 2.23, the results for the horizontal displacement is going to be presented and discussed.

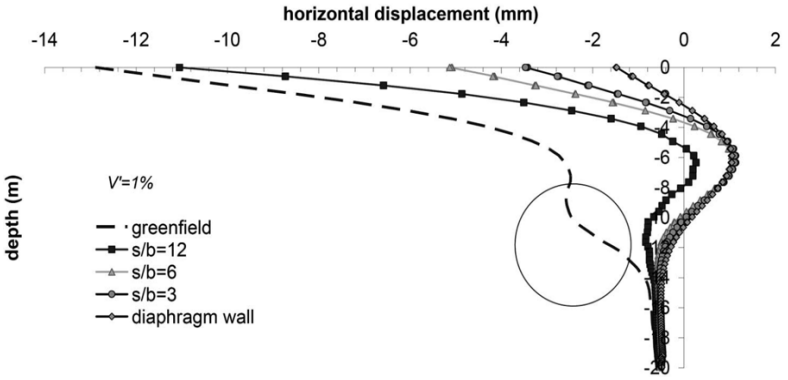

Figure 2. 23.- Horizontal displacement on a plane located 3 meters from the tunnel axis for different configurations of pile spacing. Length is L ≅ C+1.5D at V'=1% and $E_{50,ref}$ = 25 MPa. (Bilotta & Russo, 2011)

In the following section of the chapter a Benchmark test is presented in order to reproduce the same test carried out by Bilotta (2004) in which a set of physical models were developed and analysed in the centrifuge apparatus. The test is explained in section 2.6.2.4.

2.6.2.4. Experimental Benchmark

In order to validate the finite-element simulations, a set of centrifuge tests were carried out by Bilotta and Russo (2011). The idea was to develop the same test Bilotta did in 2004 in soft clays. The main difference between that test and the current one is that in 2004 the idea was to analyse the efficiency of a diaphragm wall while in that case the analysis was developed by a row of piles. (Bilotta & Russo, 2011)

The Benchmark test was divided into three groups of analysis. For each group of tests, a reference one in greenfield conditions was carried out in order to proceed with the comparison.

For this case, the previous centrifuge test was complemented in order to extent its results and analysis to a row of piles. Eight test divided in three groups were carried out. (Bilotta & Russo, 2011)

- *Group 1*: This test was carried out using an aluminium diaphragm wall embedded approximately in the tunnel axes. The length of the diaphragm wall was $\mathbf{L} \cong C + 0.5D$.
- *Group 2a*: this group has the same purpose of group 1 but with the difference that the diaphragm wall testes was longer than the one in group 1. The length of the diaphragm wall was $\mathbf{L} \cong C + 1.5D$.
- *Group 2b*: this group comprises the analysis of the row of piles considering different spacing lengths. The pile lengths were the same as in case 2a ($\mathbf{L} \cong C + 1.5D$).

In Table 2.7, the geometrical properties of the Benchmark tests are presented for the different groups of tests as well as the reference case (greenfield conditions). As in the Bioltta's centrifuge test in 2004, all the models have been tested at a rate of 160g. The **b** parameter represents both the diaphragm wall width or the pile diameter. All the structural elements were made of aluminium. (Bilotta & Russo, 2011)

GROUP	TEST	C/D	s/b	L: mm [m]	b: mm [m]	d: mm [m]
1	EB2	0.9		Greenfield		
	EB3		1	70 [11.2]	0.8 [0.136]	50 [8]
2a	EB6	1		Greenfield		
	EB13		1	120 [19.2]	0.8 [0.136]	50 [8]
2b	BB1	1	3.1	120 [19.2]	1.6 [0.316]	75 [12]
	BB2		6.2	120 [19.2]	1.6 [0.316]	75 [12]
	BB3		12.5	120 [19.2]	1.6 [0.316]	75 [12]
	BB4			Greenfield		

Table 2. 7.- Geometrical characteristics of the Benchmark Tests carried out in different groups of models. (Bilotta & Russo, 2011)

In section 2.6.2.5 of the chapter, the efficiency of the measure is analyzed. The same procedure for the diaphragm wall (Bilotta, 2004) is going to be applied.

2.6.2.5. Efficiency of the measure

As explained in the previous section, the efficiency of a structural element thought to reduce the settlements induced by tunnelling is calculated with expression 2.11:

$$\boldsymbol{\eta}[-] = \frac{[S_{ref} - S_{bp}]}{S_{ref}} \tag{2.11}$$

Where $\mathbf{S_{ref}}$ is the settlement trough in greenfield conditions and $\mathbf{S_{bp}}$ is the settlement of the ground surface immediately beyond the head of piles. (Bilotta & Russo, 2011)

In Figure 2.24, the results of the efficiency are provided by means of the envelopes. In the same figure, all the results are expressed for a constant volume loss of 1%. As an overall conclusion it can be observed that when the ratio 2/b is reduced, the efficiency increased dramatically. Also, it is observed that the results obtained by the finite-element simulations are higher than the experimental ones.

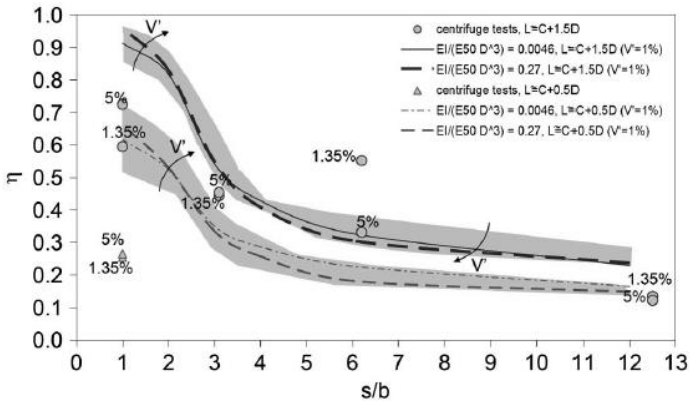

Figure 2. 24.- Efficiency at different values of spacing for the pile structural elements. As can be seen the shaded areas are the envelopes of the efficiency. (Bilotta & Russo, 2011)

As expected, the efficiency for the longer piles ($\mathbf{L} \cong C + 1.5D$), is higher and constant for low values of spacing (0.9 < s/b > 2). However, when the spacing over diameter ratio is increased the efficiency is being reduced achieving an average value of 0.3 for the value of s/b = 6.

Also as expected, analysing the results of shorter piles ($\mathbf{L} \cong C + 0.5D$), it can be seen by having a deeper look at Figure 2.24, that efficiency, appears to be lower than for the longer piles ($\mathbf{L} \cong C + 1.5D$). A fact to be highlighted is that in terms of results, the efficiency calculated for a short diaphragm wall can be compared with the results obtained for the long piles. (Bilotta & Russo, 2011)

The results between the finite-element simulations and the centrifuge tests appear to be consistent for a value of the ratio spacing over pile diameter (s/b) ≥ 3. When this ratio is decreased the differences between both results appear to be more obvious.

The last document that is going to be analysed in this chapter of the thesis belongs to a more recent case. In Barcelona the high speed tunnel beneath Sagrada Familia Basilica's foundations has been constructed.

2.6.3. Case study. Protection of World Heritage buildings in Barcelona. Row of piles constructed beside Sagrada Familia's foundations (Mallorca street) (Ledesma & Alonso, 2010)

2.6.3.1. Introduction

As part of the High Speed railway Project planned through to connect Madrid, Barcelona and the north of Catalonia with France a tunnel was designed through central Barcelona. The new tunnelling works were planned to connect both Sants and Sagrera stations. The district in which the tunnel is designed belongs to the 20th century characterized for its modernist Architecture.

The main drawback is that this type of constructions foundations is set to be shallow footings and load-bearing walls and this type of structures are so prone to suffer differential settlements which can induce heavy structural damage to the structure. Throughout the tunnel lining two of the most historical buildings of Barcelona were planned to be crossed by the tunnelling boring machine. These two buildings are the Sagrada Familia Basilica and the Casa Milà (La Pedrera). These two constructions are classified as World Heritage Buildings, so any damage during the tunnelling works would be catastrophic. Sagrada Familia Basilica was initiated during 1882 and it is still under construction. Although structural works nowadays are quite advanced it is not expected to be finished until 2026 in order to commemorate the century of Antoni Gaudí's death.

As expected, the construction of this tunnel and all the works planned generated high levels of controversy. The opposition argued that excavating that tunnel so close to the foundations of the Basilica imposed an unacceptable risk to the World Heritage Building.

2.6.3.2. Tunnel and soil characterization

The tunnel was designed to be approximately 5.6 km long from which 5 km were planned to be built by means of an earth pressure balance shield (EPB). The tunneling boring diameter is set to be 11.55 meters and the tunnel liner is made of reinforced concrete rings of 0.38-meter thickness. (Ledesma & Alonso, 2010)

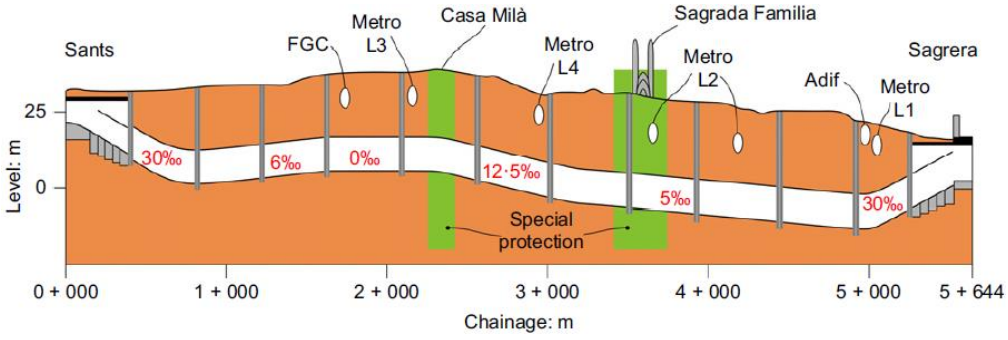

Figure 2. 25.- Longitudinal profile of the excavated tunnel. *(Ledesma & Alonso, 2010)*

The local water table is set to be between 15-16 meter Deep. It is important to notice that sandy layers below the tunnel had a piezometric level around 6 m higher than the local water table because of the presence of aquifers in the city. The average water pressure at the tunnel spring line was about 150 kPa.

Another matter of concern was that there was a groundwater flow through sandy units from hills to the sea. The problem is that the tunnel line is perpendicular to this flow and general preoccupation was generated about the possible negative effects that this groundwater flow could cause to the piezometric levels. Furthermore, the design of any diaphragm wall could worsen the negative effects. That is why a row of piles wall was designed instead of a unique diaphragm wall in order not to create a barrier to the flow. (Ledesma & Alonso, 2010)

The major preoccupation was the induced settlements due to tunnelling in surrounding structures and buildings, specially the Sagrada Familia Basilica which foundations are not prepared to receive high stresses and deformations. That is the reason why the tunnelling boring machine was fully monitored in order to have a total control of the settlements and ground movements. Another matter of monitoring the shield was because in case of sudden emergency, special measures could be adopted. (Ledesma & Alonso, 2010)

In Figure 2.26, the geotechnical profile of the site is presented showing a shaft approaching the Sagrada Familia Basilica.

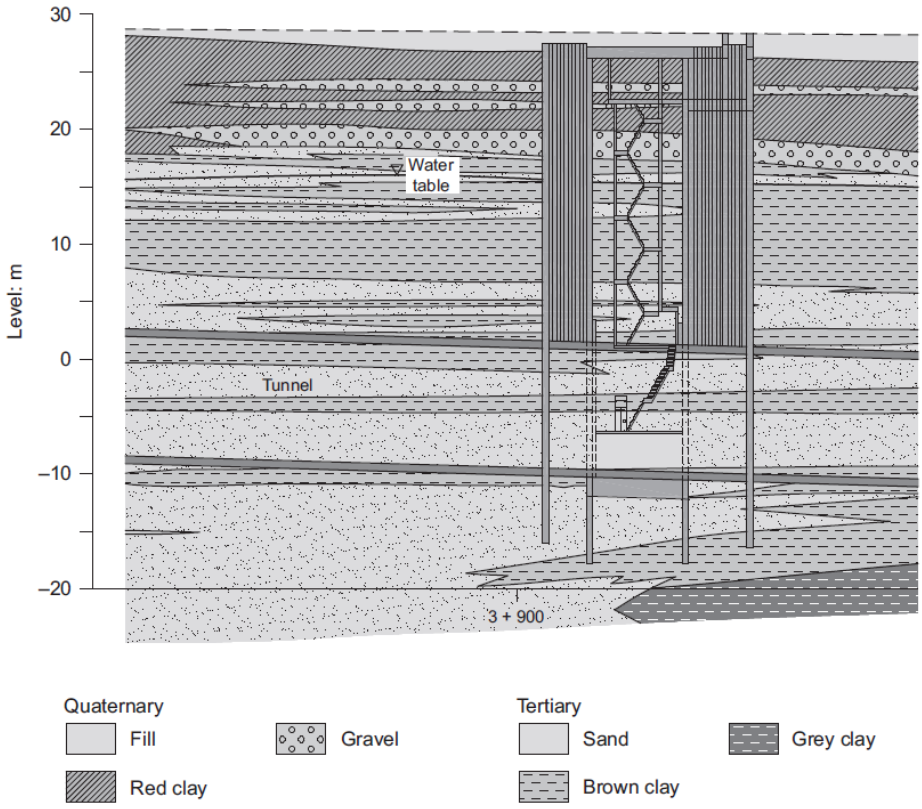

Figure 2. 26.- Geotechnical profile in the area of a vertical shaft built to proceed to a last inspection before approaching to Sagrada Familia Basilica. *(Ledesma & Alonso, 2010)*

2.6.3.3. Lateral wall to protect sensitive constructions

For both Sagrada Família Basilica and Casa Milà, a wall consisting in a row of piles was designed to protect sensitive constructions from the high speed tunnel excavation. Both lateral walls were designed under the same conditions, so the geometry of the wall planned for Sagrada Família, assumed to be the critical one, was taken as a reference and implemented in the same way for Casa Milà.

The piles were set to be 1.5 meter-diameter and 41-meter long. The separation between axis was about 2 meters giving a gap of 0.5 meters between consecutive piles. The total length of the row pile wall was 230 meters. In order to ensure higher levels of safety, after the cap beam was constructed, a concrete counterblock was designed near the pile heads. (Ledesma & Alonso, 2010)

Some finite-element simulations were carried put in order to ensure that the strcutrual solution proposed to mitigate ground movements was the most suitable one and it was found that depending on the constitutive model used to simulate the problem the results were quite different. An elasto-plastic Mohr-Coulomb was used at the design stage but for validation a Hardening Soil Model was adopted in order to increase the feasibility of the results. Finally, a Hardening Soil model with Small strains was adopted. (Ledesma & Alonso, 2010)

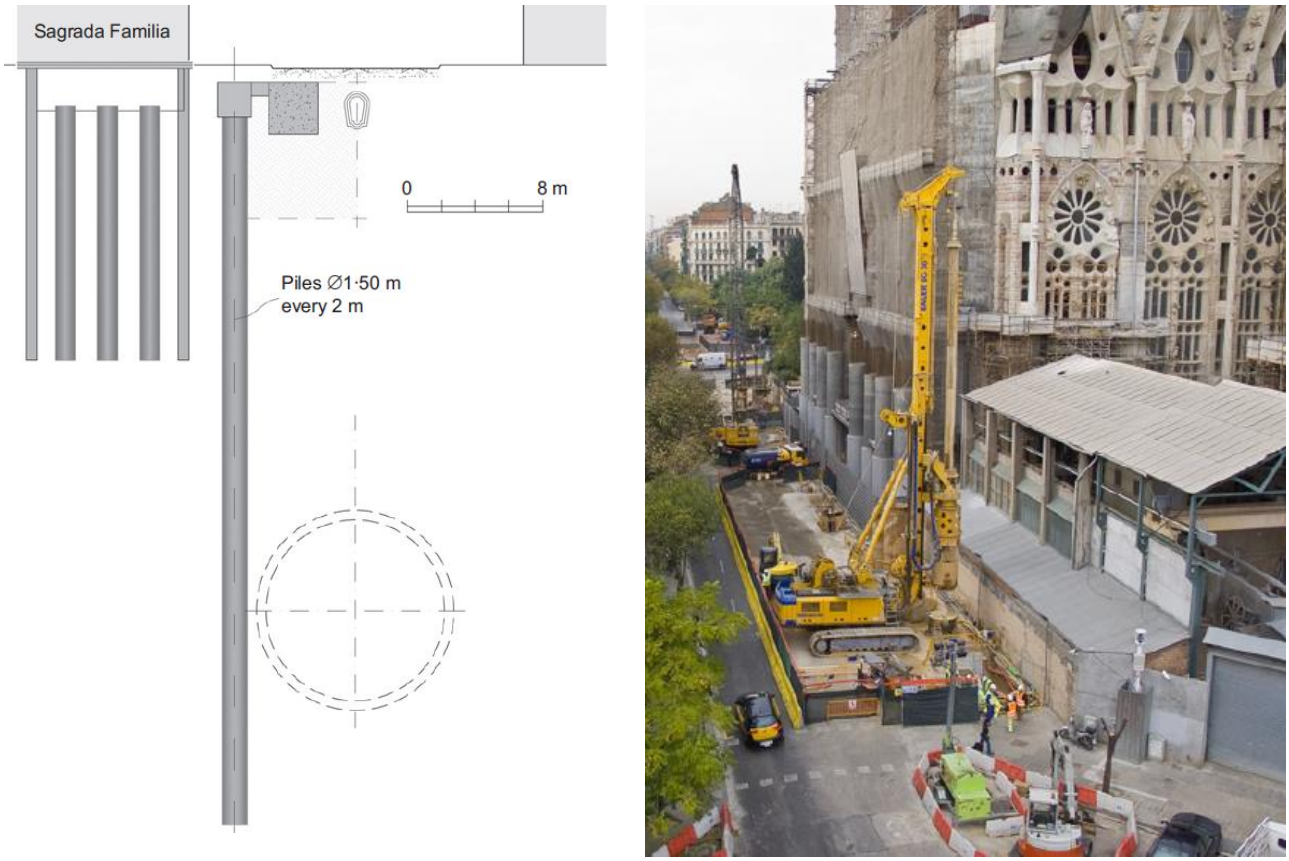

Figure 2. 27.- Cross-section of both the high-speed tunnel and the row of piles constructed beneath Sagrada Familia's foundations (left) and construction process of the pile wall (right) *(Ledesma & Alonso, 2010)*

In Figure 2.27, the geometry of the pile wall constructed to mitigate displacements induced by tunneling works is presented. As can be seen in the figure, the wall is very close to the tunnel axis. The wall was constructed prior to tunnel excavation and the results obtained of the monitoring process were very favorable concluding that the displacements were almost negligible.

It is important to notice that the success was thankful basically due to the heavy instrumentation that was installed in both the shield machine and the Sagrada Familia that was sending results in real time and also to the intense calculation process both analytical and finite-element simulations that end up with that structural solution that performed really well.

CHAPTER 3

Analysis of vertical displacements

FINAL MASTER THESIS

3.1. Introduction

As presented in previous sections of this Final Master Thesis, designing a tunnel beneath urban areas may be a challenging task if ground movements are excessive and affect buildings located in the tunnel influence area. As presented in the State of the Art, some previous work has been carried out in order to understand, predict and simulate underground settlements while a tunnelling boring machine is excavating a tunnel.

This could be potentially damaging in the case of structures supported on shallow foundations or rafts such as old temples, or World Heritage buildings such as Sagrada Familia Basilica. In these cases, the structural solution of a diaphragm walls or a row of piles has performed well. The diaphragm wall or row of piles, is build prior tunnel excavation in order to absorb a great percentage of the ground settlements. (Bilotta, 2008)

This solution has been successfully applied in real cases but is still far from routine. It is important to notice that most of the main geotechnical reports studied, analyse the effect of the tunnelling works in deep foundations such as pile foundations, which is not the aim of this Thesis. As stated in the Introduction, the aim is to study the effect of a lateral wall in the tunnelling displacement troughs either vertical or lateral. Despite that, some other contributions have been analysed in the State of the Art in which some structural solutions in order to mitigate ground displacements induced by tunnelling are proposed.

In the following sections of this chapter, the analysis of the vertical pattern of displacements is going to be presented by means of solving the 2D vertical Melan problem. The analytical procedure will be provided considering in one hand the geotechnical term and in the other hand the structural term as it will be deeply explained.

In this chapter, the vertical displacements field will be studied by analysing the problem of the tunnel-wall interaction by means of the Melan 2D formulation. Later on, in chapter 5, some numerical Plaxis models will be run in order to validate the analytical results obtained from analytical calculations with different geometries of the pile wall.

3.2. The tunnel-wall interaction problem. Vertical displacements due to vertical loads

It is obvious that the tunnel-wall interaction problem can easily be solved by means of Finite Element (FE) calculations but that applying FE in order to solve the problem is not the primary goal of this thesis. Although Finite Element methods are widely applied in order to solve complex geotechnical problems, analytical procedures are very useful in terms of understanding the mechanisms involved in the interaction and the overall problem itself.

In Figure 3.1, the tunnel-wall interaction problem it is presented. The wall is constructed at a distance “d” from the tunnel axis.

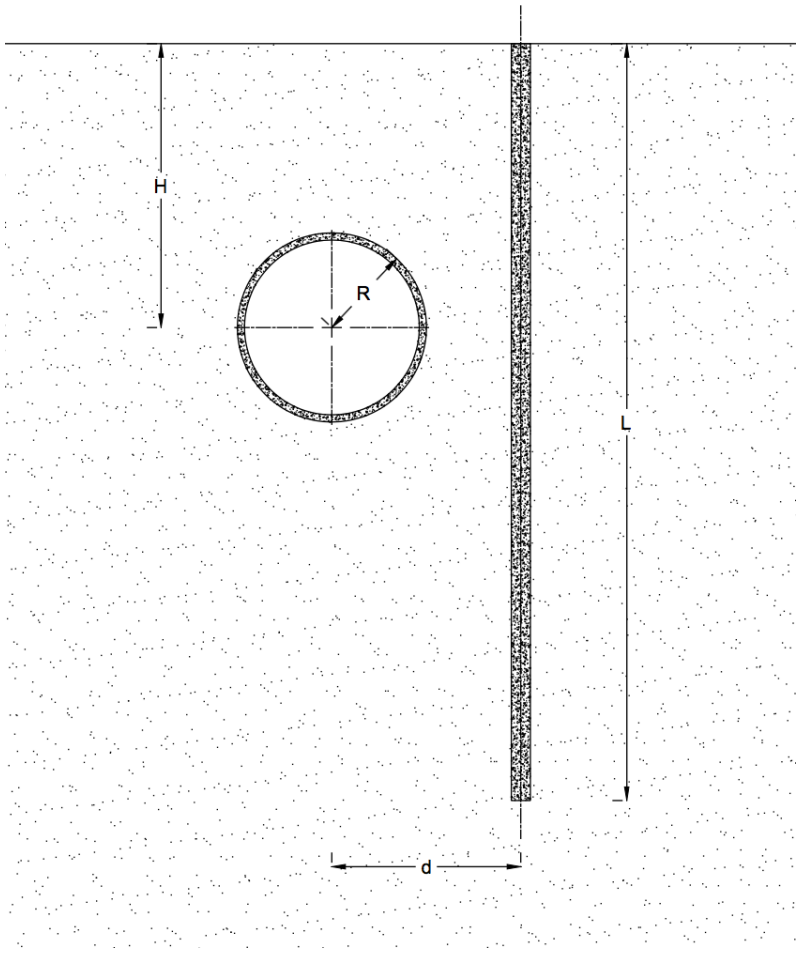

Figure 3. 1.- Basic geometry of the tunnel-wall interaction problem

3.2.1. Tunnel excavation analysis

As stated in previous chapters of this thesis, in past years' different approaches of ground settlements analysis due tot tunnel excavation have been made. Those approaches can be classified into three groups, namely, empirical methods, numerical methods and finite-element methods which are widely used in design stage of underground works. It is important to know when to apply on of these methods presented. This depends on the complexity of the problem and the need of accuracy in the results. (Loganathan & Poulos, 1998)

Ground deformations are usually described by means of empirical formulations based mainly in field observations such as the normal (Gaussian) distribution curve presented by Peck (1969). Peck's formulation has no analytic basis, but the reason why it is widely used to analyse settlement profiles is its shape.

The shape of the Gaussian distribution, is similar to the commonly observed settlement troughs and also the ease to define the curve by few parameters makes that each different case can be defined and analysed without no complications.

It has been proved, that this formulation performed well in normally consolidated clays but tend to uncertainty in both over consolidated clays and granular soils.

It is important to notice that each methodology has also its limitations when it is used. In the case of this empirical formulations there are two main limitations that one needs to be aware of them. Firstly, with Loganathan & Poulos (1998) formulation, one cannot analyse the effect of both different ground conditions and construction techniques. The input parameters of this formulae are the tunnel radius, the tunnel spring line, and both the horizontal and vertical coordinate of the studied point. There is no difference between different types of soil. The second limitation is that when concerning lateral deformations, the information provided by this methodology is quite limited. This limitation is also applicable to subsurface settlements. In order to solve that, a better method of the ones proposed above should be applied in order to analyse the effect of ground deformations due to tunnelling works. (Loganathan & Poulos, 1998)

In the past few years, some attempts to improve the formulations presented have been carried out. One example of this is Sagastea (1987) who introduced the effect of an initially isotropic and homogeneous incompressible soil due to near-surface ground loss. Verruijt and Booker (1996) presented a new formulation considering a tunnel in a homogeneous elastic half-space using a methodology proposed by Sagastea (1987) for the case of ground loss. The advantage of this solution when talking about the ground loss term is that Verruijt and Booker's (1996) solution was a generalisation of Sagastea's one, and arbitrary values of Poisson's coefficient can be introduced in the equations. Furthermore, this formula includes the effect of ovalization of the tunnel opening.

As stated before, each formulation has its pros and cons and for the case of Verruijt and Booker (1996) formulation in the case of vertical displacements troughs it has been found that they are wider than field measurements while for the case of lateral movements are in general, larger than the ones observed in experience observations. (Verruijt, 2014)

The settlement troughs are characterized by the term defined as *"ground loss".* This term is defined as a percentage of the theoretical excavated tunnel volume. Mathematically, this term will be presented below and is expressed as a percentage of the ratio of the surface settlement trough volume and the tunnel volume per unit length. (Loganathan & Poulos, 1998)

Firstly, it is important to notice that from now on, only settlements caused by tunnelling boring machines are going to be considered when analysing ground settlements from tunnel excavation. Settlements caused by tunnelling boring machines are going to be calculated in this section of the chapter. In order to do so, first of all undrained conditions are going to be assumed which means that the volume of the material remains constant leading to a value of Poisson's coefficient of 0.5. Later on in chapter 5 when talking about the validation of the analytical calculations with Plaxis software, some notes about the Poisson coefficient are going to be considered.

In order to carry out an analytical estimation of ground movements induced by tunnelling works, an approximate formulae proposed by Loganathan & Poulos (1998) will be applied. This formulation is chosen because provides reasonable displacement troughs when comparing with current field measurements. For the case of ν=0.5, vertical displacements due to tunnel excavation is obtained by applying the Equation 3.1:

$$\mathbf{u_z}[\mathbf{m}] = R^2\left[-\frac{z-H}{x^2+(z-H)^2}+\frac{z+H}{x^2+(z+H)^2}-\frac{2z[x^2-(z+H)^2]}{[x^2+(z+H)^2]^2}\right]\varepsilon \tag{3.1}$$

Where $\mathbf{u_z}(\mathbf{x},\mathbf{z})$ is the vertical displacement, considered positive downwards, **R** is the tunnel radius, **H** is the depth of the spring line and $\boldsymbol{\varepsilon}$ is the modified equivalent ground loss parameter defined as follows:

$$\boldsymbol{\varepsilon}[-] = \varepsilon_0 \exp\left[-\left(\frac{1{,}38x^2}{(H+R)^2}+\frac{0{,}69z^2}{H^2}\right)\right] \tag{3.2}$$

Where $\boldsymbol{\varepsilon_0}$ is the equivalent average ground loss (i.e. the area of the surface settlement trough divided by the tunnel area). Equation 3.2 takes into account the oval-happed ground deformation pattern around the tunnel section and provides a good estimation of ground movements. (Loganathan & Poulos, 1998)

3.2.2. Lateral wall

In this section of chapter three, the main hypothesis used to solve the Melan 2D vertical deformation system of equations are going to be presented as well as all the geometries involved in the calculation process. Finally, the results of the analysis are going to be presented.

The wall effect can be taken into account by analysing the forces acting on its surface. In Figure 3.2, a geometry of the interaction forces is presented. In following sections of this chapter this geometry is going to be updated considering different geometries used for the analysis. It has been analysed piles of length 2R, 4R, 6R and 8R in order to obtain realistic conclusions at the end of the analysis. (Ledesma & Alonso, 2010)

In structural terms it can be assured that a wall does not have any initial load but, due to displacements induced by tunnelling and skin friction, it develops internal forces and bending moments. Due to its stiffness displacements generated while tunnelling excavation works are being carried out, are dramatically reduced beyond the wall, hence the effect to any neighbouring structure is highly reduced.

The goal when solving the Melan 2D system of equations is to estimate the settlement trough when a stiff wall is constructed at a distance d from the tunnel axis using the adding principle of displacements. Soil displacements are consequence of the movements induced by the earth pressure balance on one hand and the forces induced by the wall in the other hand.

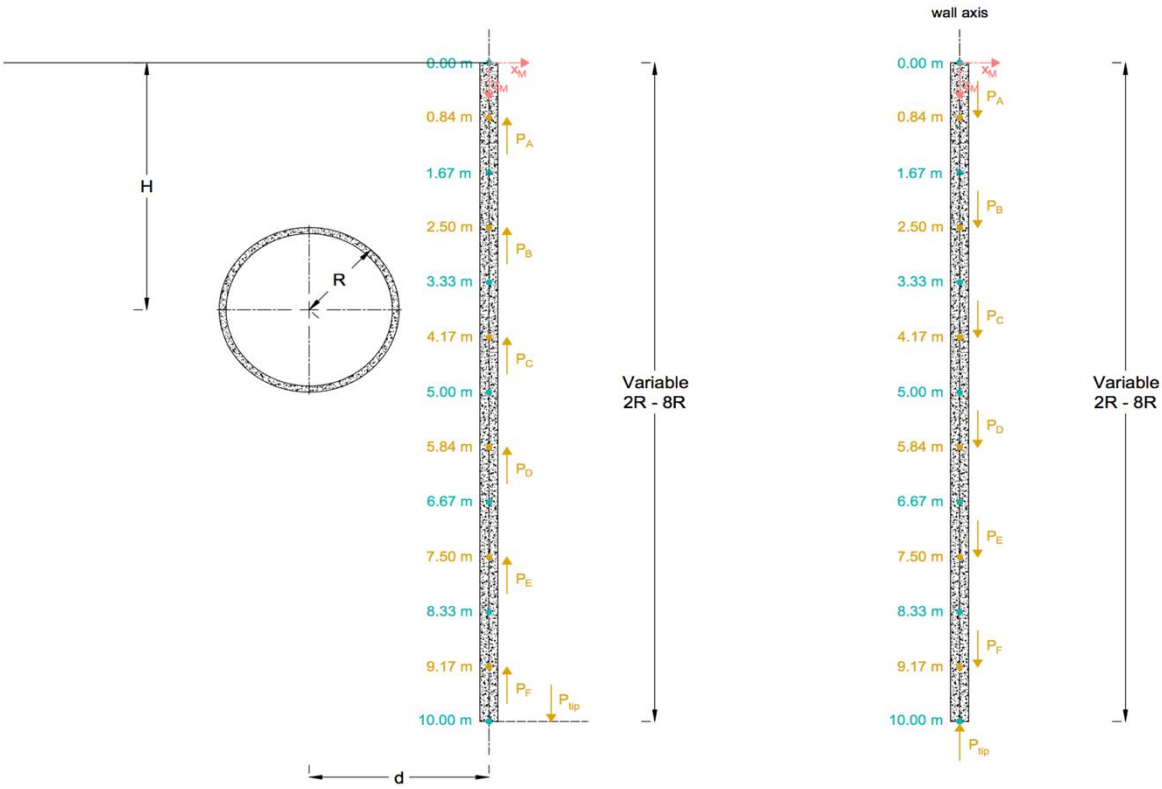

Figure 3. 2.- Basic geometry of the problem. General scheme for the interaction forces between soil and lateral wall

The problem to be solved is divided into two minor problems. In one hand, the geotechnical term is considered, which concerns the solution of the settlements caused by the tunnel excavation works and the displacements generated by the interaction forces between soil and the lateral wall. In the other hand, what is called the structural term is solved. The structural term consists mainly in the solution of the wall itself as a structural element of a cantilever beam considering the axial force passing through the discretization points of the pile wall.

Having a deeper look to Figure 3.2, $\mathbf{P_A}$ to $\mathbf{P_F}$ and $\mathbf{P_{TIP}}$ represent the action-reaction forces known also as soil-wall interaction forces.

The goal of this chapter as stated before is to solve the problem of a load applied to an inner point in the 2D elastic half-space. This procedure will allow this forces to be estimated. As presented above, this problem is widely known as Melan 2D problem which consists basically in solving the settlements due to tunnel excavation and interaction forces in one hand and the vertical deformations of the pile as structure in the other hand. Later on, the condition that both displacements must be equal needs to be imposed in order to estimate these interaction forces. Melan (1932) was the first one to provide a solution in terms of stresses. (Ledesma & Alonso, 2010)

For the case concerning this thesis the formulation used to solve the problem is the one presented in following points of this section. Firstly, the geotechnical term is presented.

For the geotechnical term, the displacements due to tunnel excavation have been presented in equation 3.1 and 3.2. The basic geometry of the Melan 2D problem with its coordinate origin is presented in the Figure 3.3.

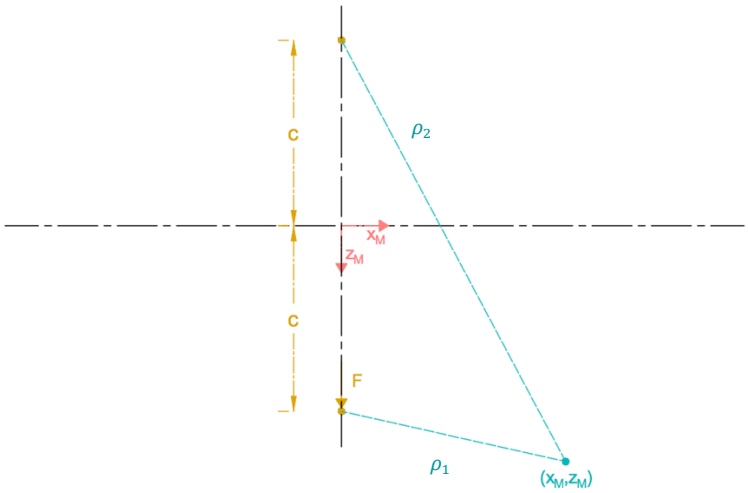

Figure 3. 3.- Geometry of the 2D Melan (vertical) problem

Equation 3.3, represents the vertical displacement, applying the Melan formulation, at point $[\mathbf{x_M}, \mathbf{z_M}]$, known as Melan coordinates as can be seen in Figure 3.3. These settlement is generated by applying a force per unit length assuming undrained conditions.

As stated previously, vertical displacements of the ground at the studied points due to a force per unit length, F, are presented in Equation 3.3. Undrained conditions mean that the volume of material remains constant, that is the reason why a Poisson coefficient of 0.5 is adopted. (Ledesma & Alonso, 2010)

$$\mathbf{u_z}[\mathbf{m}] = \frac{3F}{2\pi E_s}\left[\ln\frac{1}{\rho_2} - \frac{1}{2}\ln\frac{\rho_1}{\rho_2} + \frac{x_M^2}{2}\left(\frac{1}{\rho_1^2} - \frac{1}{\rho_2^2}\right) + \frac{(c+z_M)^2}{\rho_2^2} + cz_M\left(\frac{2(c+z_M)^2}{\rho_2^4} - \frac{1}{\rho_2^2}\right)\right] + u_o \qquad (3.3)$$

Where **c** is defined as the vertical distance between ground surface and the force application point, $[\mathbf{x_M}, \mathbf{z_M}]$ are defined as the Melan coordinates, $\mathbf{E_s}$ is the Soil's Young Modulus, $\boldsymbol{\rho_1}$ is defined as the distance between the Melan coordinates known also as the studied point and the image of the force application point and finally, $\boldsymbol{\rho_1}$ is defined as the distance between the Melan coordinates or studied point and the force application point.

It is important to highlight the term at the end of equation 3.3, $\mathbf{u_o}$. It has been noticed the presence of singularities in the equation presented above. The easiest way to deal with them is to impose that, a certain distance from the load the vertical displacement is zero. It has been considered for the current document that at 40 m far from the load application point the displacement is zero. Solving the equation imposing that condition, allows the constant u_o to be obtained. (Ledesma & Alonso, 2010)

For the case concerning this chapter, the condition of $\mathbf{x_M} = \mathbf{w} = 40$ m will be enough to solve the problem.

The formulation presented in equation 3.3 needs to be adapted to the geometrical features that are for interest in the case concerning this geotechnical problem. The goal is to calculate the vertical ground displacements at the wall axis, where the interaction forces are applied. Hence, the Melan horizontal coordinate is automatically assumed as $\mathbf{x_M = 0}$ (wall axis). This conclusion is obtained analysing Figure 3.3 in which the coordinate axis is presented. (Ledesma & Alonso, 2010)

Introducing these changes to equation 3.3, the displacements due to the interaction forces for the different studied points at the lateral wall axis becomes as follows:

$$\mathbf{u_z[m]} = \frac{3F}{2\pi E_s}\left[\ln\frac{\sqrt{c^2+w^2}}{c+z_M} - \frac{1}{2}\ln\frac{|z_M-c|}{(z_M+c)} + 1 - \frac{c^2}{c^2+w^2} + cz_M\left(\frac{1}{(c+z_M)^2}\right)\right] \quad (3.4)$$

Equation 3.4 is useful to obtain the ground deformations at a certain depth in order to solve the Melan vertical problem and build the system of equations but, it is not useful to calculate the settlement troughs at surface which is from particular interest. In order to calculate ground deformations at ground surface, $\mathbf{z_M = 0}$, Equation 3.5 needs to be applied:

$$\mathbf{u_z[m]} = \frac{3F}{2\pi E_s}\left(\ln\frac{\sqrt{c^2+w^2}}{\sqrt{c^2+x_M{}^2}} + \frac{c^2}{c^2+x_M{}^2} - \frac{c^2}{c^2+w^2}\right) \quad (3.5)$$

Applying Equation 3.5 for each interaction force obtained by solving the Melan 2D system of equations and applying the superposition principle of displacements for each point of the settlement trough, one can obtain the final vertical displacements at ground surface taking into account the overall effect of all forces. In the following section of this chapter the compatibility condition in order to solve well the system is presented.

3.2.3. Compatibility condition

These forces, ($\mathbf{P_i}$), can be obtained by imposing compatibility condition of vertical displacements at all studied points (see Figure 3.2). As stated a few paragraphs above, the geotechnical term can be calculated by combining in one hand, the Loganathan & Poulos (1998) equation which obtains the soil deformation when a tunnel is excavated at a certain depth and, in the other hand, the solution for displacements induced by inner forces $\mathbf{P_j}$ known as Melan 2D. (Ledesma & Alonso, 2010)

The structural term or wall deflection can be obtained by calculating the axial deformation. This calculation can be carried out from the axial forces acting on it. In order to proceed with the axial deformation, the wall is divided into 6 segments (n=6) as it can be seen in all geometries presented throughout the chapter. Each segment j is loaded by a force $\mathbf{P_j}$ acting at the segment midpoint ($\mathbf{P_A}, \mathbf{P_B}, \mathbf{P_C}, \mathbf{P_D}, \mathbf{P_E}$, and $\mathbf{P_F}$). Hence, the vertical deformation of a point i in the wall can be computes by applying Equation 3.5:

$$(\mathbf{u_z})_i[\mathbf{m}] = u_n + \sum_{j=i+1}^{j=n} \left[\frac{N_j}{E_w A_w}\frac{L}{n}\right] \tag{3.5}$$

It is important to notice that $\mathbf{u_6}$ is the displacement at the wall tip computed by means of the Melan equations, $\mathbf{E_w}$ is the wall's Young Modulus, $\mathbf{A_w}$ is the cross-section of the lateral wall, **n** is the number of discretization points in which the pile is divided, **L** is the total length of the pile wall and finally, $\mathbf{P_j}$ is the axial force in a particular segment *j* (force per unit length). Vertical equilibrium must be satisfied by means of verifying equation 3.6. It is trivial to understand that as a basic structural concept. (Ledesma & Alonso, 2010)

$$P_{tip} = \sum P_j \tag{3.6}$$

Finally, the compatibility condition applied to point 0 to point n – 1 is governed by the mathematical expression presented in Equation 3.7:

$$\mathbf{u_{z\ tunnel}} + \sum \mathbf{u_{z\ due\ to\ P_j}} = \mathbf{u_{z\ structural\ wall}} \tag{3.7}$$

Equation 3.7 is applied to point 0 to point n – 1. The left side term, which is composed for the settlements due to tunnel excavation calculated applying Loganathan & Poulos equation (1998) and the solution for displacements induced by inner forces $\mathbf{P_j}$ at an inner point of a half-space, conform what is called the Geotechnical term. The Loganathan & Poulos expression is defined at equation 3.1 and 3.2 while the settlements due to a force applied to an inner point of a half-space formulation is provided at equations 3.3 to 3.5 both included.

The right side term configures what is called the structural term in which the axial deformation is calculated by means of considering the pile wall as a cantilever beam with a generic point load applied on an arbitrary coordinate of its surface. In order to do that is applied what is called the superposition principle of displacements consisting in calculating the axial deformation caused for each force in all the the points in which the pile is discretized and then adding the effects of each force at each point. For instance, the effect of force $\mathbf{P_j}$ is computed for each point and then the effects are added. The formulation needed to calculate the axial deformation is provided in equations 3.5. In an overall view, equation 3.7, applied to each studied point, provides a linear system of **n** equations with **n** unknowns which is easily solved by means of excel, mat lab or any other mathematical tool. Finally, once the interaction forces are obtained, the displacements produced by these forces at ground surface by means of equation 3.5 are calculated and superposition principle of displacement is applied. In a final stage of the calculation process, those displacements are added onto the movements derived from the Loganathan and Poulos (1998) solution for the case of greenfield conditions at ground surface to obtain the final soil displacements troughs. In Figures 3.4 to 3.6, the different geometries involving different pile lengths are presented.

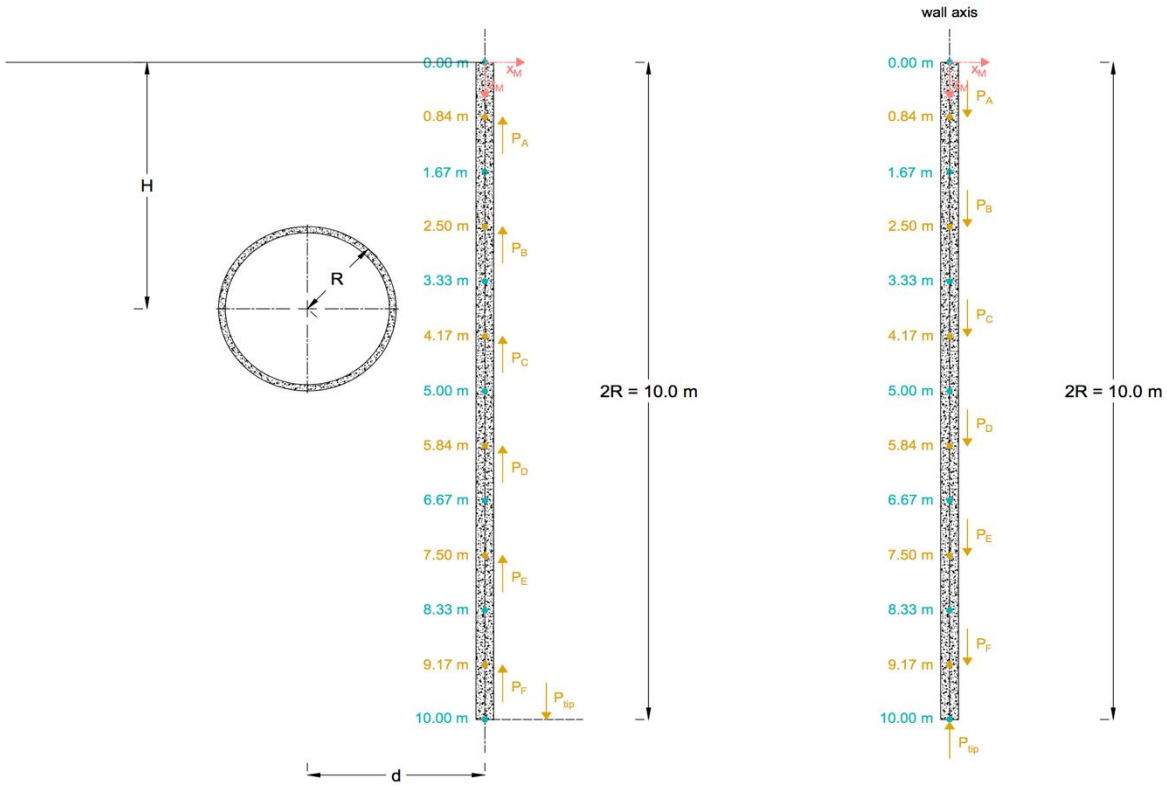

Figure 3. 4.- Basic geometry of the interaction forces for the Melan 2D vertical problem for the case of a 10-meter length lateral wall

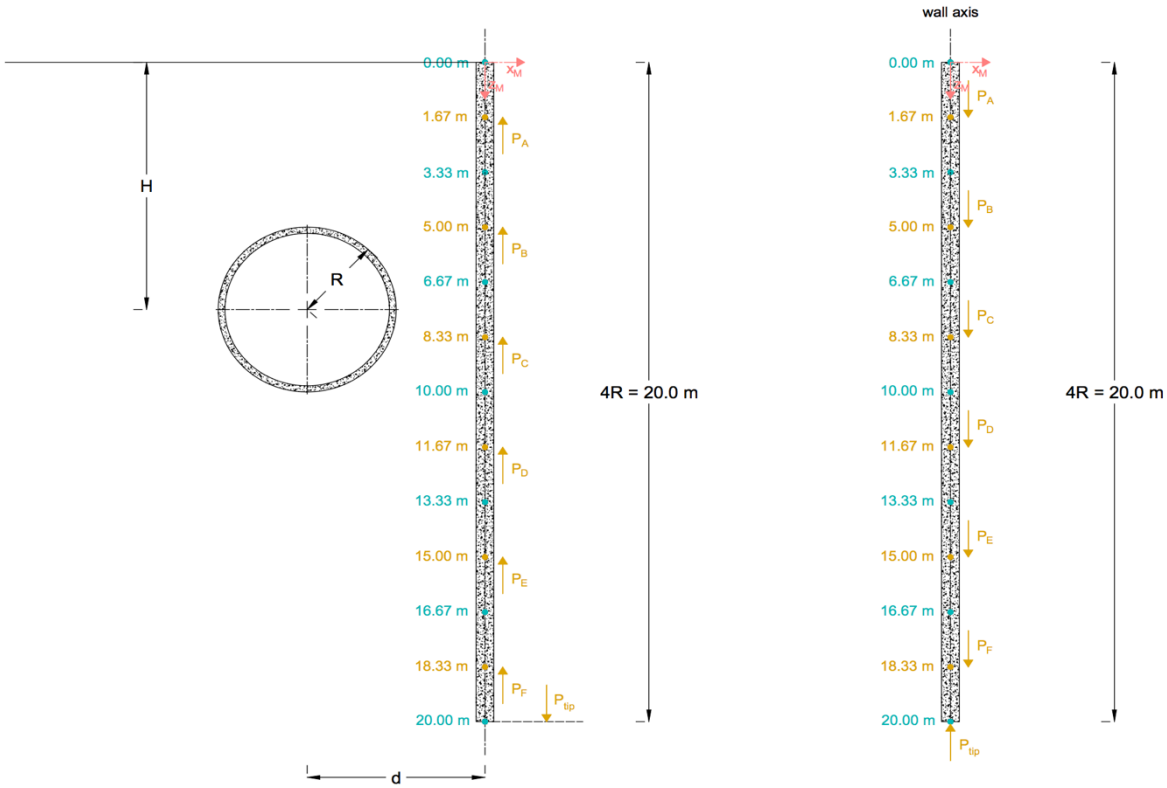

Figure 3. 5.- Basic geometry of the interaction forces for the Melan 2D vertical problem for the case of a 20-meter length lateral wall

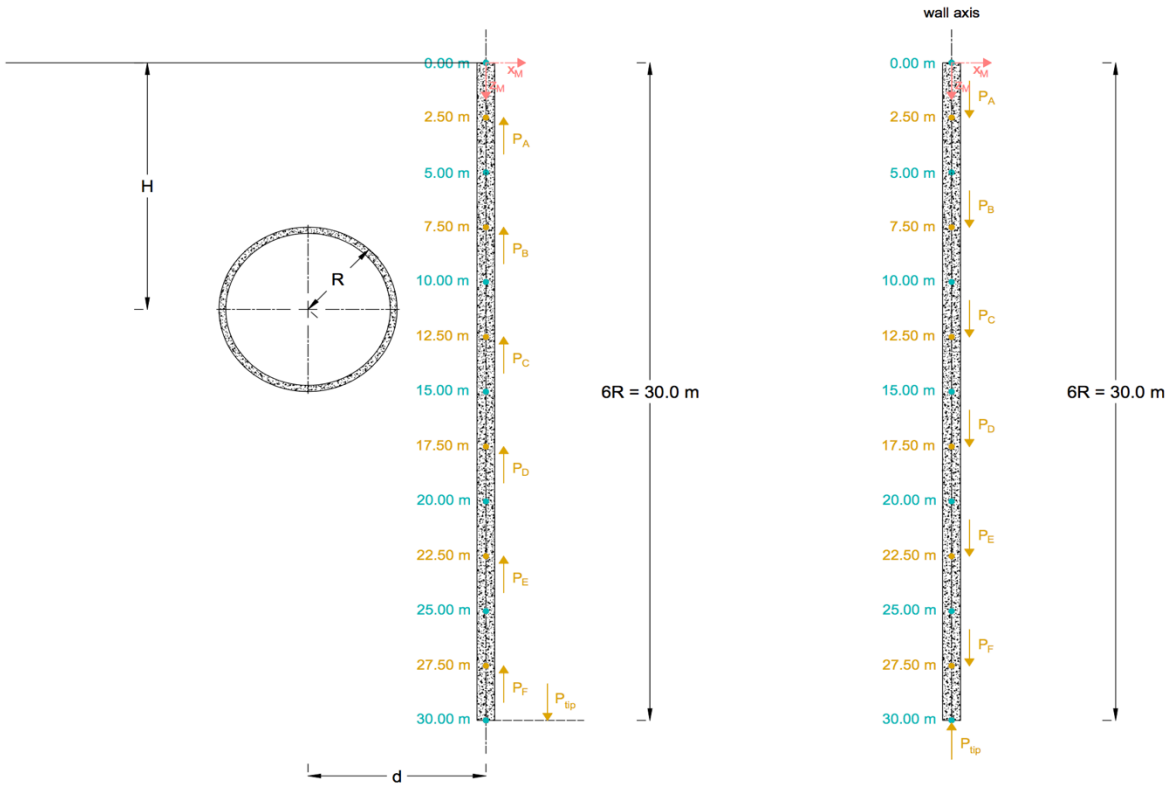

Figure 3. 6.- Basic geometry of the interaction forces for the Melan 2D vertical problem for the case of a 30-meter length lateral wall

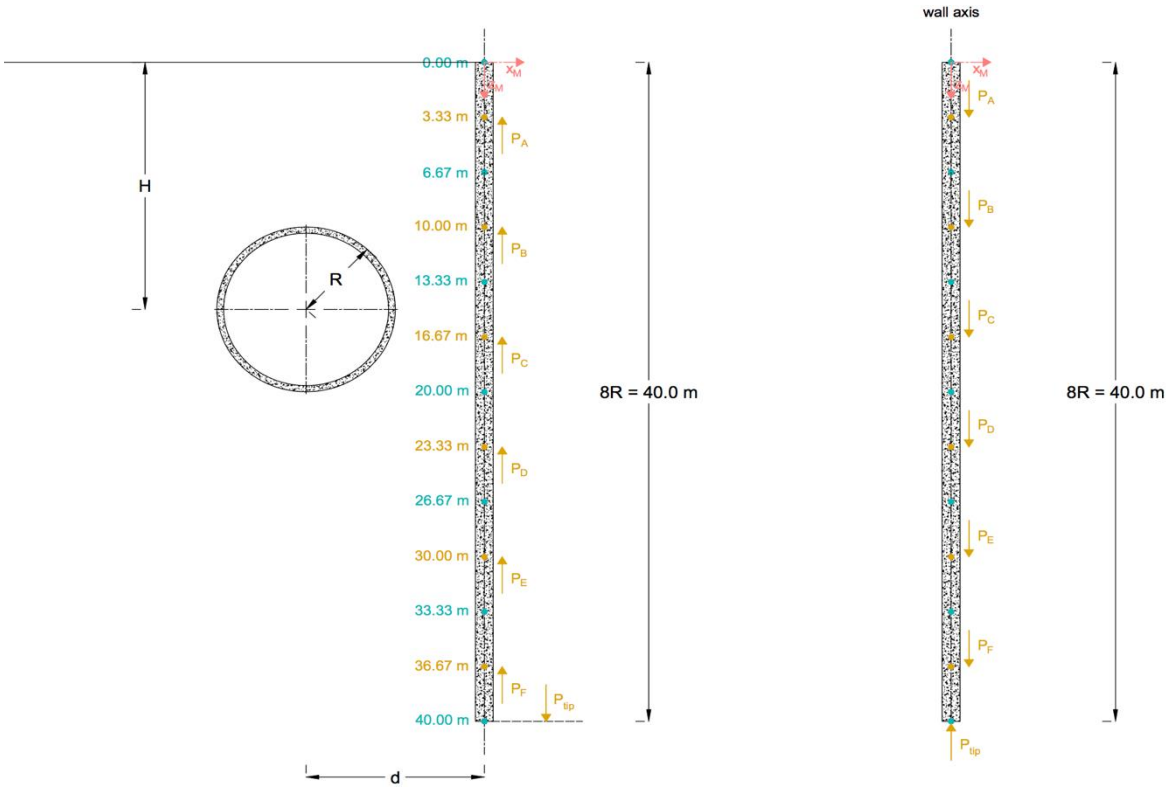

Figure 3. 7.- Basic geometry of the interaction forces for the Melan 2D vertical problem for the case of a 40-meter length lateral wall

3.2.4. Analysis and results

In this section of the chapter, the results obtained from the analysis are going to be presented. As stated in some previous paragraphs, the goal is to determine the interaction forces between the soil and the lateral and analyse its influence in the vertical displacement field.

In the case concerning this thesis, the procedure to solve the system of equation has been the following; once the coefficient matrix of the system is built, the excel solver tool is applied in order to obtain the final results of the interaction forces. It is known as coefficient matrix of the system, the one in which each column of it contains the coefficients corresponding to a variable of the system of equations and in its last column, contains the coefficients of the right side of the equations.

The goal of the analysis once having solved the system and the numerical values of the interaction forces, is to determine the influence of the lateral wall on the vertical displacements. In order to do that, firstly, a diagram representation of the "greenfield" conditions is going to be provided and after that, the influence of the lateral wall is going to be added in order to see the effects. It is important to highlight that "greenfield" conditions correspond to those in which no lateral structure is built, hence, to the vertical displacements due to tunnel excavation.

It is important also to quantify the efficiency of the wall. As stated in Chapter 2 of this thesis "State of the Art", the efficiency of a structural element designed to reduce the settlements induced by tunnelling is calculated with the mathematical expression presented below. This expression is a dimensionless ratio that quantifies the potential of a vertical diaphragm wall to reduce ground movements. (Bilotta, 2008)

$$\boldsymbol{\eta}[-] = \frac{[S_{ref} - S_{bw}]}{S_{ref}} \tag{3.8}$$

Where $\mathbf{S_{ref}}$ is defined as the settlement trough in greenfield conditions and $\mathbf{S_{bw}}$ is the settlement of the ground surface immediately beyond the diaphragm wall. When $\boldsymbol{\eta}$ is equal to 1 it means that the solution of a diaphragm wall is totally effective whereas when $\boldsymbol{\eta}$ present a value of 0, means that the wall has no positive effect when reducing the settlement trough. The analysis of the efficiency of the wall will be carried out in chapter 6.

It can be seen having a deeper analysis to Figures 3.8 to 3.13, the vertical displacements are highly influenced by the wall tip. When concerning a short wall (tip above the tunnel invert), both its tip and top will suffer from excessive ground movements which will not be the case of a wall with its tip located below the tunnel invert. Hence, when the length of the wall is increased, that helps to reduce vertical displacements and proves that the solution of a lateral wall to prevent from ground movements is effective.

In Figures 3.8 to 3.13, the results from the effect of the wall length in the displacements, are presented.

3.2.4.1. Greenfield case

In Figure 3.8, the vertical displacement trough in greenfield conditions is presented.

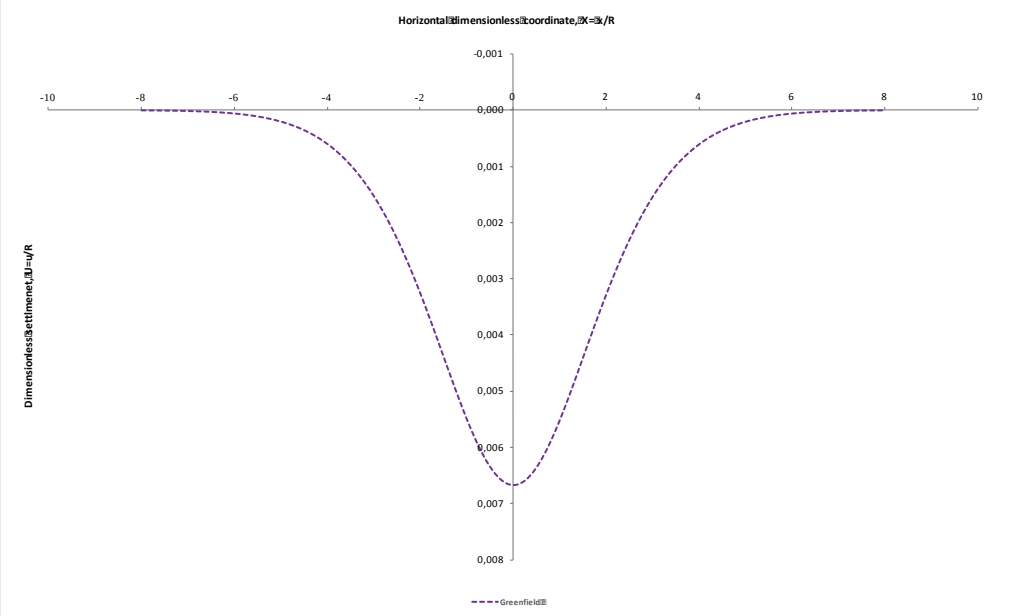

Figure 3. 8.- Vertical displacement trough due to tunnel excavation at ground surface. Greenfield conditions

3.2.4.2. Greenfield case vs. lateral wall of length 2R = 10 meters

In Figure 3.9, the vertical displacement trough due to a 10-meter length lateral wall is compared with the greenfield case.

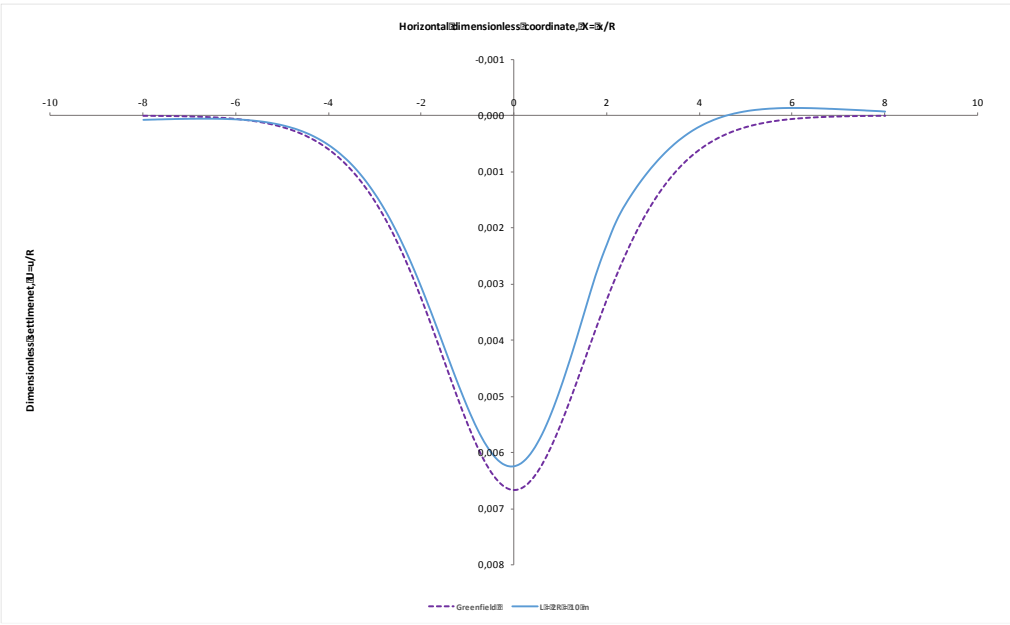

Figure 3. 9.- Effect of wall vertical length on the vertical displacements. 10-meter length lateral wall

3.2.4.3. Greenfield case vs. lateral wall of length 4R = 20 meters

The vertical displacement trough due to a 20-meter length lateral wall is compared with the greenfield case.

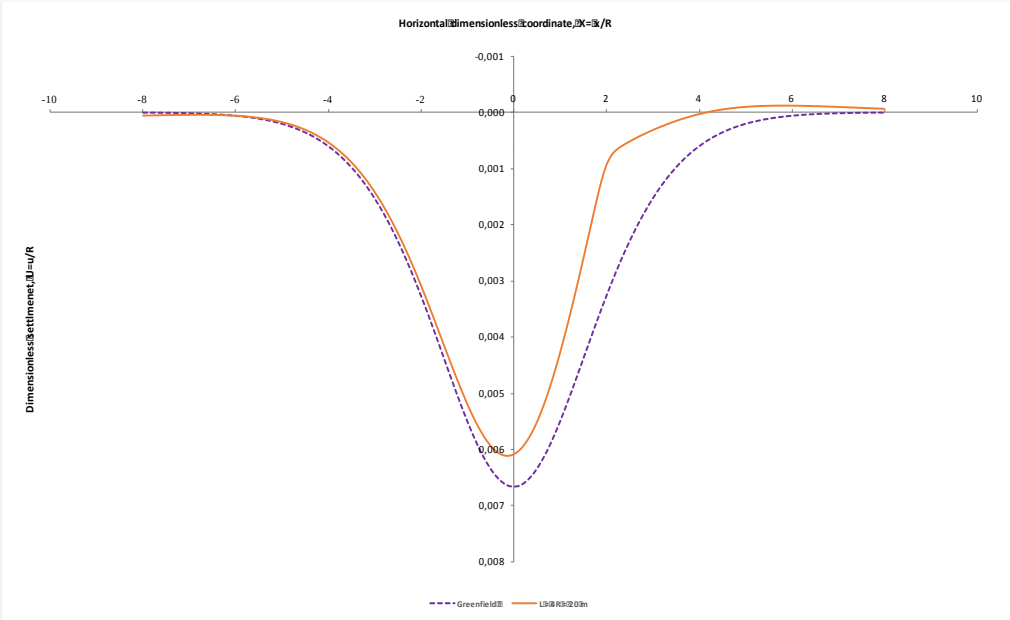

Figure 3. 10.- Effect of wall vertical length on the vertical displacements. 20-meter length lateral wall

3.2.4.4. Greenfield case vs. lateral wall of length 6R = 30 meters

In Figure 3.11, the vertical displacement trough due to a 30-meter length lateral wall is compared with the greenfield case.

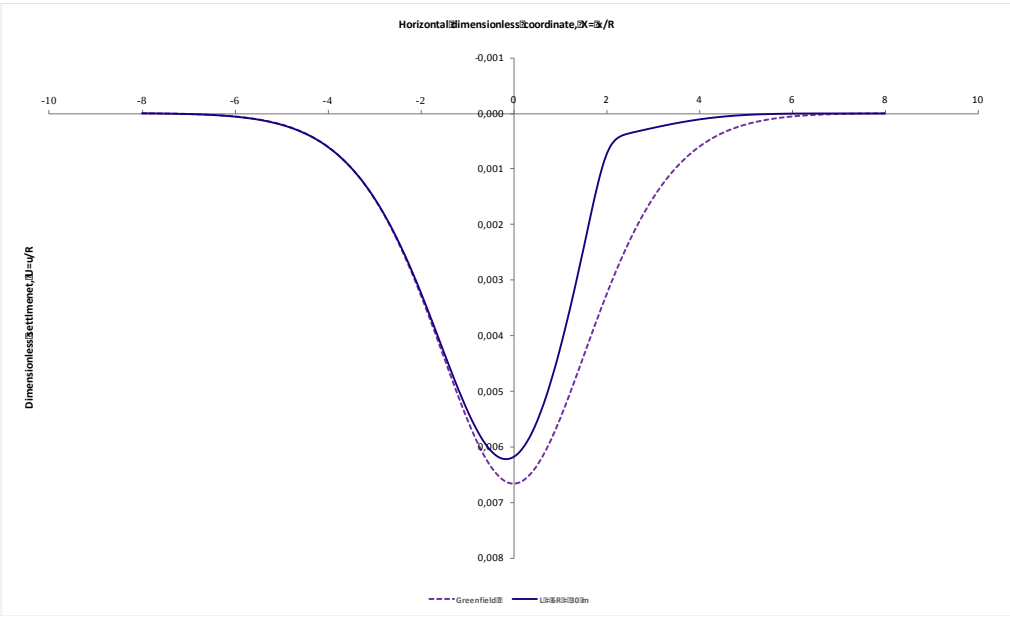

Figure 3. 11.- Effect of wall vertical length on the vertical displacements. 30-meter length lateral wall

3.2.4.5. Greenfield case vs. lateral wall of length 8R = 40 meters

The vertical displacement trough due to a 40-meter length lateral wall is compared with the greenfield case.

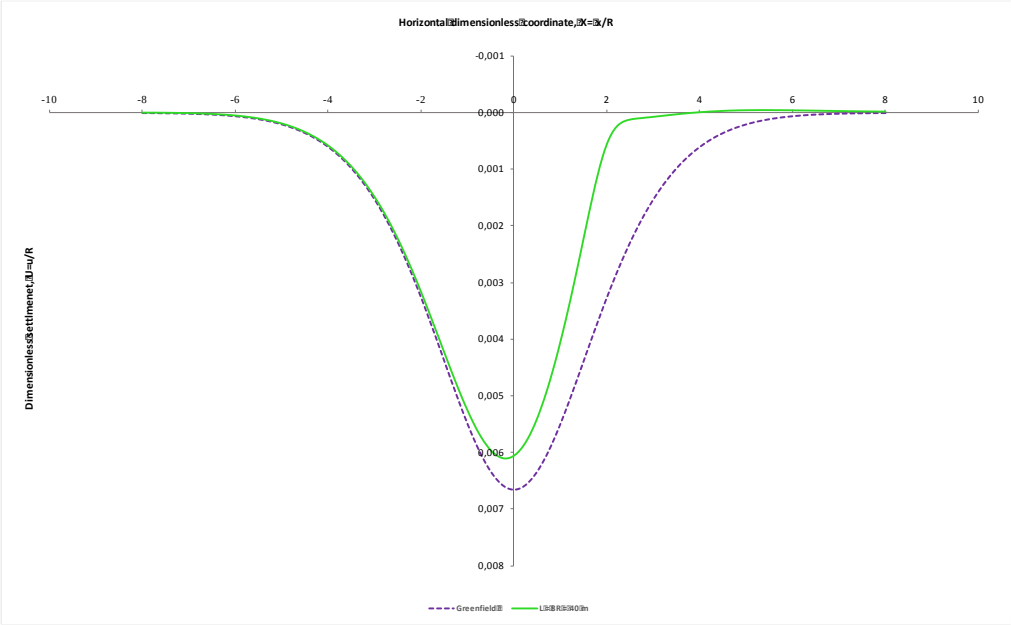

Figure 3. 12.- Effect of wall vertical length on the vertical displacements. 40-meter length lateral wall

3.2.4.6. Overall diagram

In Figure 3.13, the overall effect in the vertical displacement trough at ground surface for the different lateral wall lengths considered is presented.

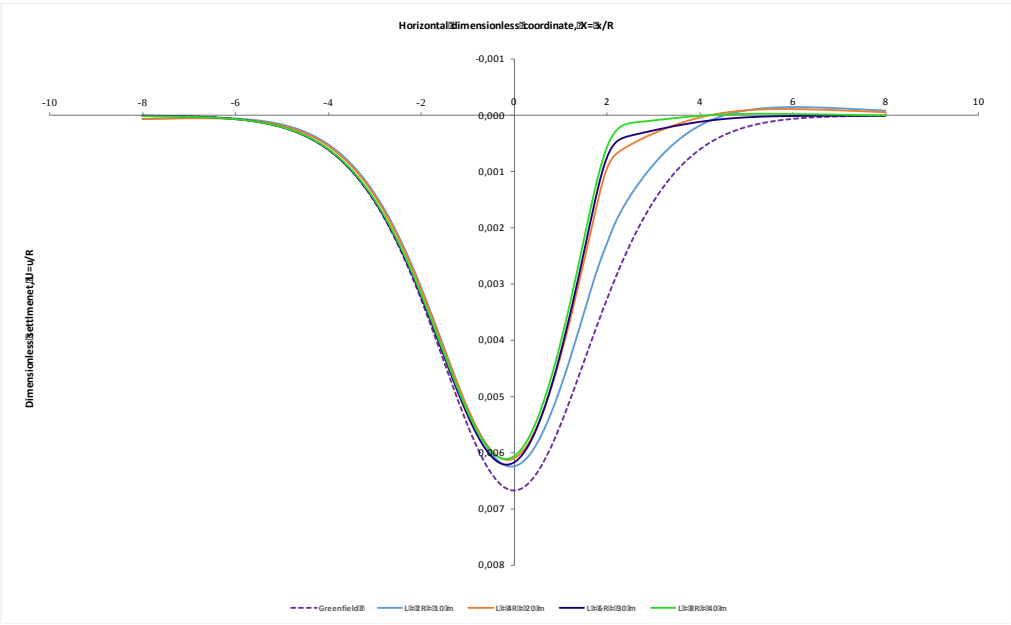

Figure 3. 13.- Effect of wall vertical length on the vertical displacements

3.2.5. General comments of the results

As stated in Figures 3.9 to 3.13, the effect of the lateral wall length has been analysed by means of solving the Melan 2D vertical problem. It has been proved that the settlements are reduced far beyond the wall, hence the aim of protecting sensitive constructions is achieved.

It can be noticed by analysing the figures provided above, that the symmetry of the settlement trough is lost when the lateral wall is built in one side of the tunnel while in the case of greenfield conditions the settlement trough was symmetric with respect to the tunnel axis. The maximum value of the displacement trough is also moved in the opposite direction of the wall axis. This phenomenon is more obvious as the length of the wall is increased. (Ledesma & Alonso, 2010)

For the analysis carried out previously, four different wall lengths have been considered in order to analyse different possible situations and the most efficient one. Later on in chapter six of this thesis a deeper analysis of the results obtained is going to be developed analysing specific parameters governing the vertical displacements troughs such as the wall stiffness and the tunnel-wall distance.

CHAPTER 4

Analysis of horizontal displacements

FINAL MASTER THESIS

4.1. Introduction

As presented in previous sections of this Final Master Thesis, designing a tunnel beneath urban areas may be a challenging task if ground movements are excessive and affect buildings located in the tunnel influence area. As presented in the State of the Art, some previous work has been carried out in order to understand, predict and simulate underground settlements while a tunnelling boring machine is excavating a tunnel.

This could be potentially damaging in the case of structures supported on shallow foundations or rafts such as old temples, or World Heritage buildings such as Sagrada Familia Basilica. In these cases, the structural solution of a diaphragm walls or a row of piles has performed well. The diaphragm wall or row of piles is build prior tunnel excavation in order to absorb a great percentage of the ground settlements. (Ledesma & Alonso, 2010)

This solution has been successfully applied in real cases but is still far from routine. It is important to notice that most of the main geotechnical reports studied, analyse the effect of the tunnelling works in deep foundations such as pile foundations, which is not the aim of this Thesis. As stated in the Introduction, the aim is to study the effect of a lateral wall in the tunnelling displacement troughs either vertical or lateral. Despite that, some other contributions have been analysed in the State of the Art in which some structural solutions in order to mitigate ground displacements induced by tunnelling are proposed.

In the following sections of this chapter, a new methodology to estimate the lateral deformations is going to be presented. As when dealing with vertical deformations, some articles and previous works could be taken as reference, and the results obtained could have been compared between them, in lateral movements no previous works has been published, so a deeper analysis of the formulation implemented in calculations is needed.

As in chapter three, the lateral displacements field will be studied by analysing the problem of the tunnel-wall interaction by means of the Melan 2D formulation. Later on, in chapter 6, some numerical Plaxis models will be run in order to validate the analytical results obtained from analytical calculations with different geometries.

4.2. The tunnel-wall interaction problem. Lateral displacements due to lateral loads

It is obvious that the tunnel-wall interaction problem can easily be solved by means of Finite Element (FE) calculations but that applying FE in order to solve the problem is not the primary goal of this thesis. Although Finite Element methods are widely applied in order to solve complex geotechnical problems, analytical procedures are very useful in terms of understanding the mechanisms involved in the interaction and the overall problem itself.

In Figure 4.1, the tunnel-wall interaction problem it is presented. The wall is constructed at a distance “d” from the tunnel axis.

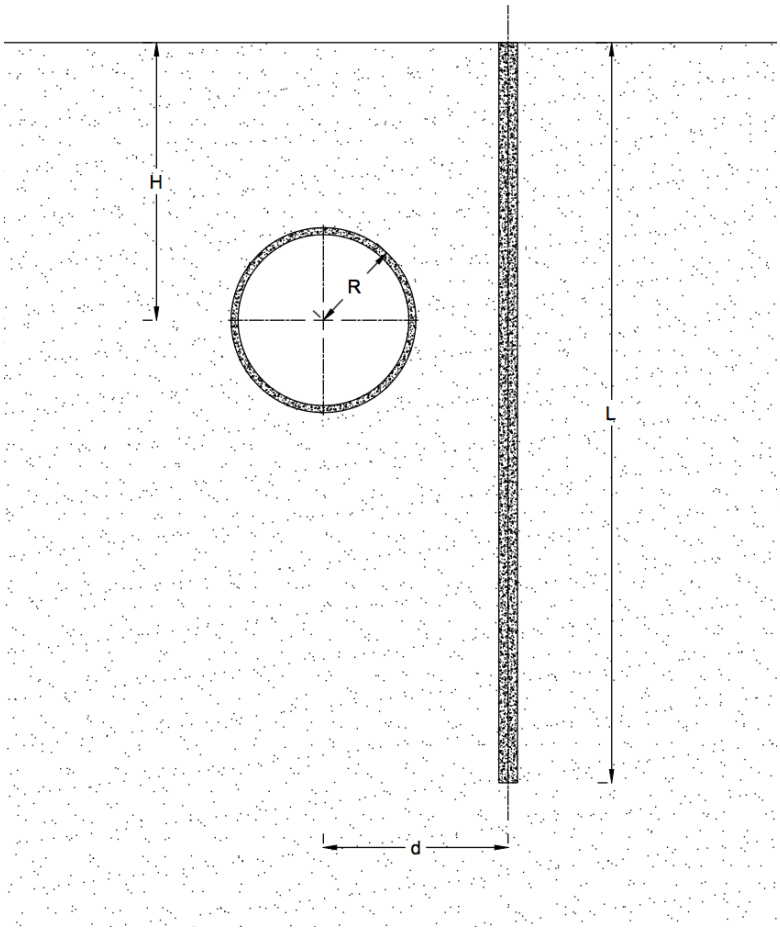

Figure 4. 1.- Basic geometry of the tunnel-wall interaction problem

4.2.1. Tunnel excavation analysis

Firstly, it is important to notice that from now on, only tunnelling boring machines are going to be considered when analysing ground settlements from tunnel excavation. The settlements caused by tunnelling boring machines are going to be calculated in this section of the chapter. In order to do so, first of all undrained conditions will be assumed which means that the volume of the material remains constant leading to a value of Poisson's coefficient of 0.5. (Loganathan & Poulos, 1998)

In order to carry out an analytical estimation of ground movements induced by tunnelling an approximate formulae proposed by Loganathan & Poulos (1998) will be applied. This formulation is chosen as they provide a reasonable displacement field when comparing with actual measurements. For the case of ν=0.5, lateral displacements due to tunnel excavation is obtained applying in Equation 4.1:

$$\mathbf{u_x[m]} = -R^2 x\left[\frac{1}{x^2+(H-z)^2}+\frac{3-4\nu}{x^2+(H+z)^2}-\frac{4z(z+H)}{[x^2+(H+z)^2]^2}\right]\varepsilon \qquad (4.1)$$

Where $\mathbf{u_x(x,z)}$ is the vertical displacement, considered positive downwards, **R** is the tunnel radius, **H** is the depth of the spring line and **ε** is the modified equivalent ground loss parameter defined as follows:

$$\boldsymbol{\varepsilon}[-] = \varepsilon_0 \exp\left[-\left(\frac{1{,}38x^2}{(H+R)^2} + \frac{0{,}69z^2}{H^2}\right)\right] \tag{4.2}$$

Where $\boldsymbol{\varepsilon_0}$ is the equivalent average ground loss (i.e. the area of the surface settlement trough divided by the tunnel area). Equation 4.2 takes into account the oval-happed ground deformation pattern around the tunnel section and provides a good estimation of ground movements.

4.2.2. Previous work for Melan Lateral equations

As stated in some previous sections of this chapter, no reference work of this methodology could be used in terms of comparison because it does not exist. The first step was to build the general equation for the Melan 2D lateral problem by means of analysing all the available information presented by J.C.F Telles and C.A. Brebbia on its publication: *Boundary Element Solution for Half-Plane problems.* (Telles & Brebbia, 1981)

The Melan 2D fundamental solution for the displacements due to a unit load applied to a half-plane consists basically in two parts. The first part is the Kelvin solution which represents the solution to an infinite space. Secondly, the complementary solution which when added to the kelvin solution gives the solution for an elastic half-space. The fundamental solution can be written as:

$$\mathbf{u^*_{ij}[m]} = u^k_{ij} + u^c_{ij} \tag{4.3}$$

Where $\mathbf{u^*_{ij}}$ is the displacement in the ***i*** direction due to a unit load in the ***j*** direction. The geometry of both the Kelvin and the Complementary problems is provided in Figure 4.2. (Kupussamy, Zarco, & Ebeling, 1992)

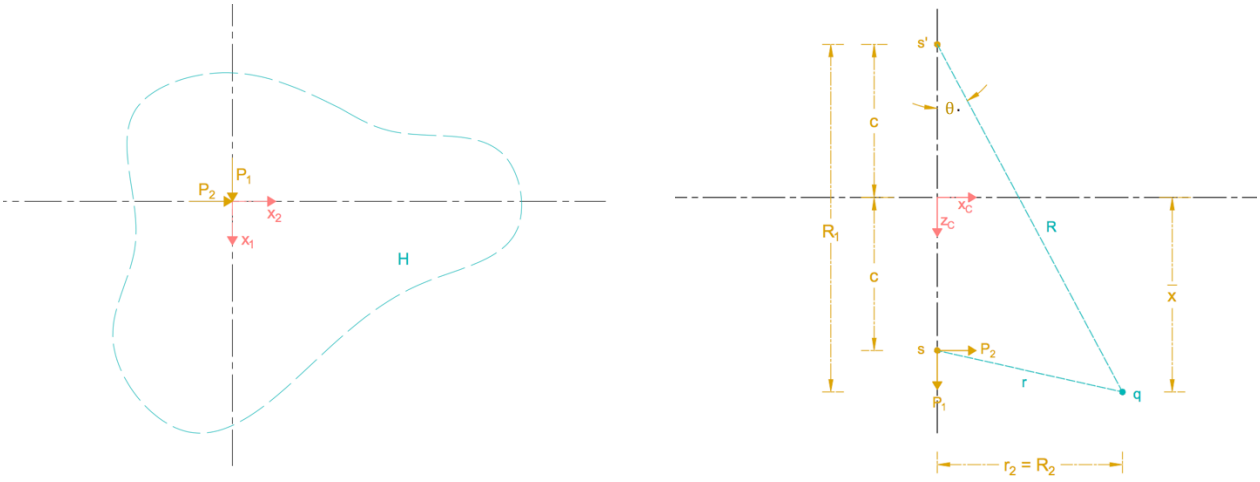

Figure 4. 2.- Definition of both the Kelvin and Complementary problems

Analysing the previous figures, it is important to notice that both Kelvin and Complementary geometries have not the same coordinate origin. For the Kelvin problem, the origin will be the load application point, leading to as many origins as forces the problem has. For the complementary solution, the origin of coordinates will be the ground elevation level. Equation 4.4, defines both the Kelvin and Complementary problems:

The Kelvin formulation for lateral displacements due to a horizontal unit load can be defined by means of Equation 4.4. As explained before, the Kelvin formulation takes into account an infinite space.

$$\mathbf{u_{22}^{k}[m]} = \frac{1}{8\pi G(1-\nu)}\left[(3-4\nu)\ln\left(\frac{1}{r}\right)+\frac{y^2}{r^2}\right]+u_0 \tag{4.4}$$

The Complementary formulation for lateral displacements due to a horizontal unit load can be defined by means of Equation 4.5. As explained before, the Complementary formulation, when added to the Kelvin formulation gives as a result the Melan formulation. The complementary equation can be expressed by means of Equation 4.5. (Telles & Brebbia, 1981)

$$\mathbf{u_{22}^{c}[m]} = K_d\left\{-[8(1-\nu)^2-(3-4\nu)]\ln R+\frac{[(3-4\nu)r_2^2+2c\bar{x}]}{R^2}-\frac{4c\bar{x}r_2^2}{R^4}\right\}+u_0 \tag{4.5}$$

The value of $\mathbf{K_d}$ can be obtained by applying Equation 4.6.

$$\mathbf{K_d[m]} = \frac{1}{8\pi G(1-\nu)} \tag{4.6}$$

It has been noticed that the formulation presented above had some singularities. The easiest way to deal with them is to impose that, a certain distance from the load the displacements is zero. For the case concerning this thesis it has been considered that at 40 meters from the application point the displacement is zero. Solving the equation imposing that condition for both the Kelvin and the Complementary solution, allows the constant u_0 to be obtained.

As a previous work to understand the meaning of these equations, it has been considered the basic geometry of the interaction soil-wall problem presented in Figure 4.3. It has been calculated the lateral deformation for each force independently for both Kelvin and Complementary equations in order to obtain the general Melan diagram for each force. As stated before, what has been carried out is not to solve the system of equations but, to develop an individual analysis of each force applied at each application point for both Kelvin and Complementary formulations to analyse the behaviour of the results.

In Figures 4.4 to 4.9, the results for each Melan diagram resulting from applying equations 4.4 and 4.5 are presented.

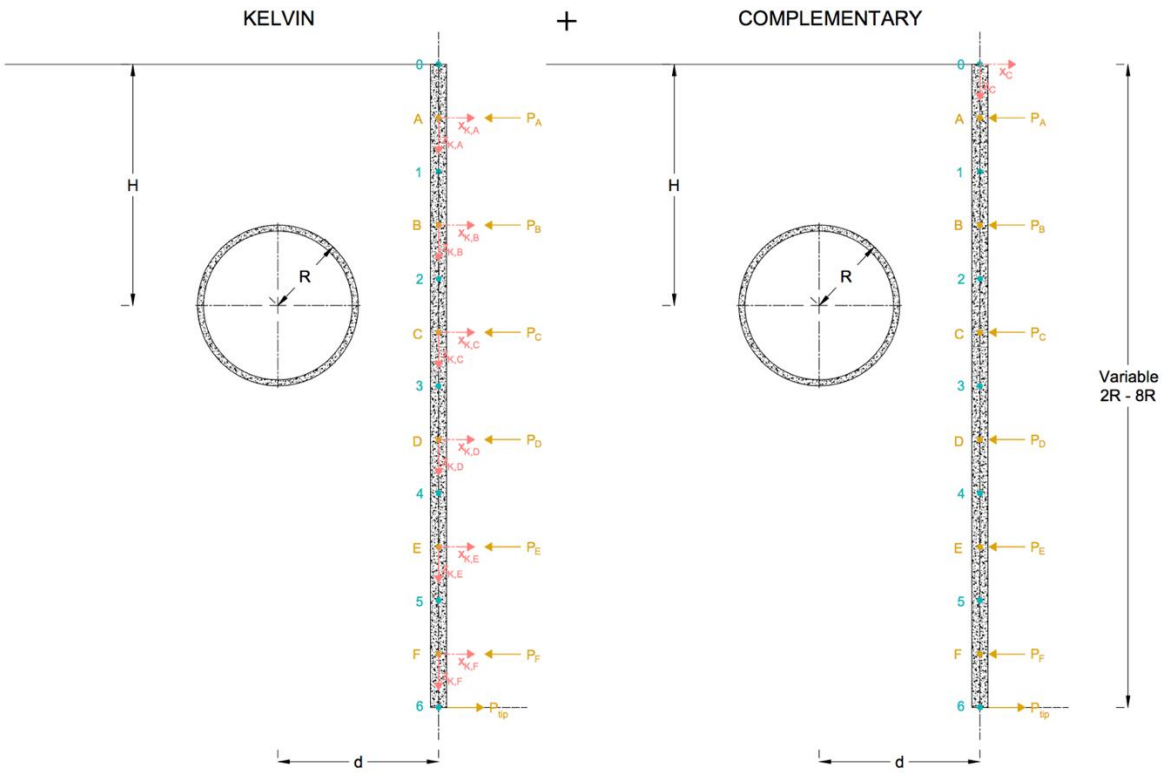

Figure 4. 3.- Basic geometry of the problem. General scheme for the interaction forces between soil and wall.

For each figure, three diagrams are presented. The first one in green corresponds to the Kelvin solution, the gold one, corresponds to the Complementary solution and finally the blue one corresponds to the addition of both Kelvin + Complementary resulting on the Melan 2D lateral.

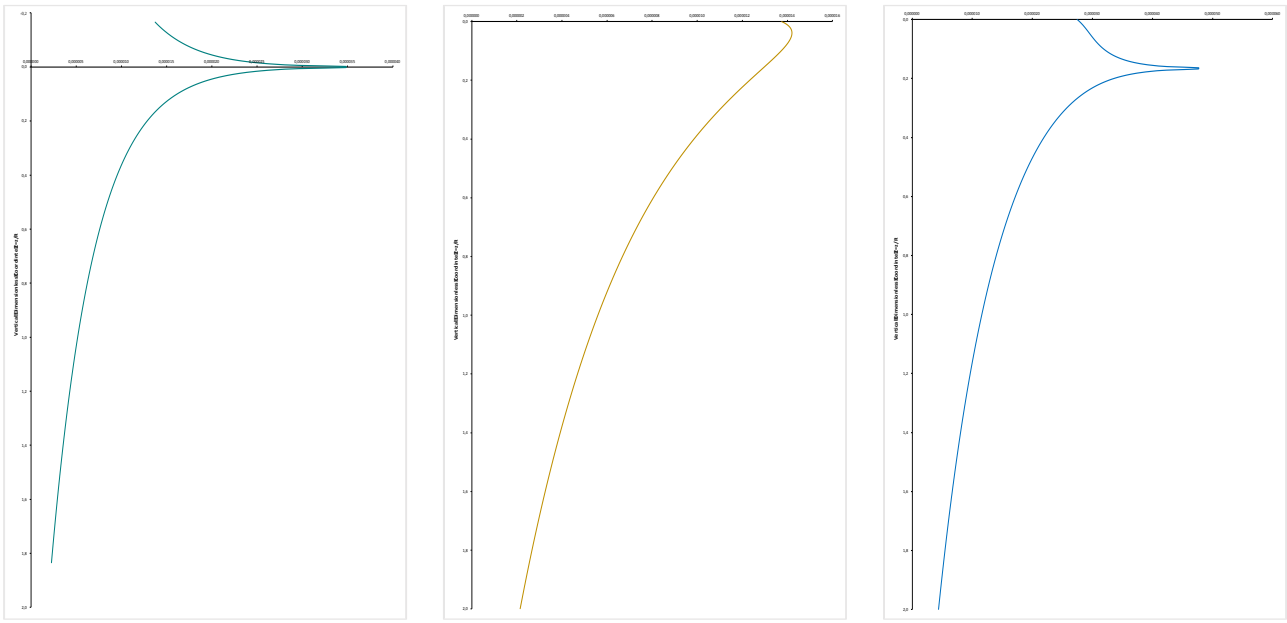

Figure 4. 4.- Analysis of Melan 2D lateral deformation for a point load applied at point A

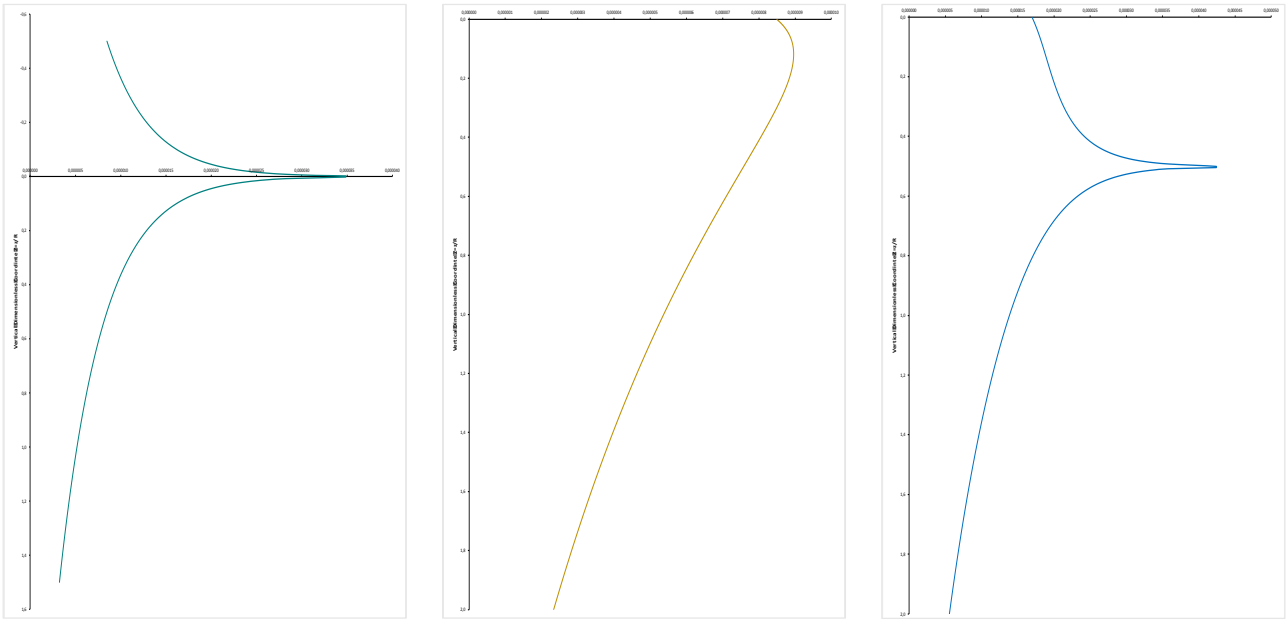

Figure 4. 5.- Analysis of Melan 2D lateral deformation for a point load applied at point B

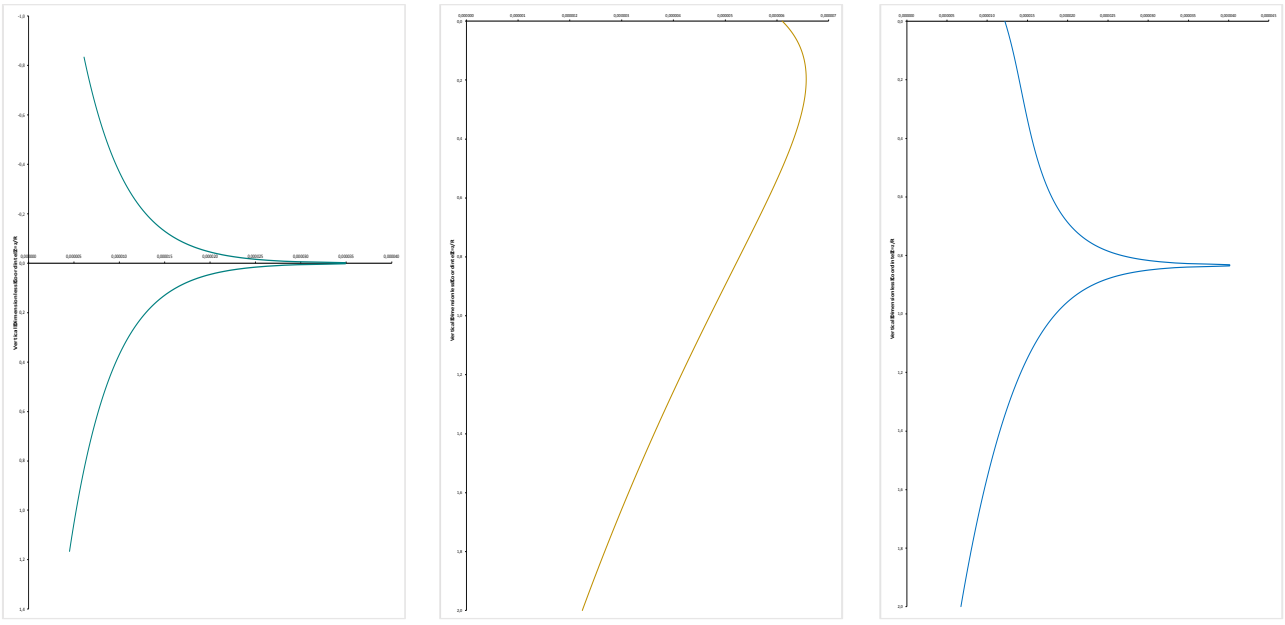

Figure 4. 6.- Analysis of Melan 2D lateral deformation for a point load applied at point C

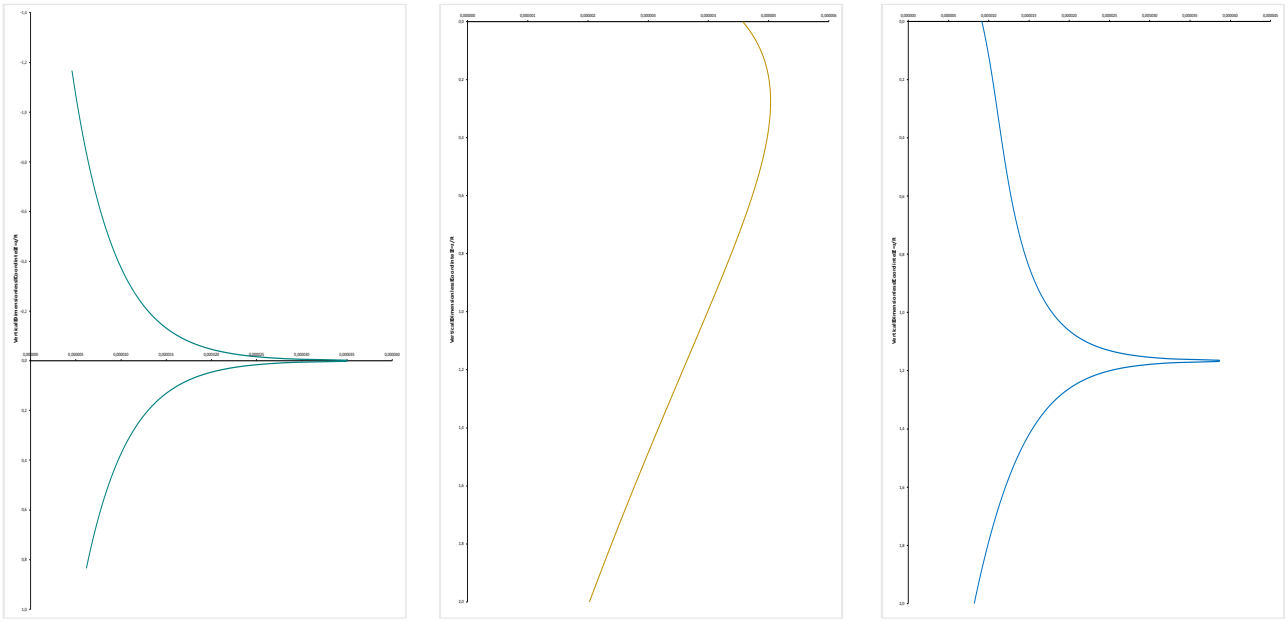

Figure 4. 7.- Analysis of Melan 2D lateral deformation for a point load applied at point D

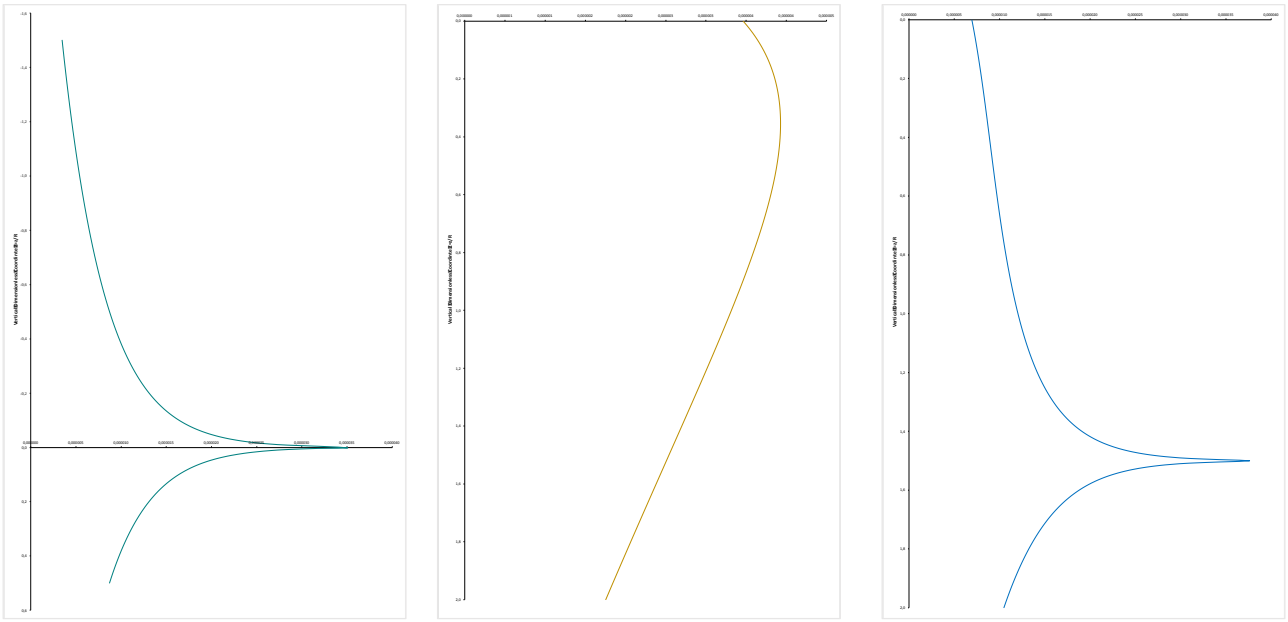

Figure 4. 8.- Analysis of Melan 2D lateral deformation for a point load applied at point E

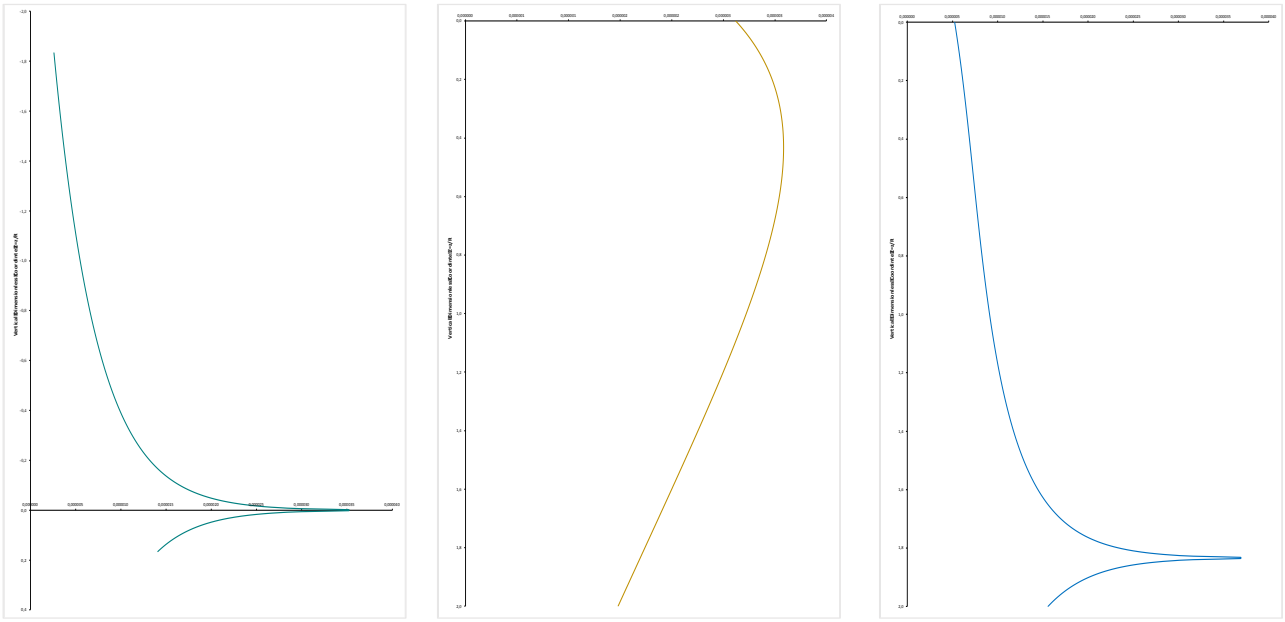

Figure 4. 9.- Analysis of Melan 2D lateral deformation for a point load applied at point F

By doing this individual analysis, a deeper understanding of the equations and its behaviour is pretended. Also an analysis of discontinuities is carried out in order to determine the constant u_0 to adopt which is already implemented in the diagrams presented above.

Once this analysis is carried out successfully, it is time to solve the overall system of equations for the Melan lateral deformations which takes into account the effect of the lateral wall on the soil in order to prevent or reduce the soil deformations while tunnelling works are being developed.

4.2.3. Lateral wall

In this section of chapter four, the main hypothesis used to solve the Melan 2D lateral deformation system of equations are going to be presented as well as all the geometries involved in the calculation process. Finally, the results of the analysis are going to be provided.

The wall effect can be taken into account by analysing the forces acting on its surface. In Figure 4.3, a geometry of the interaction forces is presented. In following sections of this chapter this geometry is going to be updated considering different geometries used for the analysis. It has been analysed piles of length 2R, 4R, 6R and 8R in order to obtain realistic conclusions in the analysis. (Ledesma & Alonso, 2010)

In structural terms, a wall does not have any initial load but, due to the displacements induced by tunnelling and skin friction, it develops internal forces and bending moments. Due to its stiffness, displacements generated while tunnelling excavation are reduced beyond the wall, hence, the effect to any structure is dramatically reduced.

Having a deeper look to figure 4.2, $\mathbf{P_A}$ to $\mathbf{P_F}$ and $\mathbf{P_{TIP}}$ represent the action-reaction forces between the soil and the pile or diaphragm wall known also as the interaction forces.

The goal of this chapter is to solve the problem of a load applied to an inner point in the 2D elastic half-space. This procedure will allow this forces to be estimated. As stated before this problem is widely known as Melan 2D problem which consists basically in the addition of the Kelvin and the Complementary equations. Melan (1932) was the first to provide a solution in terms of stresses. For the case concerning this thesis the formulae used to solve the Melan problem will be the one presented in previous equations.

As stated previously, the lateral displacement at the studied points due to a force per unit length, F, is expressed again assuming undrained conditions which means that the volume remains constant and the Poisson's coefficient is adopted as 0.5. (Ledesma & Alonso, 2010) (Perez-Garcia & Guardiola-Víllora, 2012)

4.2.4. Compatibility condition

These forces, ($\mathbf{P_i}$), can be obtained by imposing compatibility condition of lateral displacements at all studied points (see Figure 4.3, 4.10 and 4.11). As stated a few paragraphs above, the geotechnical term can be calculated by combining in one hand, the Loganathan & Poulos (1998) equation which obtains the soil deformation when a tunnel is excavated at a certain depth and, in the other hand, the solution for displacements induced by inner forces $\mathbf{P_j}$ by adding the Kelvin and Complementary formulation.

The structural term or movements in the wall can be calculated by calculating the shear deformation. This calculation can be carried out from the shear forces acting on it. In order to proceed with the shear deformation, the wall is divided into 6 segments (n=6) as it can be seen in all geometries presented throughout the chapter. Each segment *j* is loaded by a force $\mathbf{P_j}$ acting at the segment midpoint ($\mathbf{P_A}, \mathbf{P_B}, \mathbf{P_C}, \mathbf{P_D}, \mathbf{P_E}$, and $\mathbf{P_F}$). Hence, the lateral deformation of a point *i* in the wall can be computes by applying Equation 4.7:

$$\mathbf{u_{AC}}[\mathbf{m}] = u_6 + \frac{P_j b^2}{6E_w I_w}[3(L-x)-b] \text{ for } x \in AC \tag{4.7}$$

$$\mathbf{u_{CB}}[\mathbf{m}] = u_6 + \frac{P_j}{6E_w I_w}(L-x)^2(2b-a+x) \text{ for } x \in CB \tag{4.8}$$

In Figure 4.10, an arbitrary geometry is provided showing for each studied point (0, 2, 3, 4 and 5), the location of points A, B and C which helps to decide which equation is necessary to apply depending on the position of the *x* coordinate (equation 4.7 or equation 4.8). (Perez-Garcia & Guardiola-Víllora, 2012)

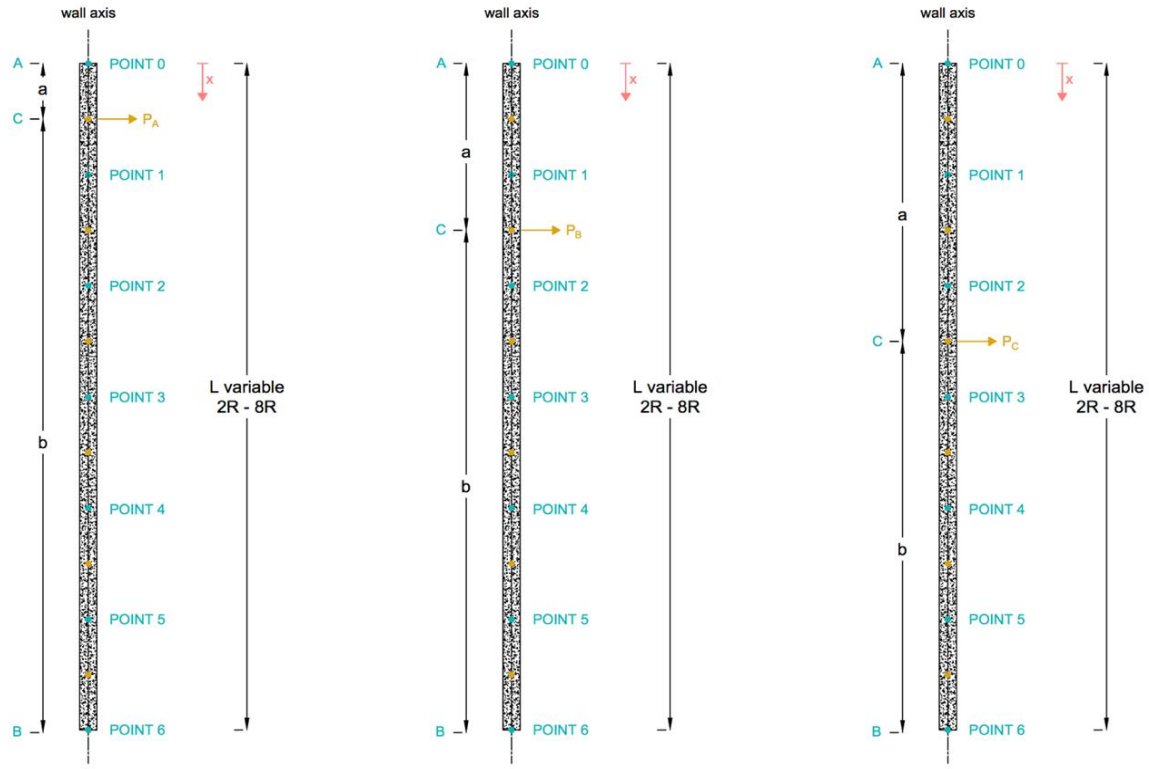

Figure 4. 10.- Development of the shear deformation calculation process (I)

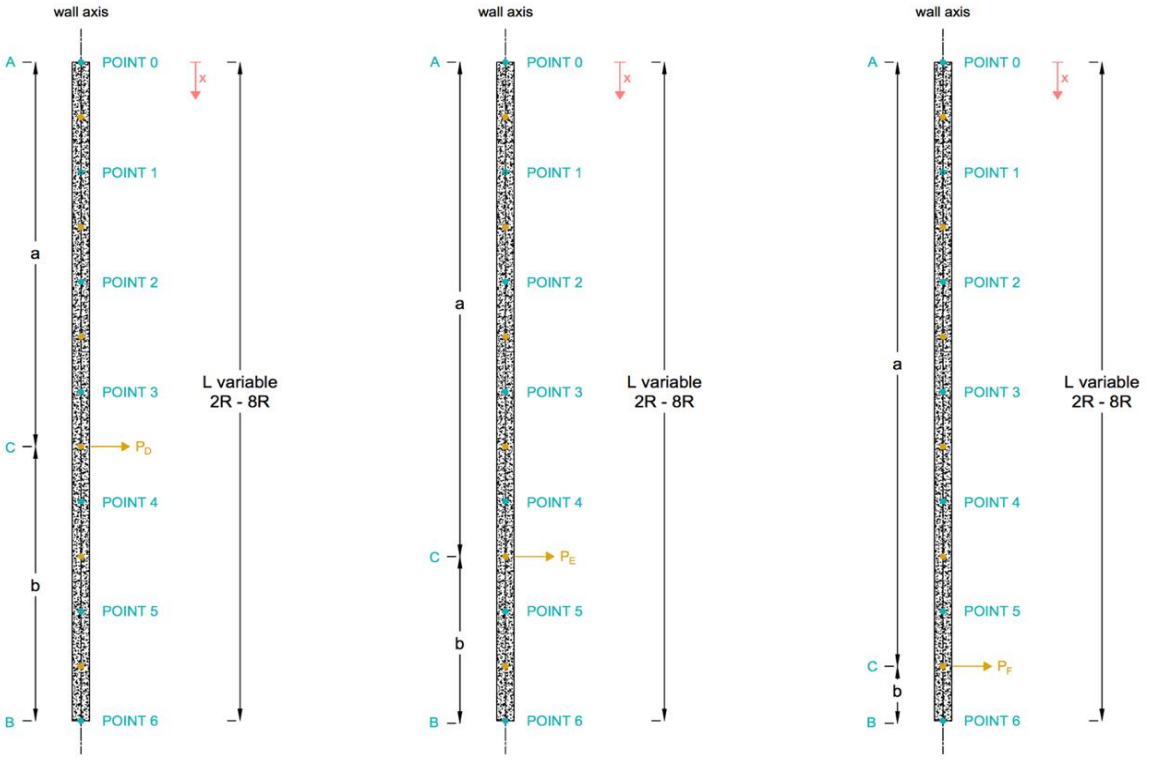

Figure 4. 11.- Development of the shear deformation calculation process (II)

It is important to notice that $\mathbf{u_6}$ is the displacement at the wall tip, $\mathbf{E_w}$ is the wall's Young Modulus, $\mathbf{I_w}$ is the wall Second Moment of Inertia, **L** is the total length of the pile wall and finally, $\mathbf{P_j}$ is the shear force in a particular segment *j* (force per unit length). For the first segment, between points 0 and 1, the shear force is $\mathbf{P_A}$, between points 1 and 2, the shear force is $\mathbf{P_B}$, between points 2 and 3, the shear force is $\mathbf{P_C}$, between points 3 and 4, the shear force is $\mathbf{P_D}$, between points 4 and 5, the shear force is $\mathbf{P_E}$, and finally between points 5 and 6, the shear force is $\mathbf{P_F}$.

It is important to verify lateral equilibrium at the wall tip $\mathbf{P_{TIP}}$. It is trivial to see that lateral equilibrium is satisfied by imposing a basic structural concept:

$$\mathbf{P_{tip}} = \sum \mathrm{P_j} \tag{4.9}$$

Finally, the compatibility condition applied to point 0 to point n – 1 is governed by the mathematical expression presented in Equation 4.10: (Ledesma & Alonso, 2010)

$$\mathbf{u_{z\ tunnel}} + \sum \mathbf{u_{z\ due\ to\ P_j}} = \mathbf{u_{z\ structural\ wall}} \tag{4.10}$$

Equation 4.10 is applied to point 0 to point n – 1. The left side term, which is composed for the settlements due to tunnel excavation calculated applying Loganathan & Poulos equation (1998) and the solution for displacements induced by inner forces $\mathbf{P_j}$ by adding the Kelvin and Complementary formulation conform what is called the Geotechnical term. The Loganathan & Poulos expression is defined at equation 4.1 and 4.2 while Kelvin and Complementary formulation is provided at equations 4.3 to 4.6 both included.

The right side term configures what is called the structural term in which the shear deformation is calculated by means of considering the pile wall as a cantilever beam with a generic point load applied on an arbitrary point of its surface. In order to do that is applied what is called the superposition principle consisting in calculating the shear deformation caused for each force in all the the points in which the pile is discretized and then adding the effects of each force at each point. For instance, the effect of force $\mathbf{P_j}$ is computed for each point and then the effects are added. The formulation needed to calculate the shear deformation is provided in equations 4.7 and 4.8.

In an overall view, equation 4.10, applied to each studied point, provides a linear system of **n** equations with **n** unknowns which is easily solved by means of excel, mat lab or any other mathematical tool. Finally, once the interaction forces are obtained, the displacements produced by these forces are calculated and in a final stage of the calculation process, those displacements are superposed onto the movements derived from the Loganathan and Poulos (1998) solution for greenfield case at ground surface to obtain the final soil displacements.

In Figures 4.12 to 4.15, the different geometries involving different pile lengths are presented.

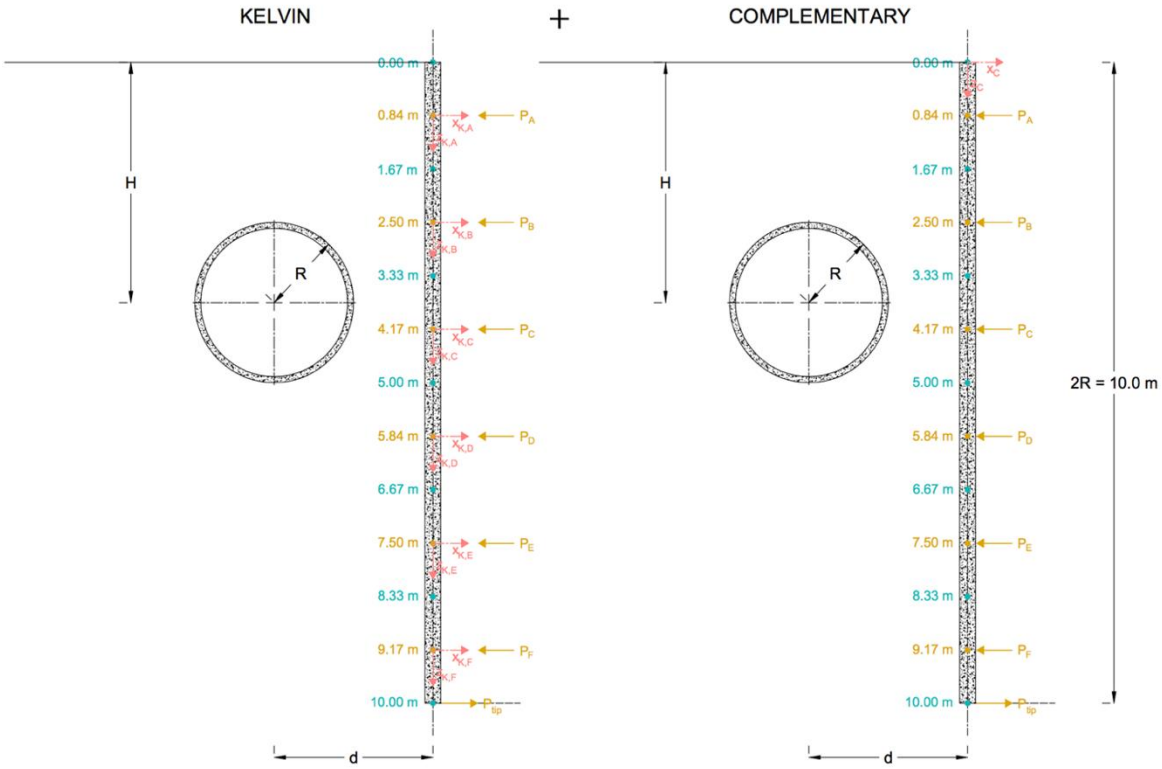

Figure 4. 12.- Basic geometry of the interaction forces for both Kelvin and Complementary equations. Length = 10 m.

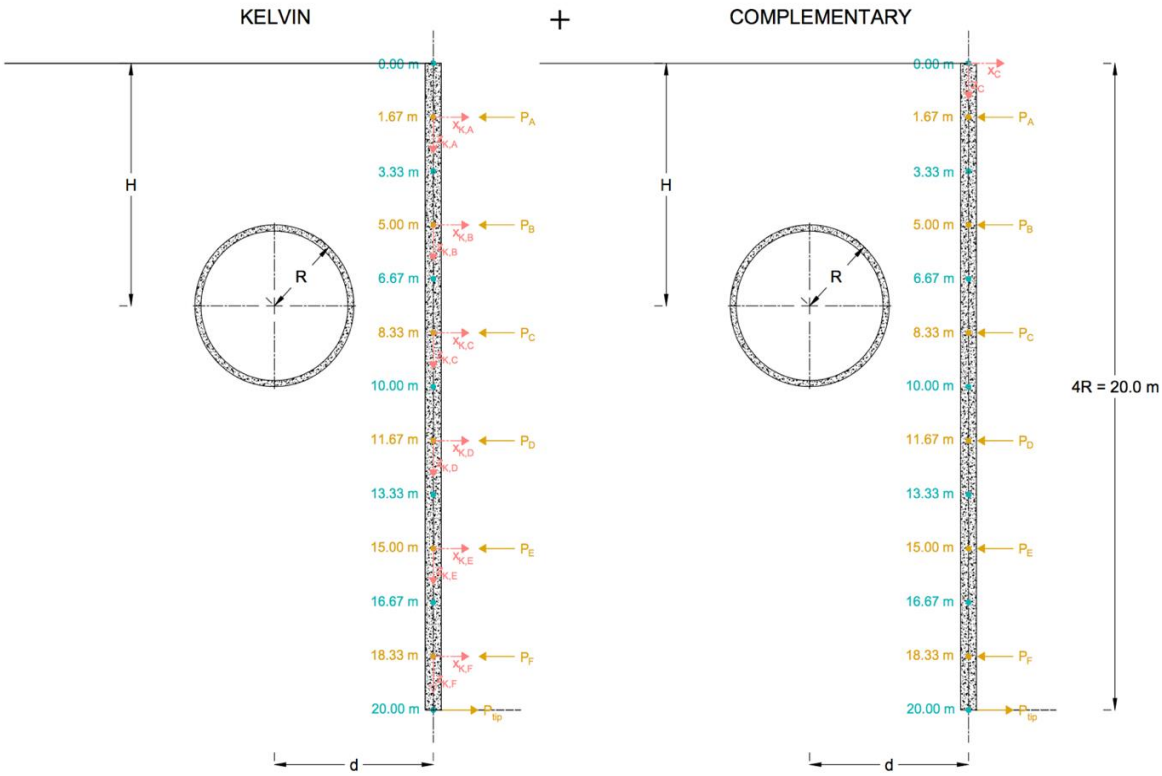

Figure 4. 13.- Basic geometry of the interaction forces for both Kelvin and Complementary equations. Length = 20 m.

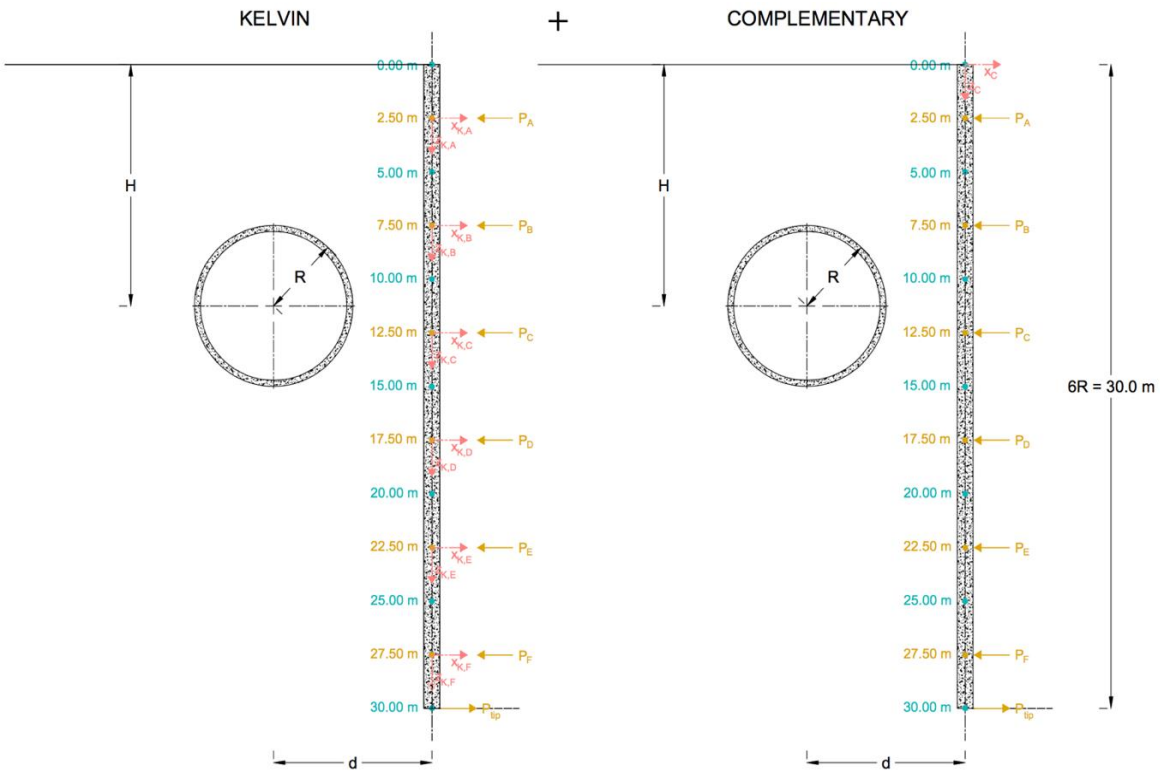

Figure 4. 14.- Basic geometry of the interaction forces for both Kelvin and Complementary equations. Length = 30 m.

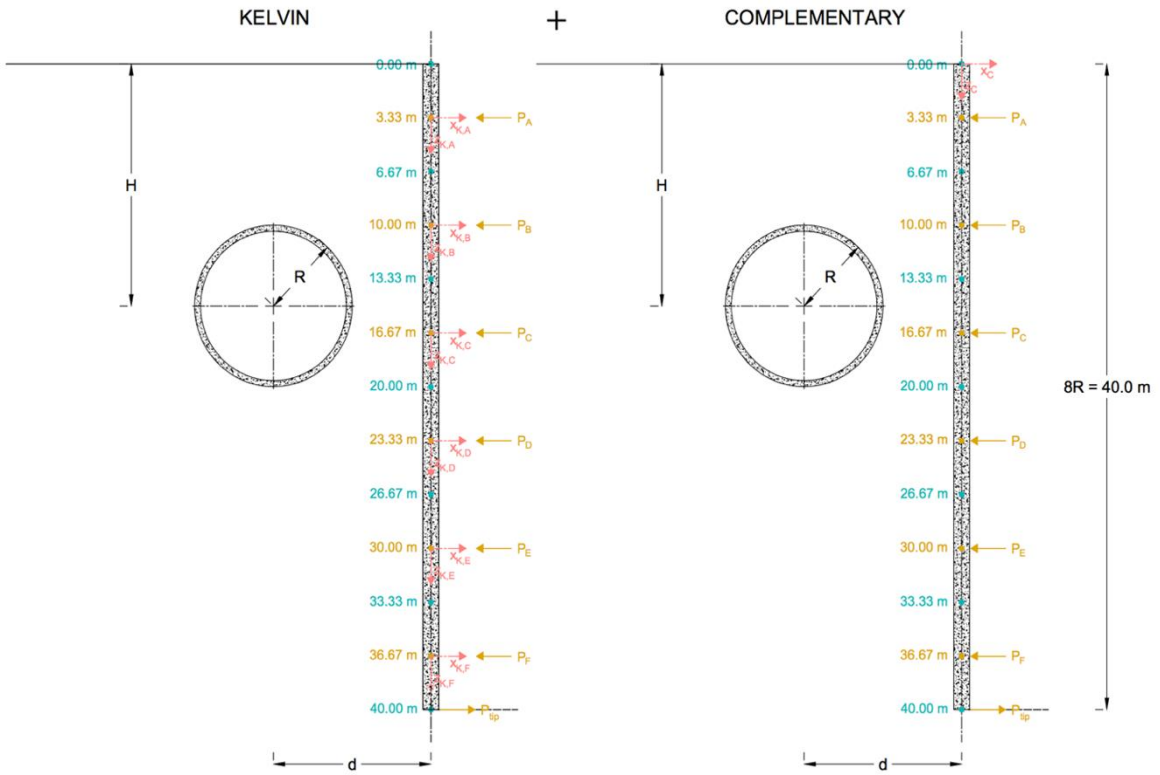

Figure 4. 15.- Basic geometry of the interaction forces for both Kelvin and Complementary equations. Length = 40 m.

4.2.5. Analysis and results. Lateral displacements due to lateral loads

In this section of the chapter, the results obtained from the analysis are going to be presented. As stated in some previous paragraphs, the goal is to determine the interaction forces and compute its effect in the lateral displacement trough.

In the case concerning this thesis, the procedure to solve the system of equation has been the following; once the coefficient matrix of the system is built, the Excel solver tool is applied in order to obtain the final results of the interaction forces. It is known as coefficient matrix of the system, the one in which each column of it contains the coefficients corresponding to a variable of the system of equations and in its last column, contains the coefficients of the right side of the equations.

The goal of the analysis once having solved the system and the numerical values of the interaction forces, is to determine the influence of the lateral wall on the lateral displacements. In order to do that, firstly, a diagram representation of the *"greenfield"* conditions is going to be provided and after that, the influence od the lateral wall is going to be added in order to see the effects. It is important to highlight that *"greenfield"* conditions correspond to those in which no lateral structure is built, hence, to the lateral displacements due to tunnel excavation.

It is important also to quantify the efficiency of the wall. As stated in Chapter 2 of this thesis "*State of the Art*", and as published in Bilota's article, the efficiency of a structural element designed to reduce the settlement induced by tunnelling is calculated with the mathematical expression presented below. This expression is a dimensionless ratio that quantifies the potential of a vertical diaphragm wall to reduce ground movements.

$$\boldsymbol{\eta}[-] = \frac{[S_{ref} - S_{bw}]}{S_{ref}} \tag{4.11}$$

Where $\mathbf{S_{ref}}$ is defined as the settlement trough in greenfield conditions and $\mathbf{S_{bw}}$ is the settlement of the ground surface immediately beyond the diaphragm wall. When $\boldsymbol{\eta}$ is equal to 1 it means that the solution of a diaphragm wall is totally effective whereas when $\boldsymbol{\eta}$ present a value of 0, means that the wall has no positive effect when reducing the settlement trough. (Bilotta, 2008)

It can be seen having a deeper analysis to Figures 4.16 to 4.18, that the results obtained are highly influenced by the wall tip location. As in vertical displacements, when having a short wall (tip above the tunnel invert), both its wall top and tip can suffer from excessive ground displacements. Hence, when the length of the wall is increased, it helps to reduce lateral displacements and proves that the solution of a lateral wall to prevent from ground movements is effective.

In Figures 4.16 to 4.18, the results from the analysis are presented and discussed.

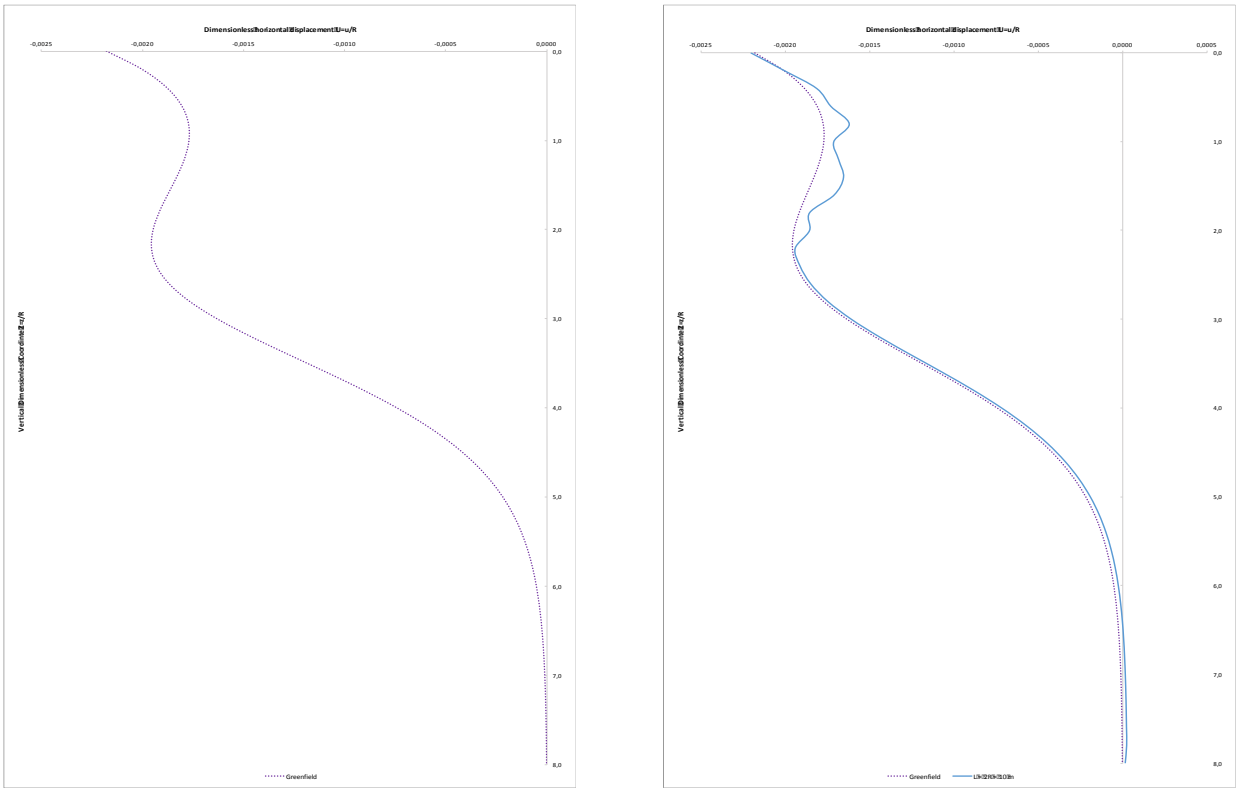

Figure 4. 16.- Effect of wall vertical length on the lateral displacement trough. Lateral wall of 10-meter length.

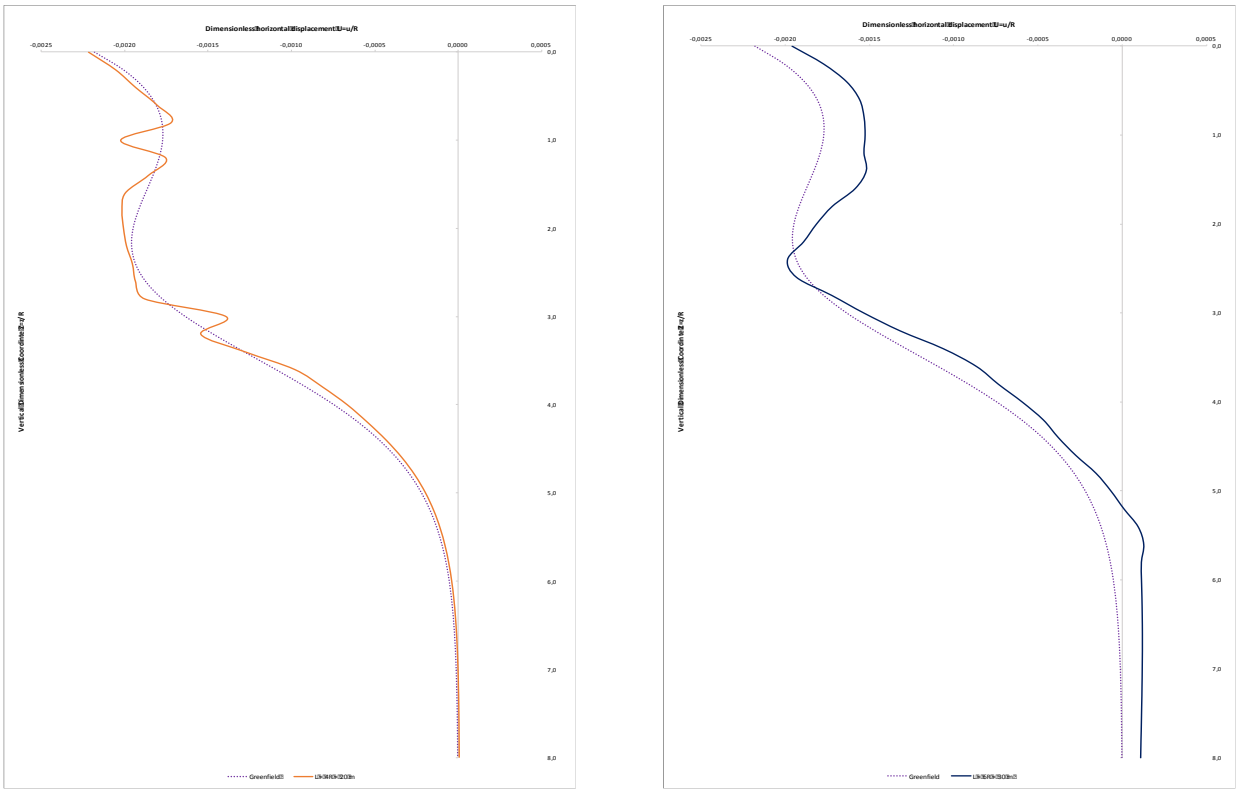

Figure 4. 17.- Effect of wall vertical length on the lateral displacement trough. Lateral wall of 20 and 30-meter length.

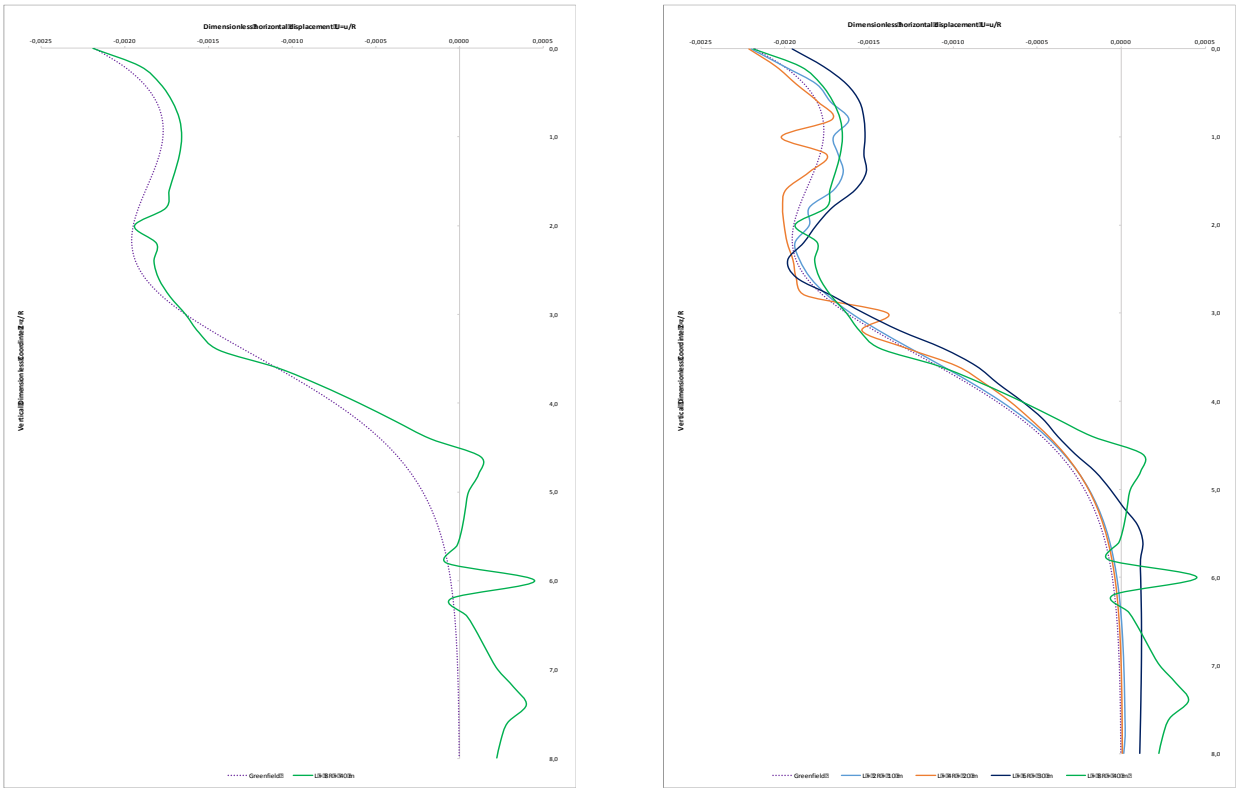

Figure 4. 18.- Effect of wall vertical length on the lateral displacement trough. Lateral wall of 40-meter length.

4.2.6. General comments on the results. Lateral displacements due to lateral loads.

As stated in Figures 4.16 to 4.18, the effect of the lateral wall length has been analysed by means of solving the Melan 2D horizontal problem which is constituted by the addition of the Kelvin and the Complementary Solution. For the case of horizontal displacements, it can be seen that the effect of reducing the settlements far beyond the wall is achieved but, in general, the maximum lateral displacement that coincides with the tunnel spring line remains almost the same without suffering important variations.

As stated in chapter three, the vertical displacement trough was symmetric with respect to the tunnel axis in greenfield conditions when no lateral wall is implemented. This is not the case for lateral displacements, which the it has already lost the symmetry for the case of greenfield conditions because the analysis distance is 10 meters far form respect the tunnel axis. Furthermore, it is trivial to understand that if in greenfield conditions there is no symmetry, when the wall is implemented the effect will be the same. (Ledesma & Alonso, 2010)

For the analysis carried out previously, four different wall lengths have been considered in order to analyse different possible situations and the most efficient one. Later on in chapter six of this thesis a deeper analysis of the results obtained is going to be developed analysing specific parameters governing the lateral displacements troughs such as the wall stiffness and the tunnel-wall distance.

4.3. The tunnel-wall interaction problem. Lateral displacements due to vertical loads

In chapter three, the analysis of vertical displacements has been developed by means of solving the Melan 2D vertical problem presented and discussed in the corresponding chapter. As stated in previous chapters and sections the result of solving the Melan problem, either vertical or lateral, are the interaction forces between the soil and the lateral wall. It is trivial to understand that these interaction forces for the case of vertical displacement troughs will be vertical forces while for the case of lateral displacements will be horizontal interaction forces.

So, in order to proceed with a deeper analysis of the lateral deformations, in this section of the chapter, the vertical interaction forces obtained from chapter three are going to be used to calculate the effect of them in the lateral displacement fields.

For the case concerning the lateral displacements due to vertical load, a slightly different formulation with respect to the one presented previously will be applied as the forces are not acting in the same direction. As presented previously the Melan 2D fundamental solution is made of two parts: The Kelvin solution and the Complementary solution. The Kelvin solution gives the solution for an infinite space while the complementary when added to the Kelvin one gives the solution for a half-space which is the one of interest. Hence, the fundamental solution can be written as follows: (Kupussamy, Zarco, & Ebeling, 1992) (Telles & Brebbia, 1981)

$$\mathbf{u_{ij}^{*}[m]} = u_{ij}^{k} + u_{ij}^{c} \tag{4.12}$$

Where $\mathbf{u_{ij}^{*}}$ is the displacement in the ***i*** direction due to a unit load in the ***j*** direction. The geometry of both the Kelvin and the Complementary problems is presented in Figure 4.2.

The Kelvin formulation for lateral displacements due to a vertical unit load can be defined by means of Equation 4.13. As explained above, the Kelvin solution takes into account an infinite space.

$$\mathbf{u_{21}^{k}[m]} = \frac{1}{8\pi G(1-\nu)}\left[\frac{xy}{r^2}\right] + u_0 \tag{4.13}$$

The Complementary solution for lateral displacements due to a unit vertical load can be defined by means of Equation 4.14. It is important to highlight that, when the Complementary solution is added to the Kelvin one, the result is the solution for the half-space. As it can be noticed in the previous work for lateral displacements due to lateral loads it is not trivial to understand the graphical meaning of the complementary solution.

$$\mathbf{u_{12}^{c}[m]} = K_d\left\{\frac{[(3-4\nu)r_1r_2 + 2c\bar{x}]}{R^2} + \frac{4c\bar{x}R_1r_2}{R^4} - 4(1-\nu)(1-2\nu)\theta\right\} + u_0 \tag{4.14}$$

The value of $\mathbf{K_d}$ can be obtained by applying the mathematical expression presented in Equation 4.15:

$$\mathbf{K_d[m]} = \frac{1}{8\pi G(1-\nu)} \tag{4.15}$$

Again, the formulation presents some singularities that have been solved by imposing that at a certain distance from the load application point, the displacement must be zero. For the case concerning this thesis, it has been considered that at 40 meters from the application point the displacement is zero. Hence, the value of the constant u_0 can be obtained. (Ledesma & Alonso, 2010)

4.3.1. Analysis and results. Lateral displacements due to vertical loads

In this section of the chapter the effect of the vertical loads computed in chapter three are going to be analysed by means of applying the previous equations and plotting the results. In Figures 4.19 to 4.21, the results concerning the effect lateral displacements due to vertical loads is presented. The first curve corresponds to the one in greenfield conditions and the remaining ones compare the greenfield trough with the effect of each wall length.

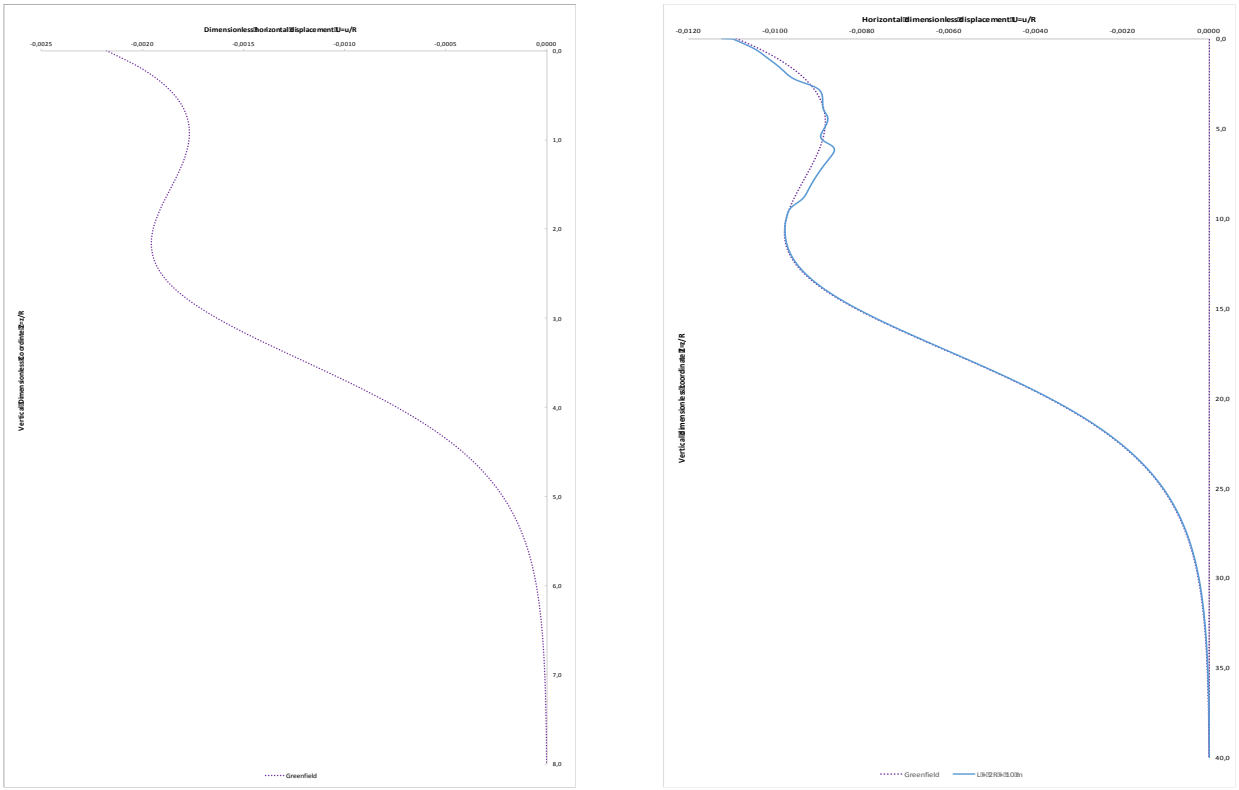

Figure 4. 19.- Lateral displacement due to vertical loads. Effect of a 10-meter lateral wall

It can be noticed that the lateral displacements generated by the vertical loads are not as important as the lateral displacements due to lateral load or the vertical displacements due to vertical loads. The results plotted in Figures 4.19 to 4.21 show that in general the displacement fields suffer the effect of the lateral wall at the tunnel centre line while the wall tip does not experience any variation for the case studied in this section.

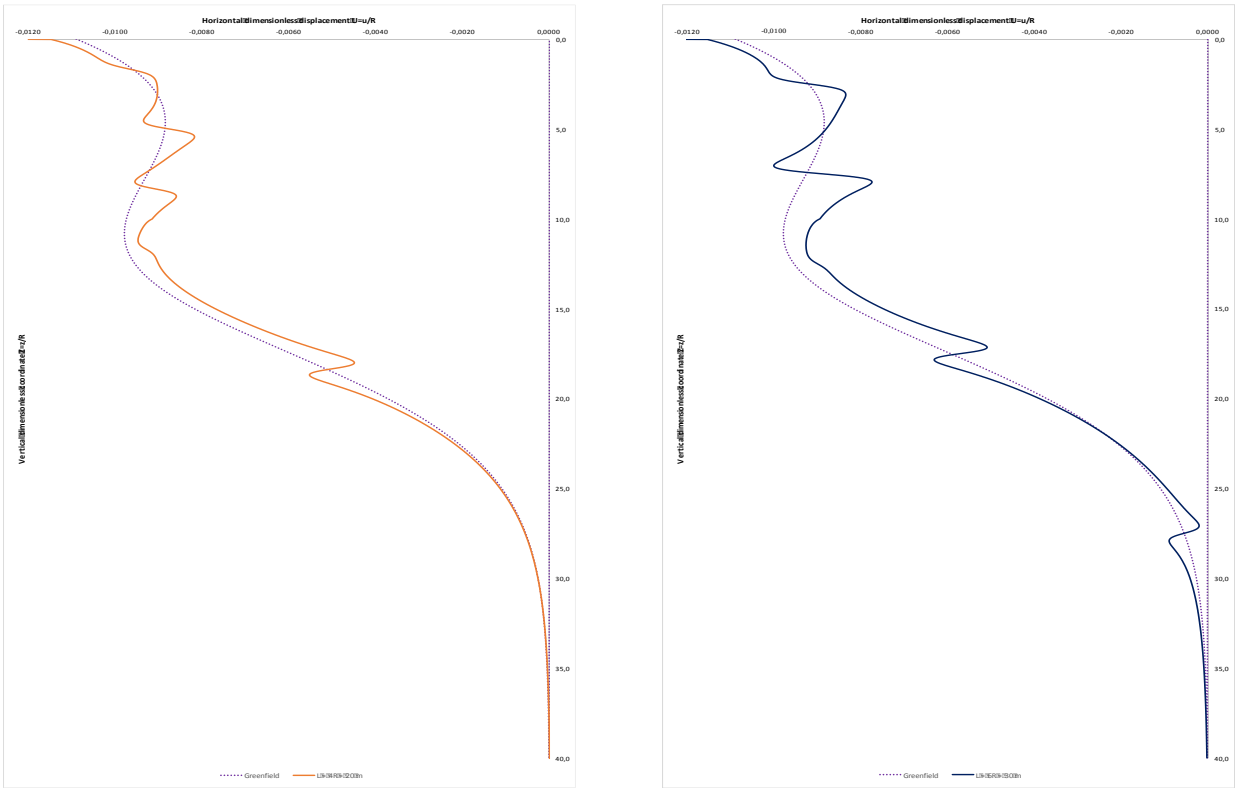

Figure 4. 20.- Lateral displacement due to vertical loads. Effect of a 20 and 30-meter lateral wall

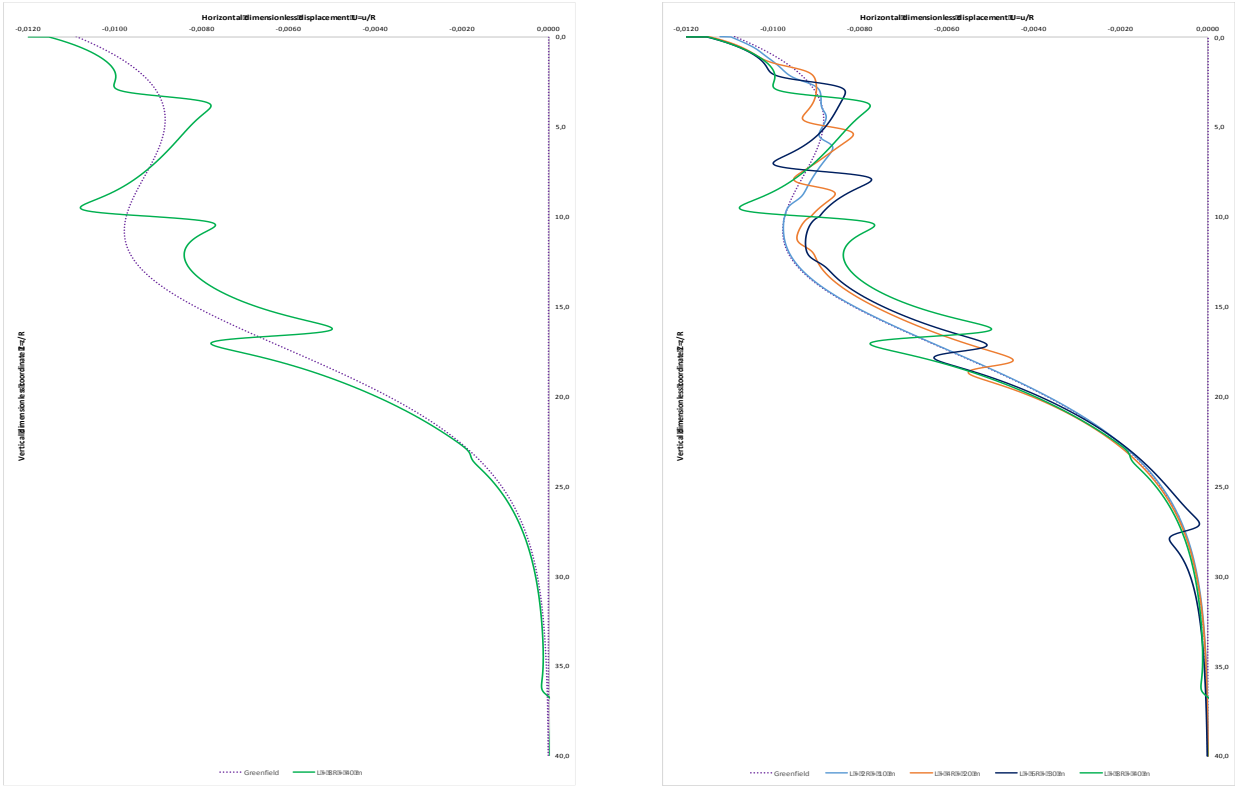

Figure 4. 21.- Lateral displacement due to vertical loads. Effect of a 40-meter lateral wall

4.3.1. General comments on the results. Lateral displacements due to vertical loads.

As developed in the previous section, the effect of the lateral wall length due to vertical loads has been computed by means of solving the Melan 2D horizontal problem which is, as explained throughout the current chapter, made basically from the addition of the Kelvin and the Complementary solution. For the case concerning this section is noticed that the ground displacement at the tunnel centreline is reduced as the wall increases its length but, is slightly increased at ground surface.

As stated in chapter three, the vertical displacement trough was symmetric with respect to the tunnel axis in greenfield conditions when no lateral wall is implemented. This is not the case for lateral displacements, which the it has already lost the symmetry for the case of greenfield conditions because the analysis distance is 10 meters far form respect the tunnel axis. Furthermore, it is trivial to understand that if in greenfield conditions there is no symmetry, when the wall is implemented the effect will be the same.

For the analysis carried out previously, four different wall lengths have been considered in order to analyse different possible situations and the most efficient one. Later on in chapter six of this thesis a deeper analysis of the results obtained is going to be developed analysing specific parameters governing the lateral displacements troughs such as the wall stiffness and the tunnel-wall distance.

CHAPTER 5

Finite-Element analysis

FINAL MASTER THESIS

5.1. Introduction

At this point of the thesis it is important to validate the analytical results obtained in previous chapters of this document. In chapter three, the vertical deformations have been studied while in chapter four, the same analysis has been carried out for horizontal displacements. Basically, the previous work consisted in the analytical solution of the Melan 2D system of equations both for vertical displacements and lateral displacements in order to obtain the numerical values of the interaction forces between the soil and the lateral wall designed to protect sensitive constructions from tunnelling.

In this chapter, a finite-element code is used to validate the empirical methods applied in previous chapters. The analysis will be carried out by means of Plaxis 2D software. Plaxis is a widely used software in geotechnical Engineering when designing underground works such as tunnels, deep foundations or retaining walls and any kind of soil-structure interaction problem. Its friendly interface allows the user to define and understand the geotechnical problem and its results in an easy way.

The geometry considered in this chapter will be the same one considered for the previous chapters in which the analytical calculations were developed. The goal is to conclude with a comparison between the simplified methodology (Melan problem) and the results obtained by using a tool adapted to the current design needs. It is obvious that with the classical formulations it is not trivial to simulate all the conditions and phenomenon that take place while the excavation works are developed. However, while using a finite-element program such as Plaxis, one can take into account and control almost all parameters governing soil conditions and behaviours.

In this chapter, the same geometries applied in previous chapters are implemented to the Program. The analysis is carried out by means of the Linear-elastic model with the aim to reproduce in the most accurate way the empirical results obtained applying elastic solutions. Hence, five different geometries are going to be calculated; the greenfield case and four different lengths considered for the lateral wall.

5.2. Plaxis 2D description

As stated before, Plaxis software is a Geotechnical Engineering tool developed to carry out deformability and stability of underground structures in both soil and rock mechanics. It is a widely used software in most geotechnical consultant institutions in order to design and develop projects with the most accurate level of detail.

Plaxis is thought to solve problems involving simple excavations, tunnel constructions including its staging and the installation of the liner, deep or shallow foundations, retaining walls made of diaphragm or pile walls, slope stability by means of micro piles or bolts, etc. The first stage is to develop the geometry in a similar interface as CAD in order to introduce facilities to the user. (Brinkgreve, Kumarswamy, & Swolfs et al., 2019)

Plaxis has the ability to create accurate models defining in a well manner both complex geotechnical profiles and structural elements such as piles, micro piles, anchors, geogrids, loads and prescribed displacements as boundary conditions. In case of complex geotechnical profiles, these can be imported with CAD. That can be the case when simulating a landslide for instance, where the soil profile may be quite difficult to represent in Plaxis and with the main topographic drawing one can import the transversal cross-section in an easy way.

Another important feature that has this software is the way in which the model is run. After the mesh is generated, the staged construction tab is opened. There the user can define and simulate with high levels of accuracy the way in which the excavation or the underground works are going to be developed or planned. That is achieved by means of activating or deactivating the structural or soil elements in each calculation phase.

A wide range of geotechnical problems can be analysed with that software such as safety analysis, consolidation analysis or plastic analysis. There is also a wide range of constitutive models. The main constitutive models range from linear elastic to non-linear models with strong features to develop at a high level of accuracy the real conditions of the soil. (Brinkgreve, Kumarswamy, & Swolfs et al., 2019)

The output interface it is widely used also to analyse the results obtained by the simulations. In the output tab, it is possible to analyse the forces, displacements, stresses, pore water pressures in the way that the user is most interested in. Also the stresses in the structural elements can be analysed in order to proceed with the reinforcement calculations. (Brinkgreve, Kumarswamy, & Swolfs et al., 2019)

5.3. Model geometries and input parameters

As stated before, the analysis is going to be developed using the linear-elastic model in order to be consistent with the analytical calculations developed in previous chapters. The models will be developed considering a unique type of soil. The mesh geometry involves a rectangle 160-meter-wide and 100-meter-deep. The lateral wall will be modelled as a plate.

It is important to notice that in order to perform well the simulation it has been considered for the linear elastic calculations the presence of a tunnel liner made of reinforced concrete rings of 0.4-meter thickness. The mechanical properties of all the structural elements and soil considered for the simulation are going to be presented in the following tables.

The lateral earth pressure is calculated by means of the expression presented in equation 5.1. The coefficient of lateral earth pressure is defined as the ratio of the horizontal effective stress, σ'_H, to the vertical effective stress, σ'_V. It can also be calculated by means of the Poisson coefficient of the soil as presented in the equation. For the the different models considered, the lateral earth pressure it has been properly calculated.

PARAMETER	SYMBOL	VALUE	UNIT
Material ID	[-]	Soil and interfaces	Soil
Material model	[-]	Linear elastic	[-]
Drainage type	[-]	Undrained (A)	[-]
Unit weight	γ	20.00	kN/m^3
Young Modulus	E_s	10,000	kPa
Poisson coefficient	ν	0.49	[-]
Interfaces	R_{inter}	0.67	[-]
Earth pressure coefficient	k_0	Automatic	[-]

Table 5. 1.- Mechanical and geotechnical properties of the soil used for the simulations with Plaxis 2D

PARAMETER	SYMBOL	VALUE	UNIT
Material ID	[-]	Lateral wall	[-]
Material type	[-]	Plate	Linear elastic
Isotropic	[-]	Yes	[-]
Unit weight	γ	25.00 (reinforced concrete)	kN/m^3
Young Modulus	E_w	20,000,000.00	kPa
Cross section	A_w	1	[m^2/m]
Poisson coefficient	ν	0.2	[-]
Second moment of inertia	I_2	0.0833	[m^4]

Table 5. 2.- Mechanical properties of the structural element representing the lateral wall

PARAMETER	SYMBOL	VALUE	UNIT
Material ID	[-]	Tunnel liner	[-]
Material type	[-]	Plate	Linear elastic
Isotropic	[-]	Yes	[-]
Unit weight	γ	25.00 (reinforced concrete)	kN/m^3
Young Modulus	E_w	100,000.00	kPa
Cross section	A_w	0.40	[m^2/m]
Poisson coefficient	ν	0.2	[-]
Second moment of inertia	I_2	0,00533	[m^4]

Table 5. 3.- Mechanical properties of the structural element representing the tunnel liner

Furthermore, it is important to consider that for the tunnel simulation it has been considered a line contraction of 1% corresponding to the values of ground loss assumed for the analytical calculations.

$$\mathbf{k_o}[-] = \frac{\nu}{1-\nu} \tag{5.1}$$

In section 5.3.1, the geometries considered for the simulations are going to be presented. Firstly, a drawing made by AutoCAD showing the main features of the model and then the screenshot of the Plaxis staged construction tab. When talking about the construction staging followed to develop the models first of all the pile wall is constructed prior to the tunnel excavation in order to analyse the desired goal.

As it is going to be observed, first the greenfield case will be presented, then the case of L=2R, L=4R, L=6R and finally the pile length corresponding to the case of L=8R. After that the results will be provided and in the sensitivity analysis chapter, will be compared with the analytical ones.

5.3.1. Greenfield case (No lateral wall)

As stated in previous chapters, the greenfield case is the base case. The results obtained with the lateral walls are going to be compared with the base case in terms of settlements and ground deformations. As stated before, greenfield conditions refer to those ones in which no structural element is built in order to protect from settlements and the ground deformations are only expected to be due to tunnel excavation process.

In Figures 5.1 to 5.10, both the drawing and the model geometry from Plaxis 2D software are presented. Later on the results will be shown.

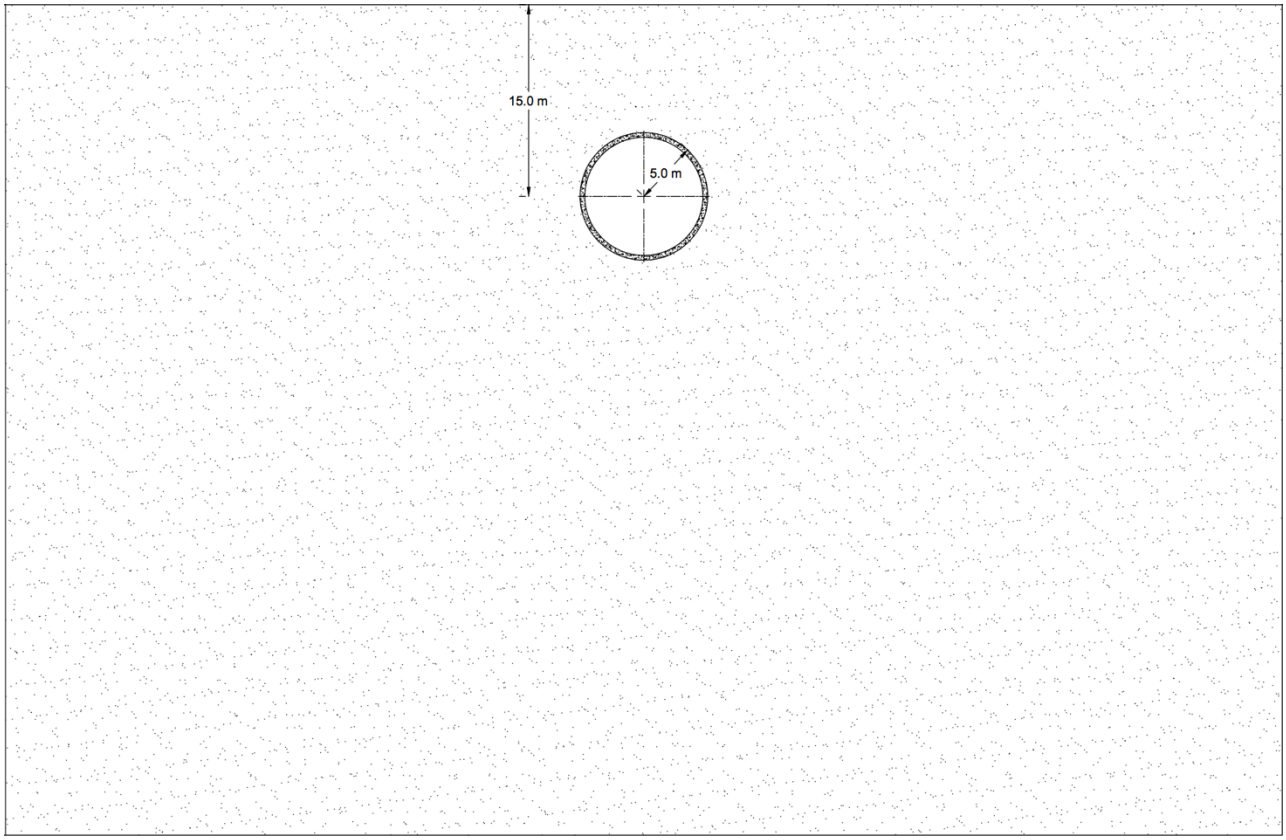

Figure 5. 1.- Drawing corresponding to greenfield conditions in which no structural element is imposed

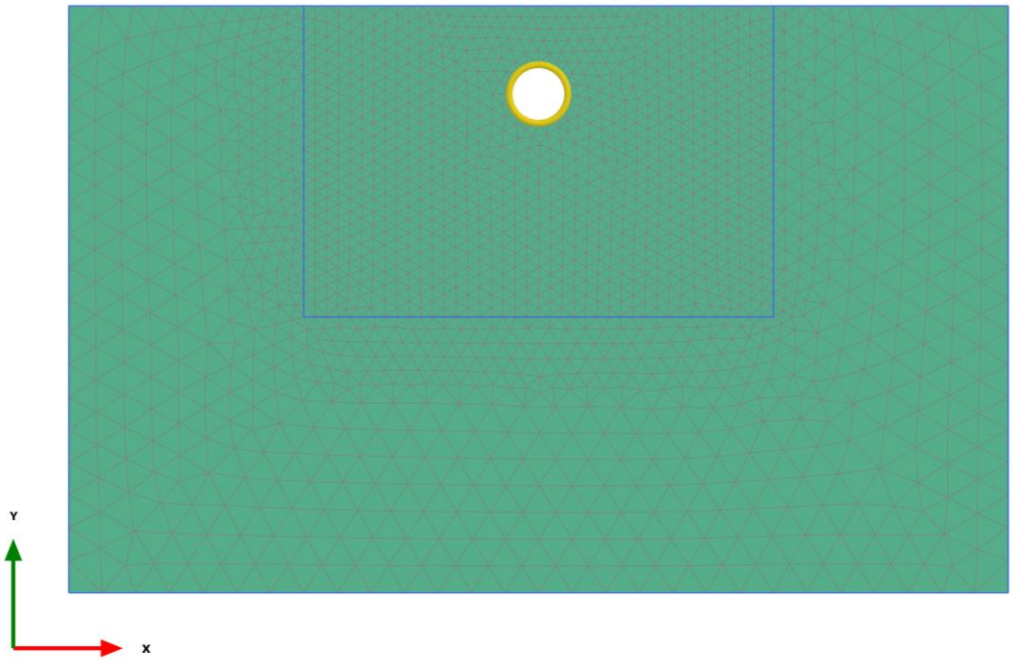

Figure 5. 2.- Plaxis model corresponding to the greenfield case without no structural element.

5.3.1. Wall of length L = 2R = 10 m

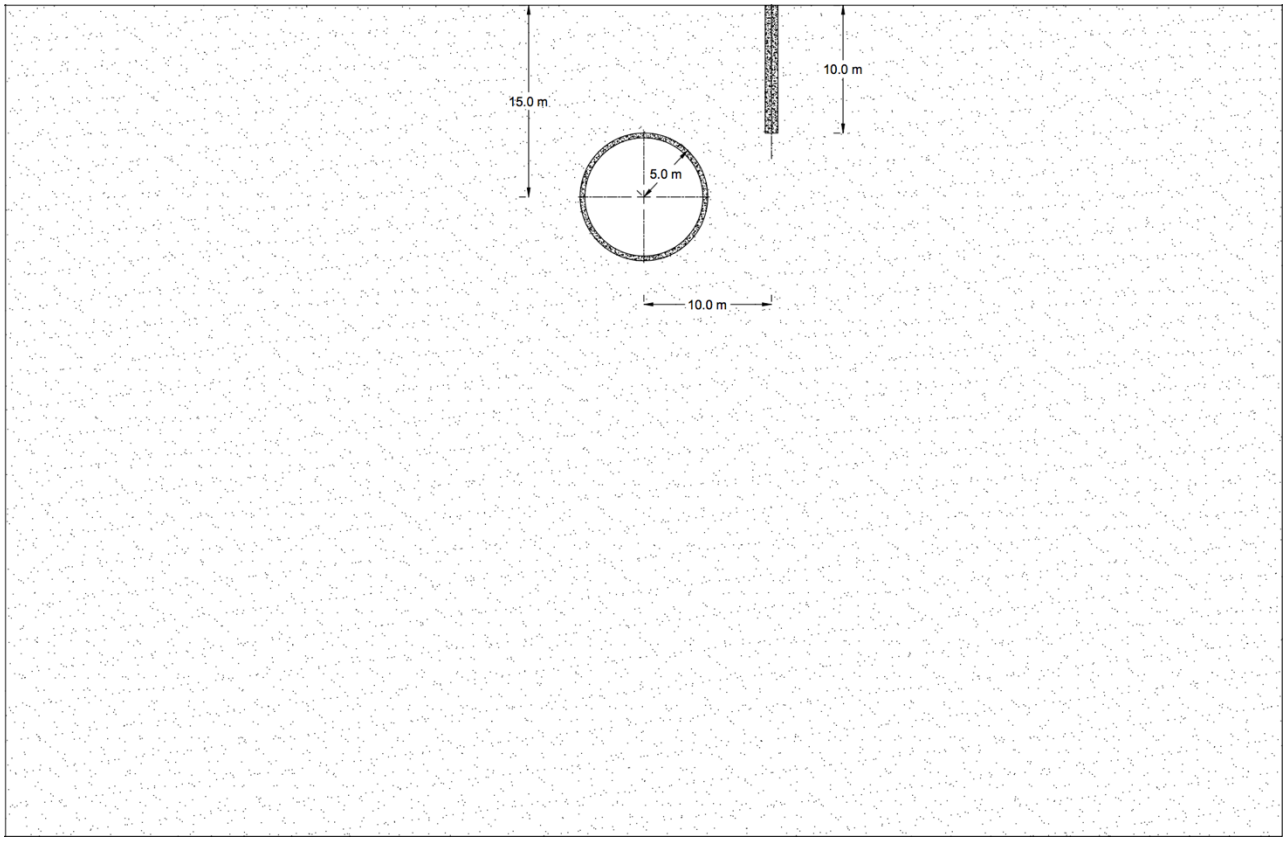

Figure 5. 3.- Drawing corresponding to the installation of the lateral wall of length L = 2R = 10 meters

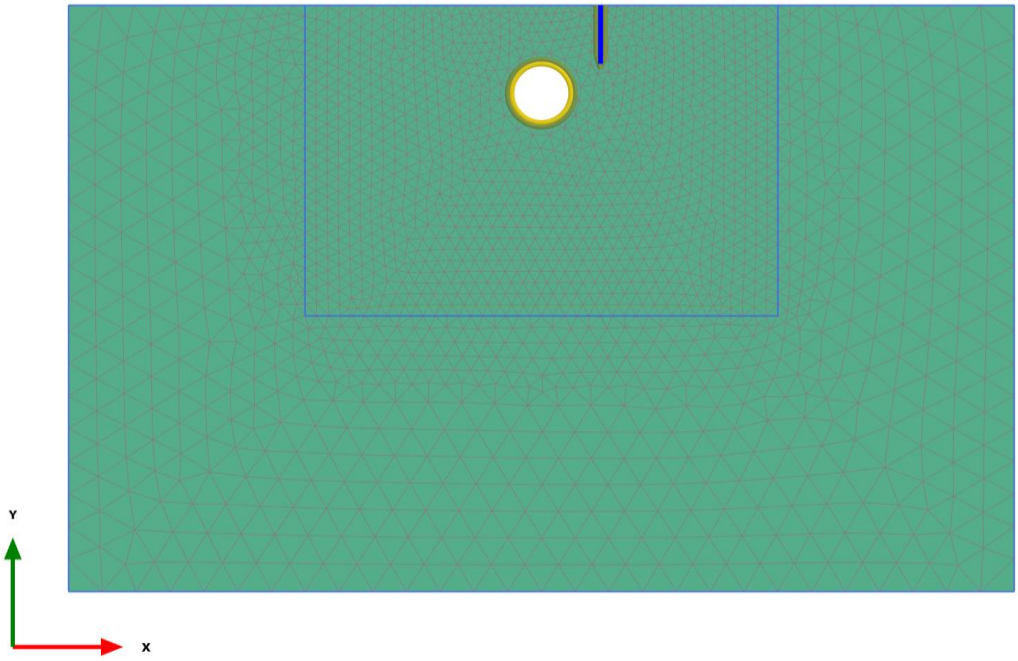

Figure 5. 4.- Plaxis model corresponding to the installation of the lateral wall of length L = 2R = 10 meters

5.3.1. Wall of length L = 4R = 20 m

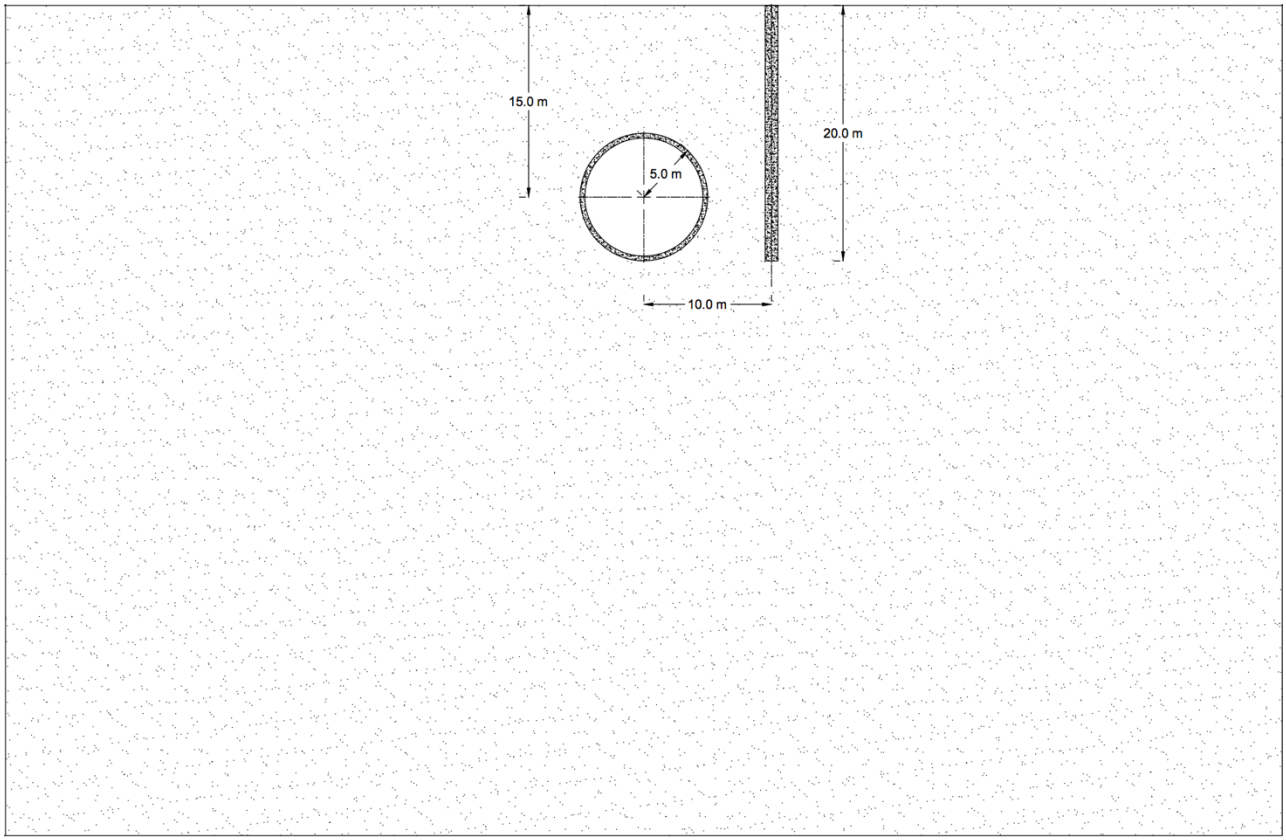

Figure 5. 5.- Drawing corresponding to the installation of the lateral wall of length L = 4R = 20 meters

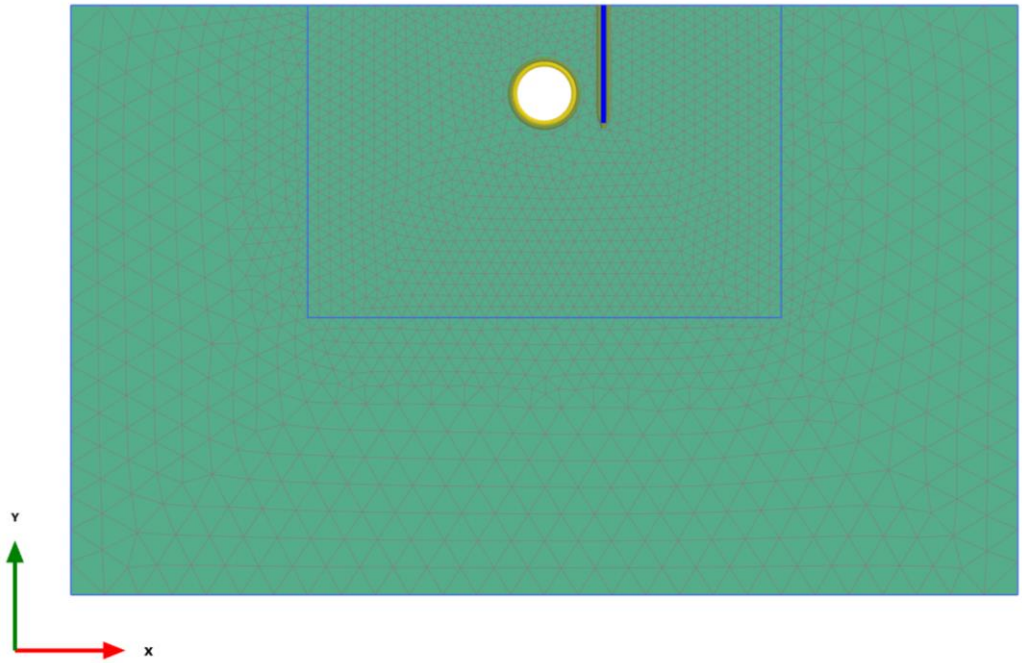

Figure 5. 6.- Plaxis model corresponding to the installation of the lateral wall of length L = 4R = 20 meters

5.3.1. Wall of length L = 6R = 30 m

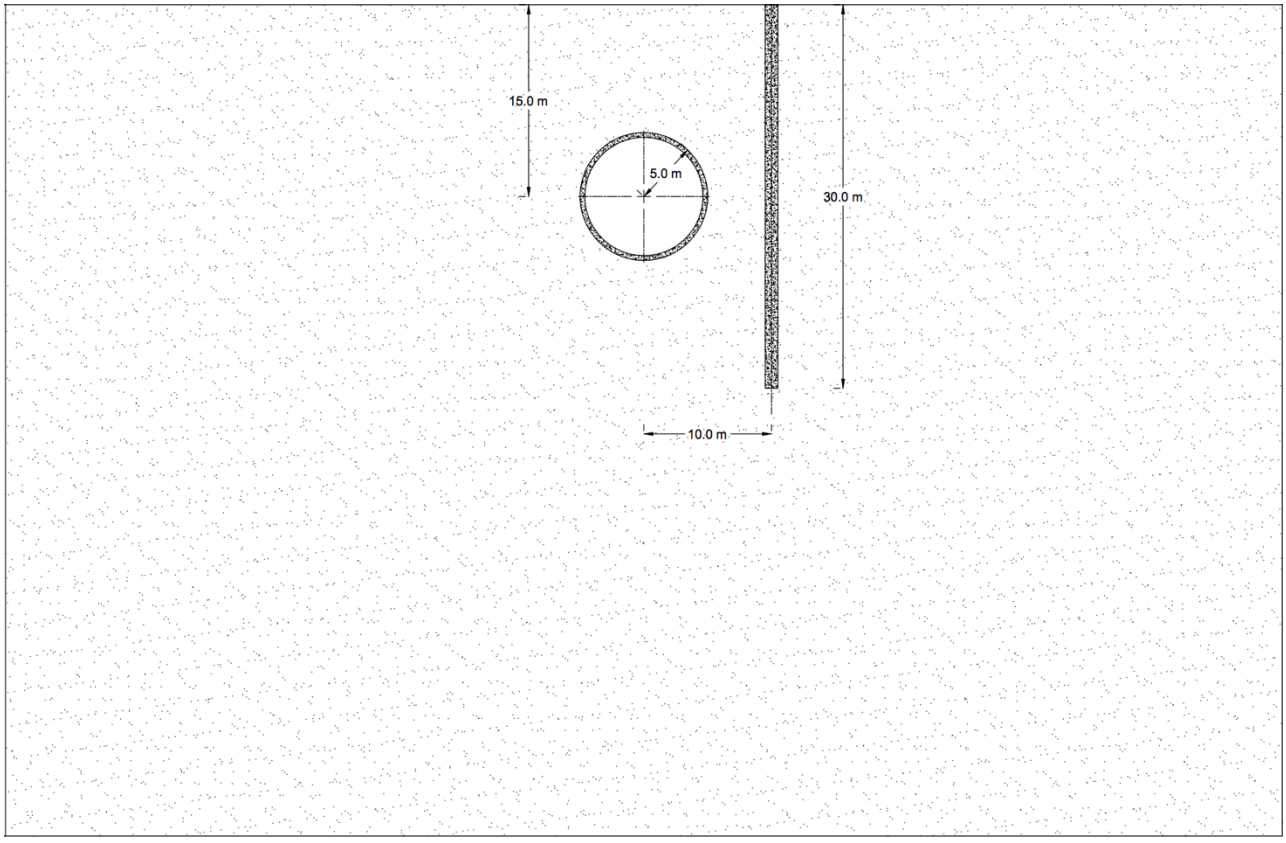

Figure 5. 7.- Drawing corresponding to the installation of the lateral wall of length L = 6R = 30 meters

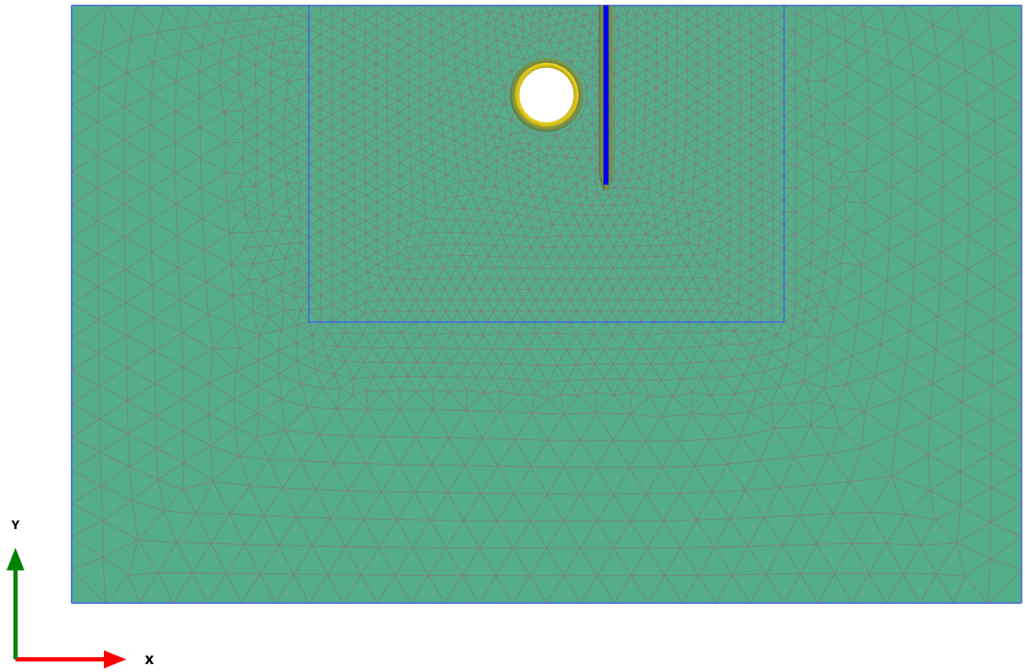

Figure 5. 8.- Plaxis model corresponding to the installation of the lateral wall of length L = 6R = 30 meters

5.3.1. Wall of length L = 8R = 40 m

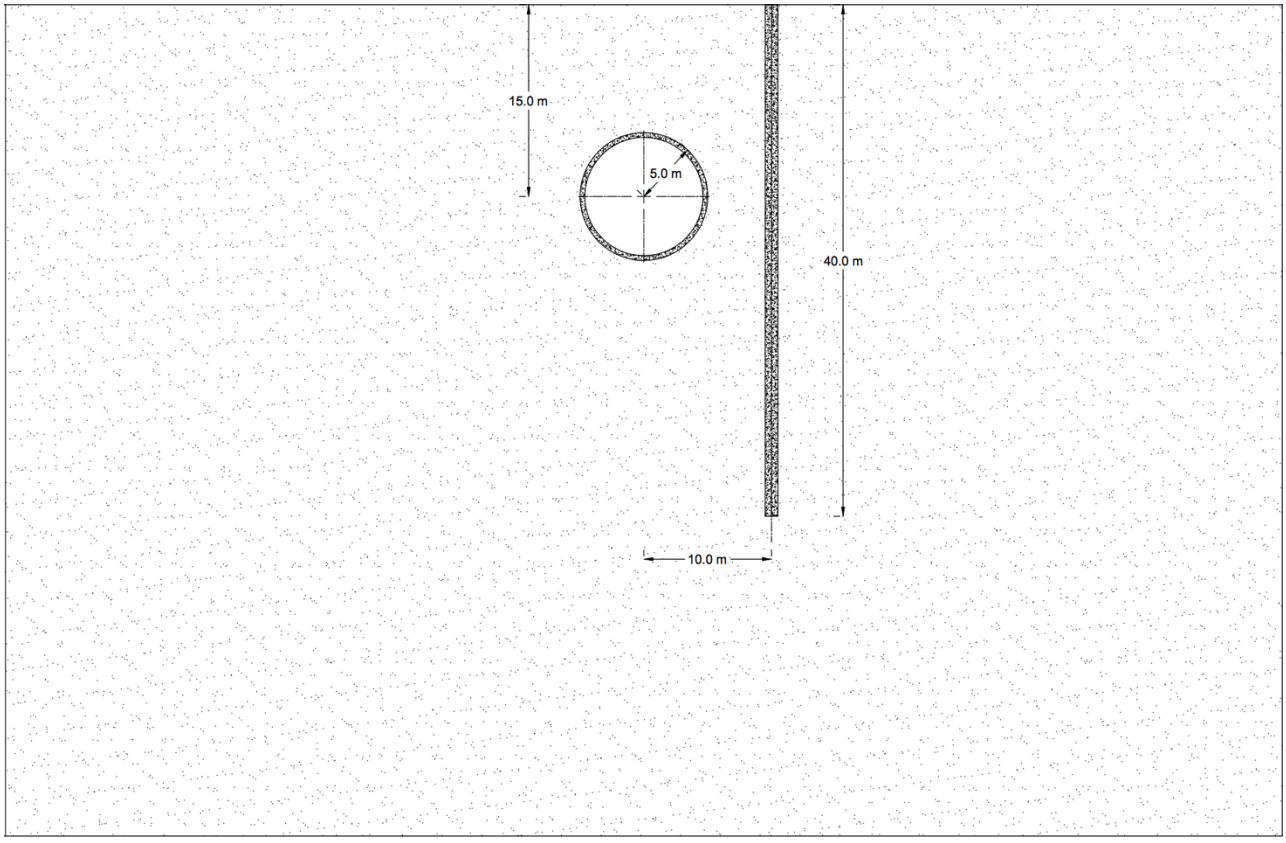

Figure 5. 9.- Drawing corresponding to the installation of the lateral wall of length L = 8R = 40 meters

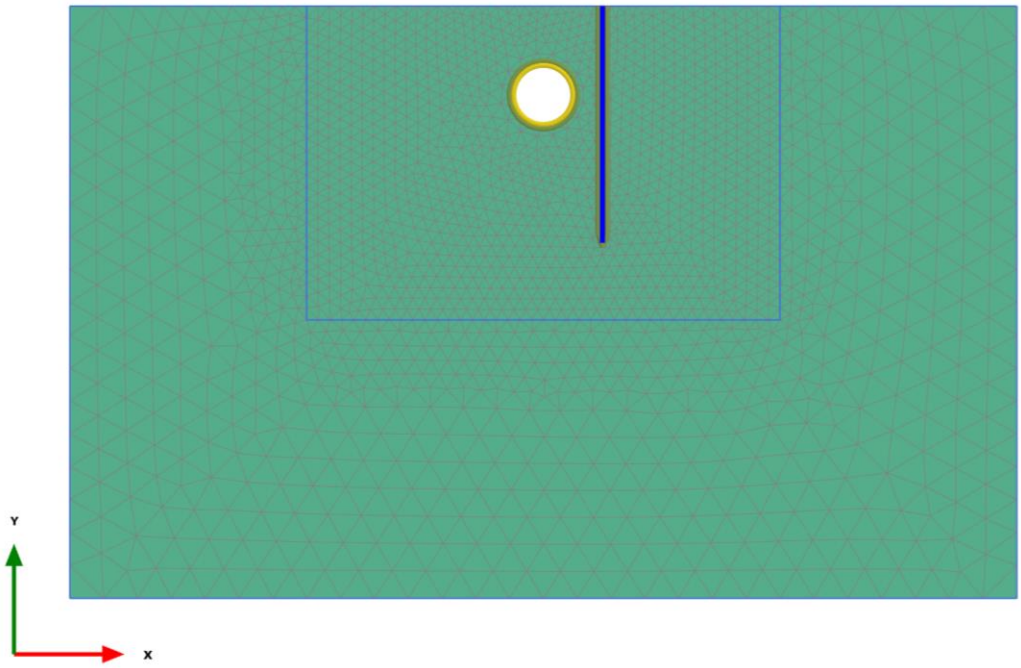

Figure 5. 10.- Plaxis model corresponding to the installation of the lateral wall of length L = 8R = 40 meters

Once the different geometries taken into account in the simulations are presented and discussed it is time to proceed with the results obtained from the simulations. Contour displacements of total, vertical and horizontal movements will be provided.

5.1. Results

In this section of the chapter the results of the finite-element simulations are going to be presented and discussed. Once the basic geometry of the model is finished, the mesh is created. As can be seen in the figures presented above, there is a rectangular shape in which the mesh has been refined in order to obtain a more accurate settlement trough.

Once the mesh is generated the ground flow tab is opened. Due to the fact that in the analytical calculations the ground water table cannot be taken into account, in the case of the simulations, water table is set to be under the excavation.

As explained before, after the initial phase, and in each phase of tunnel excavation the displacements and strains are reset to zero in order to take into consideration only the ground deformations induced by tunnel excavation. In the cases, in which the lateral wall is implemented, this one is constructed prior to the tunnel excavation and both the wall and the interfaces are activated. In the phases in which the tunnel is being excavated, a line contraction corresponding to a ground loss of a 1% is activated as well as a structural element corresponding to a tunnel liner of 0.40 meter-thickness.

In Figure 5.11, the results for the total ground deformations are presented as well as the contour displacements fields.

5.1.1. Total displacements trough

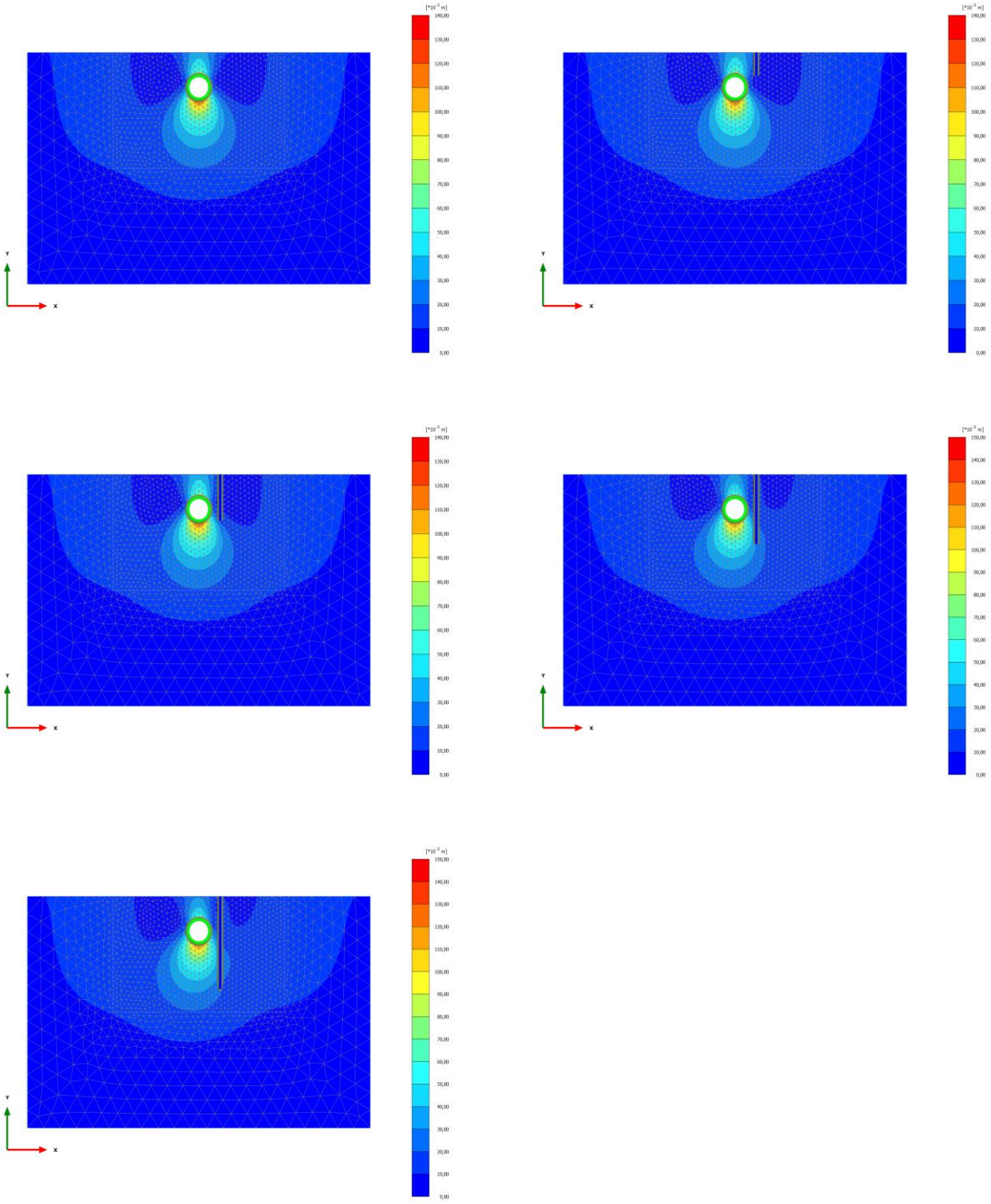

Figure 5. 11.- Total settlement trough for different lateral wall lengths with the properties defined in Table 5.2

In Figure 5.12, the results for vertical ground deformations are presented as well as the contour displacements fields.

5.1.2. Vertical deformation troughs

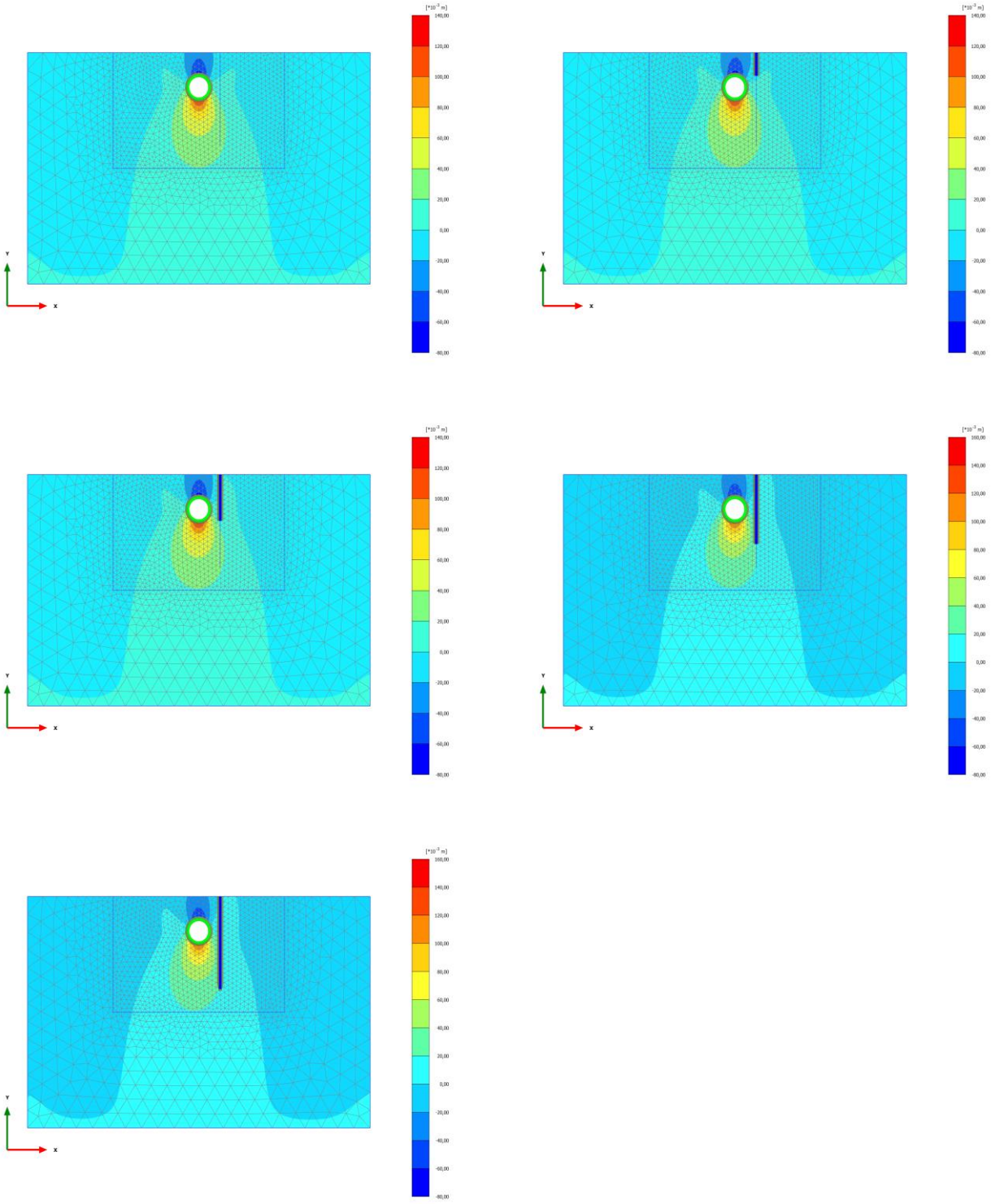

Figure 5. 12.- Vertical settlement trough for different lateral wall lengths with the properties defined in Table 5.2

In Figure 5.13, the results horizontal ground deformations are presented as well as the contour displacements fields.

5.1.3. Horizontal deformation troughs

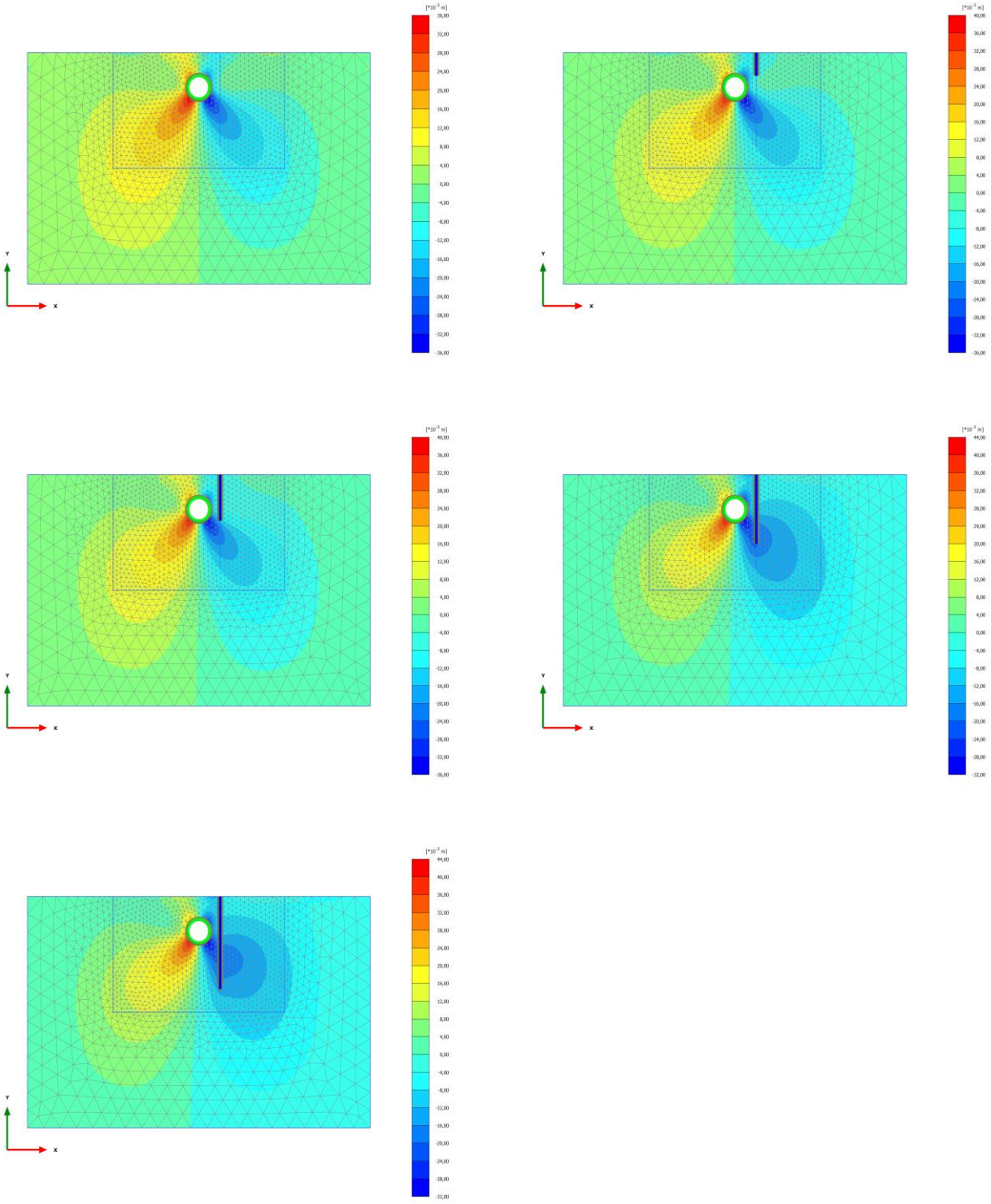

Figure 5. 13.- Horizontal displacement trough for different lateral wall lengths with the properties defined in Table 5.2

5.1.1. General comments on the results

In Figures presented in sections 5.1.1, 5.1.2 and 5.1.3 the contour displacements field for the total displacements as well as both vertical and lateral displacement troughs have been presented. The contour displacements are useful because they give an overall idea of the magnitude of the displacement trough, but then, these results need to be plotted in order to deeply analyse the effect.

In Figure 5.14, the effect of the wall length in the vertical displacement field is plotted against the greenfield displacement curve. As stated in previous sections of this chapter, a linear elastic constitutive model has been used in order to simulate the problem because it is the one that represents in a most accurate way the elastic equations presented for the Melan problem.

However, it needs to be stated that, real problems cannot be solved by means of elasticity because in fact, they are non-linear so, more accurate constitutive models implemented in Plaxis may have been used.

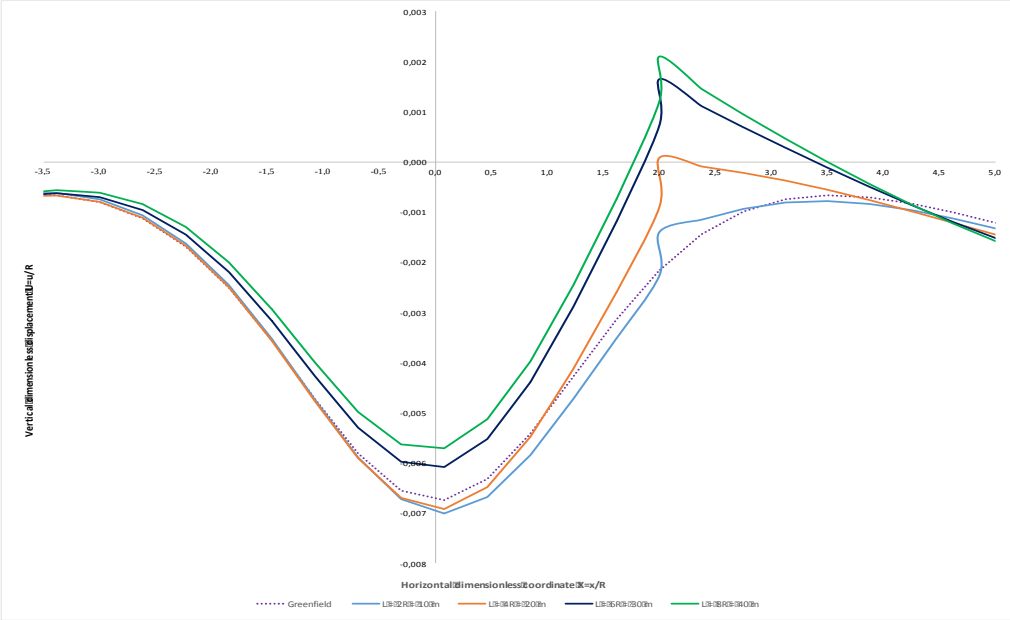

Figure 5. 14.- Effect of wall length length in the vertical displacement trough. Results from Plaxis 2D

Analysing Figure 5.14, it can be clearly noticed the effect of the lateral wall and the effect of its length in the vertical displacement field. However, it needs to be noticed that finite-element simulations carried out by means of an elastic constitutive model are very sensitive to the model boundaries and the results may not represent the reality. However, if the analysis had been carried out by means of a Hardening soil model, which is widely used in terms of geotechnical design, these positive displacements in Figure 5.14 would not exist.

In Figure 5.15, the same analysis has been developed for the lateral displacement trough. The effect of the lateral wall length has been computed against the greenfield curve.

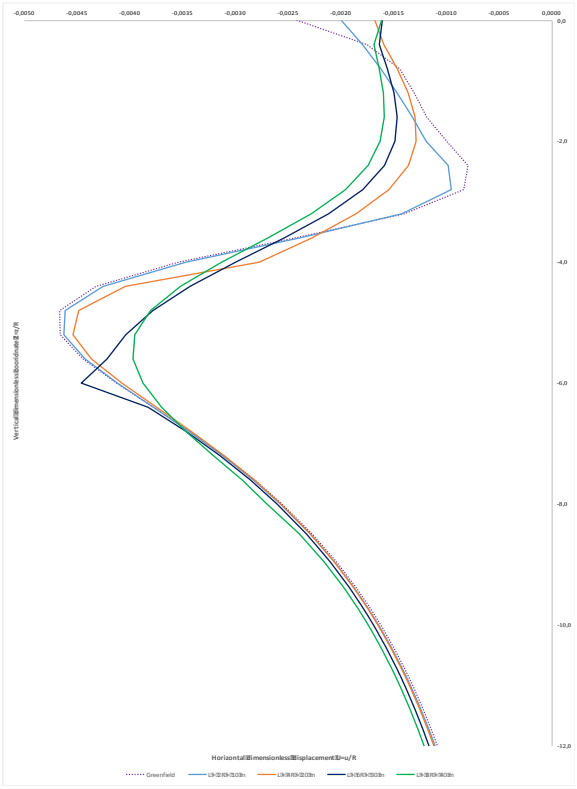

Figure 5. 15.- Effect of wall length length in the lateral displacement trough. Results from Plaxis 2D

In Figure 5.15, the effect of implementing a lateral wall in the horizontal displacements is computed. It can be noticed that the maximum lateral displacement is reduced as the length of the wall is increased. As stated in section 5.2, the effect of the constitutive model also influences the horizontal displacement. If one needs to solve a real problem more sophisticated models need to be applied. In the case concerning this thesis, linear elasticity has been used to make a comparison between the analytical results.

In Chapter 6 a sensitivity analysis is carried out for both vertical and horizontal displacement fields. Also the results of the finite-element simulations are going to be compared with those obtained by means of applying the Melan equations presented in previous chapters of this thesis.

CHAPTER 6

Sensitivity analysis of the results

FINAL MASTER THESIS

6.1. Introduction

From chapter two to four, the basic theory involved throughout this thesis has been presented as well as the formulations and mathematical procedures used to carry out the analytical calculations. Firstly, in chapter two, State of the Art, all the relevant geotechnical data has been analysed and presented. Later on, in the same chapter, some case studies related to structural elements to protect buildings from tunnelling have also been provided and discussed the main conclusions.

In both chapters three and four, the vertical and horizontal displacements are analysed by means of solving the Melan problem. As it has been explained in each chapter, the Melan problem is defined as the problem of a load applied to an inner point in the 2D elastic half-space. By solving this problem, the interaction forces between soil and wall are obtained. Then, by applying the superposition principle of displacements for each force, the soil displacements can be calculated at ground surface. Finally, by adding the greenfield ground displacements calculated by means of Loganathan & Poulos (1998) the final soil displacements are obtained. The goal of this chapter is to develop a sensitivity analysis of the analytical results from both chapters three and four and study the main parameters governing the tunnel-wall interaction problem. In the following sections of the chapter this analysis is developed and the main results are highlighted.

6.2. Vertical displacements

6.2.1. Analytical results (Melan 2D)

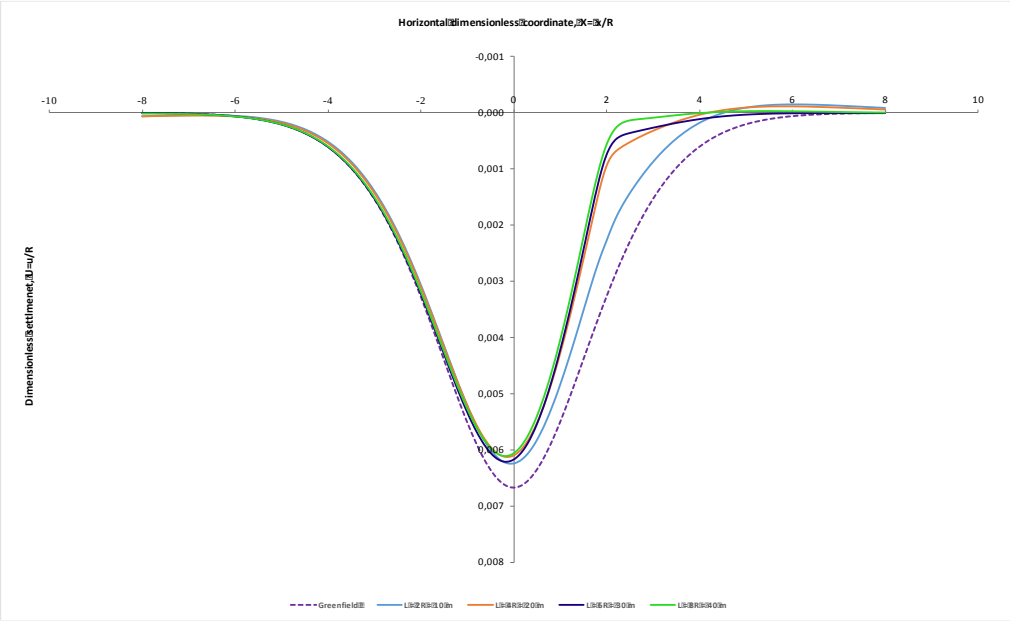

Figure 6. 1.- Effect of wall vertical length on the vertical displacements

In Figure 6.1, the effect of the length of the wall is computed for different values of its it. The purple dashed line belongs to the vertical settlement trough for greenfield conditions. The blue line belongs to the settlement trough for the case of the 2R length meter wall, the orange line belongs to the settlement trough for the case of the 4R length meter wall, the dark-blue line belongs to the settlement trough for the case of the 6R length meter wall and finally the green line belongs to the settlement trough for the case of the 8R length meter wall.

It is trivial to see that as the wall length is increased, the settlements far beyond the wall are reduced so the goal of reducing the vertical settlement trough by means of a lateral wall is reduced. In Table 6.1, the design parameters governing the results provided in Figure 6.1 are presented. This results will be assumed as a starting point, and will be compared with the results obtained by changing parameters such as the tunnel-wall distance and the wall stiffness. (Ledesma & Alonso, 2010)

PARAMETER	UNIT	VALUE
Tunnel radius [R]	meters [m]	5.00
Soil Modulus [E_s]	kilopascals [kPa]	10,000
Tunnel spring line [H]	meters [m]	15.00
Tunnel-wall distance [d]	meters [m]	10.00
Wall Modulus [E_w]	kilopascals [kPa]	20,000,000.00
Wall cross section [A_w]	squared-meter per unit length [m^2/m]	1.00
Wall length / tunnel radius (1)	Dimensionless [-]	2.00
Wall length / tunnel radius (2)	Dimensionless [-]	4.00
Wall length / tunnel radius (3)	Dimensionless [-]	6.00
Wall length / tunnel radius (4)	Dimensionless [-]	8.00
E_sR/E_wA_w [Π_4]	Dimensionless [-]	0.0025

Table 6. 1.- Parameters governing the results presented in Figure 6.1. Case of vertical displacements

It is important also to quantify the efficiency of the wall. As stated in Chapter 2 of this thesis "State of the Art", and as published in Bilota's article, the efficiency of a structural element designed to reduce the settlements induced by tunnelling is calculated with the mathematical expression presented below. This expression is a dimensionless ratio that quantifies the potential of a vertical diaphragm wall to reduce ground movements.

$$\boldsymbol{\eta}[-] = \frac{[S_{ref} - S_{bw}]}{S_{ref}} \tag{6.1}$$

Where $\mathbf{S_{ref}}$ is defined as the settlement trough in greenfield conditions and $\mathbf{S_{bw}}$ is the settlement of the ground surface immediately beyond the diaphragm wall. When $\boldsymbol{\eta}$ is equal to 1 it means that the solution of a diaphragm wall is totally effective whereas when $\boldsymbol{\eta}$ present a value of 0, means that the wall has no positive effect when reducing the settlement trough. In Figure 6.2, the efficiency is computed. (Bilotta, 2008)

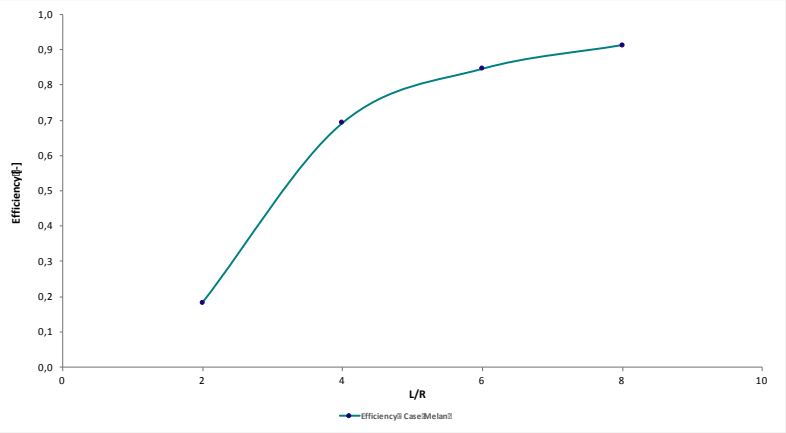

Figure 6. 2.- Efficiency of the wall as a function of the wall length presented in a dimensionless form

In Figure 6.2, the efficiency of the wall is computed for the cases concerning Figure 6.1. For the case of the 20-meter length lateral wall, the efficiency is 69% (Case L = 4R). For this case, the wall tip is located at the level of the tunnel invert. It can be concluded that lateral walls designed to mitigate ground displacements present acceptable levels of efficiency when their wall tip is located below the tunnel invert. (Ledesma & Alonso, 2010)

Hence, it can be concluded that the parameter governing the wall efficiency is the displacement at its tip. For cases in which the lateral wall has its tip above the tunnel invert, both the tip and wall head will suffer excessive ground displacements when the tunnelling works are carried out. In conclusion it can be assured, that increasing the wall length is an effective measure when the aim is to reduce the vertical displacement trough.

Another point to highlight, which also has been commented in the corresponding chapter, is that the symmetry of the displacement trough is lost when the wall is constructed. Furthermore, the maximum value for the settlement trough is moved in the opposite direction in which the wall is installed. This phenomenon is accentuated for the cases in which the lateral wall increases its length. For the following sections the effect of the wall stiffness and the tunnel-wall distance is going to be analysed and discussed. (Ledesma & Alonso, 2010)

6.2.1.1. Effect of the wall stiffness

The dimensionless parameter that controls the stiffness of the lateral wall is defined in equation 6.2, where all the variables have been presented and defined in Table 6.1.

$$\Pi_4[-] = \frac{E_s R}{E_w A_w} \tag{6.2}$$

In order to study the influence of the wall stiffness, this dimensionless parameter has been changed keeping constant the remaining parameters. In conclusion, as varying the value of this parameter, different values of the wall modulus can be easily obtained. These values of the wall modulus are presented in the Table 6.2.

PARAMETER	UNIT	VALUE	WALL MODULUS [kPa]
E_sR/E_wA_w $[\Pi_4]$ (1)	Dimensionless [-]	0.25	200,000.00
E_sR/E_wA_w $[\Pi_4]$ (2)	Dimensionless [-]	0.025	2,000,000.00
E_sR/E_wA_w $[\Pi_4]$ (3)	Dimensionless [-]	0.0025	20,000000.00
E_sR/E_wA_w $[\Pi_4]$ (4)	Dimensionless [-]	0.000025	2,000,000,000.00

Table 6. 2.- Different values of the wall modulus that have been considered for the sensitivity analysis

In Figures 6.3 to 6.6, the effect of the soil-wall relative stiffness in the settlement trough is presented. The calculations have been carried out for all wall lengths in order to analyse if the wall length has any influence in the settlement troughs.

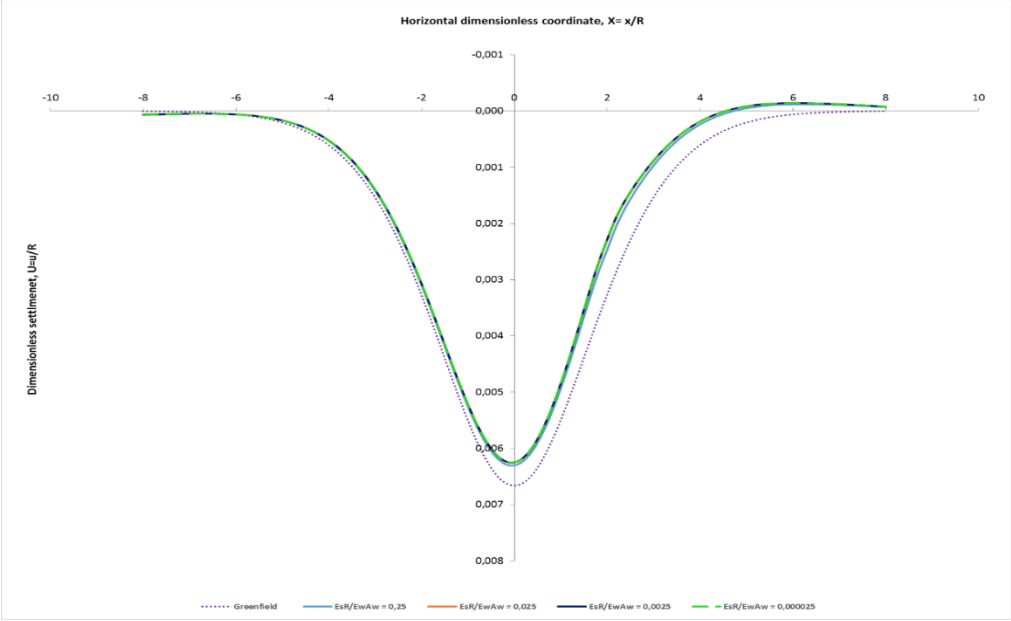

Figure 6. 3.- Effect of the soil-wall relative stiffness on the settlement trough for the 10-meter length lateral wall

As can be noticed analysing the figures presented, in which the settlement troughs are presented for different values of the dimensionless parameter, the soil-wall relative stiffness also is influenced by the wall length. As stated in previous sections of this chapter, for those values of length lower than the tunnel invert depth, the effect of the soil-wall relative stiffness is almost imperceptible. However, when the lateral wall has its tip below the tunnel invert, the effects of the relative stiffness are more evident. (Ledesma & Alonso, 2010)

Despite that, it can be noticed that there is a certain value of the wall stiffness from which the settlement troughs calculated at ground surface do not show significant changes.

So in a different way, it is proved that, ground movements at ground surface are governed by the movement experienced suffered by the wall tip. Hence, in a practical way, it is more efficient to increase the length of the lateral wall rather than increasing its modulus.

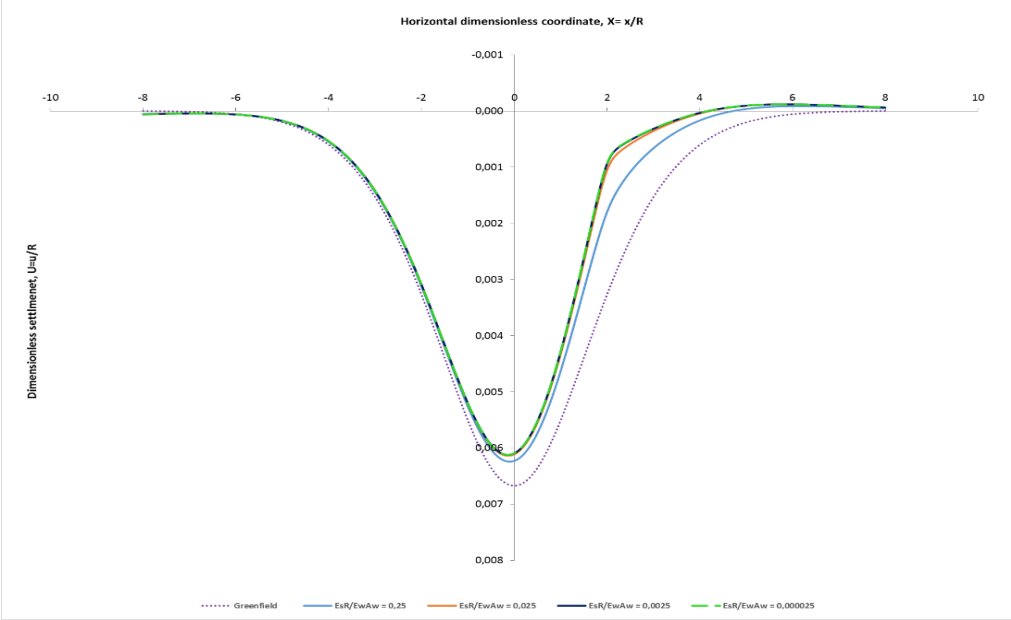

Figure 6. 4.- Effect of the soil-wall relative stiffness on the settlement trough for the 20-meter length lateral wall

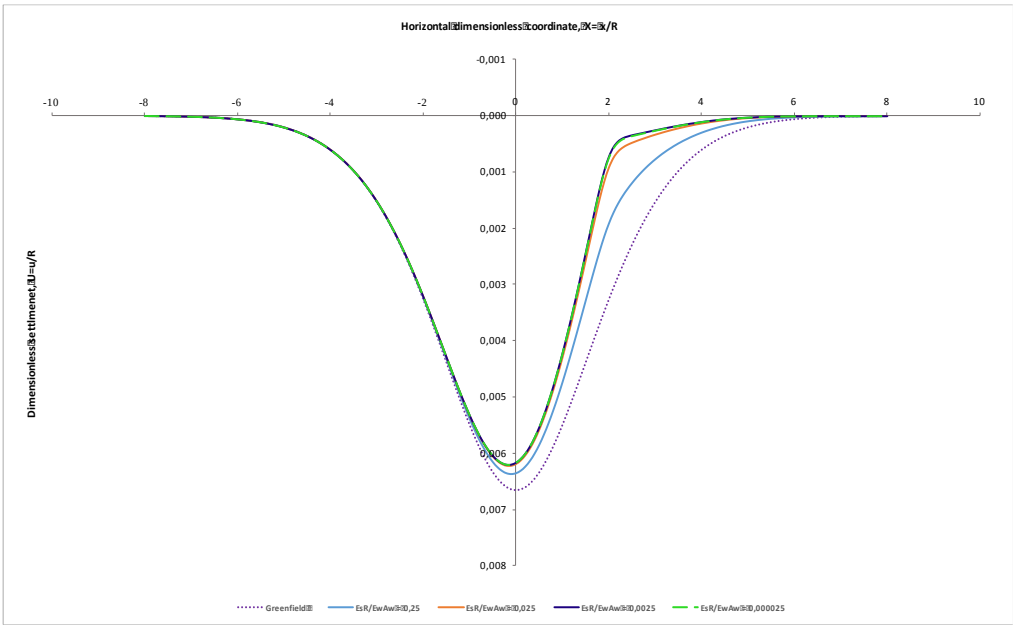

Figure 6. 5.- Effect of the soil-wall relative stiffness on the settlement trough for the 30-meter length lateral wall

It is important also to quantify the efficiency of the wall when the relative soil-wall stiffness is modified. As stated in Chapter 2 of this thesis "State of the Art" and in previous sections of this document, the efficiency of a structural element designed to reduce the settlements induced by tunnelling is calculated with the mathematical expression presented in equation 6.1. This expression is a dimensionless ratio that quantifies the potential of a vertical diaphragm wall to reduce ground movements. As noticed above, the efficiency has been computed for all the wall lengths studied in this thesis in order to analyse its contribution to the efficiency. (Bilotta, 2008)

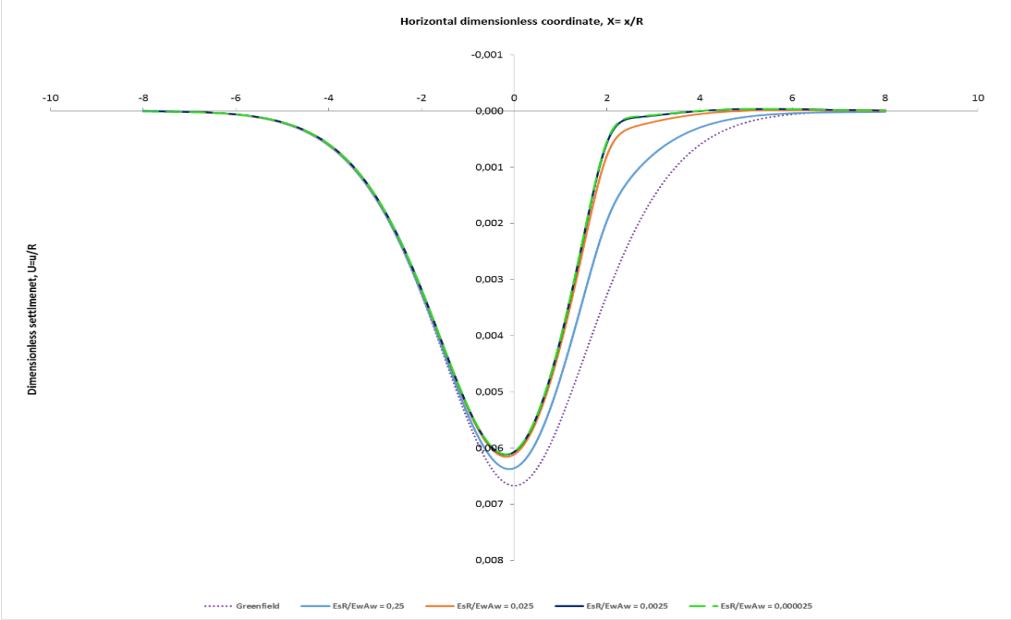

Figure 6. 6.- Effect of the soil-wall relative stiffness on the settlement trough for the 40-meter length lateral wall

In Figure 6.7, the efficiency is computed and presented. As can be noticed, as higher as the lateral wall is, more efficiency presents. Also it can be seen that, for values of the dimensionless parameter lower than 0.0025, the effect of the wall modulus in the efficiency is almost imperceptible. (Ledesma & Alonso, 2010)

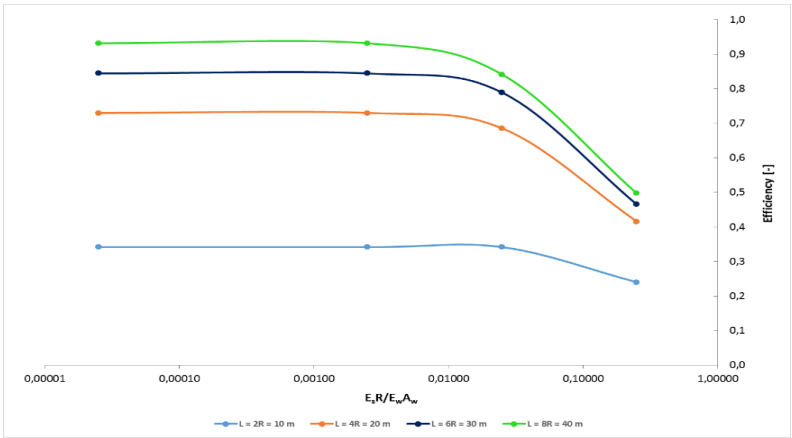

Figure 6. 7.- Efficiency against dimensionless parameter [Π_4] for the different lateral wall lengths

6.2.1.2. Effect of the tunnel-wall distance

As stated before, the sensitivity analysis provided in this section involves the study of different variables. For the case concerning this section, the influence of the tunnel-wall distance has been studied. The dimensionless parameter that controls the influence of the tunnel-wall distance is presented in Equation 6.3:

$$\mathbf{\Pi_2}[-] = \frac{\mathrm{d}}{\mathrm{R}} \tag{6.3}$$

In order to study the influence of the wall stiffness, this dimensionless parameter has been changed keeping constant the remaining parameters. In conclusion, as varying the value of this parameter, different values of the tunnel-wall distance can easily be obtained. These values are presented in the Table 6.3.

PARAMETER	UNIT	VALUE	TUNNEL-WALL DISTANCE [m]
$d/R\ [\Pi_2]$ (1)	Dimensionless [-]	1.25	6.25
$d/R\ [\Pi_2]$ (2)	Dimensionless [-]	1.50	7.50
$d/R\ [\Pi_2]$ (3)	Dimensionless [-]	2.00	10.00
$d/R\ [\Pi_2]$ (4)	Dimensionless [-]	2.50	12.50
$d/R\ [\Pi_2]$ (5)	Dimensionless [-]	3.00	15.00

Table 6. 3.- Different values of the tunnel-wall distance that have been considered for the sensitivity analysis

In Figure 6.8 to 6.11, the effect of the tunnel wall distance in the settlement trough is presented. The calculations have been carried out for all wall lengths considered in this thesis in order to analyse the effects that the length may induce.

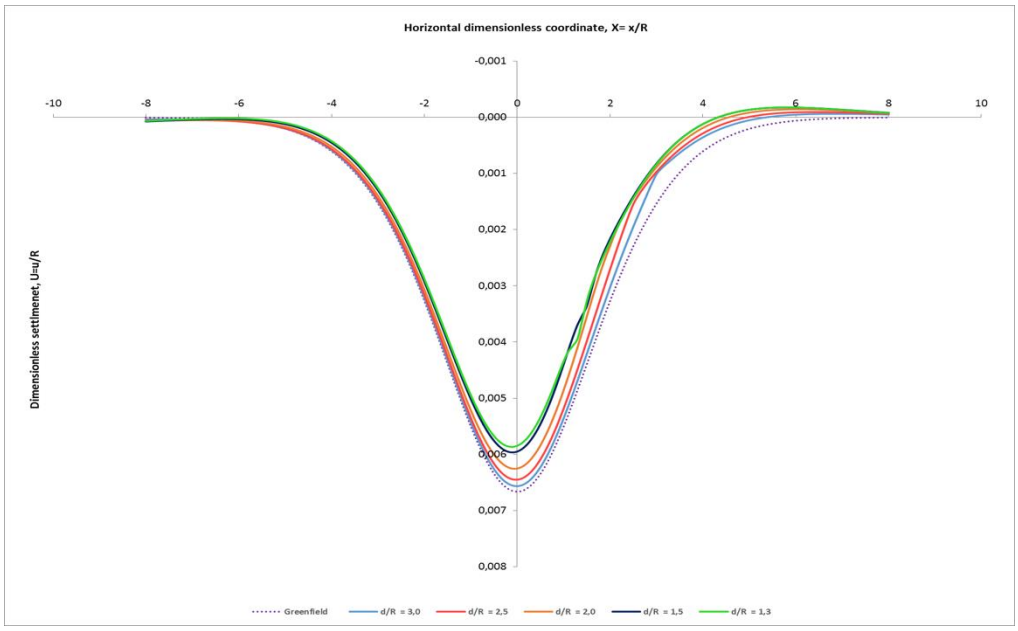

Figure 6. 8.- Effect of the tunnel-wall distance on the settlement trough for a 10-meter lateral wall length

As can be noticed analysing the figures presented, in which the settlement troughs are presented for different values of the dimensionless parameter, the tunnel-wall distance is also influenced by the wall length. As stated in previous sections of this chapter, for those values of length lower than the tunnel invert depth, the effect of the tunnel-wall distance is almost imperceptible (see Figure 6.8). However, when the lateral wall has its tip below the tunnel invert, the effects are more evident. (Ledesma & Alonso, 2010)

However, for all the cases analysed, varying the tunnel-wall distance, does not affect substantially in the efficiency diagram as it can be seen Figure 6.12.

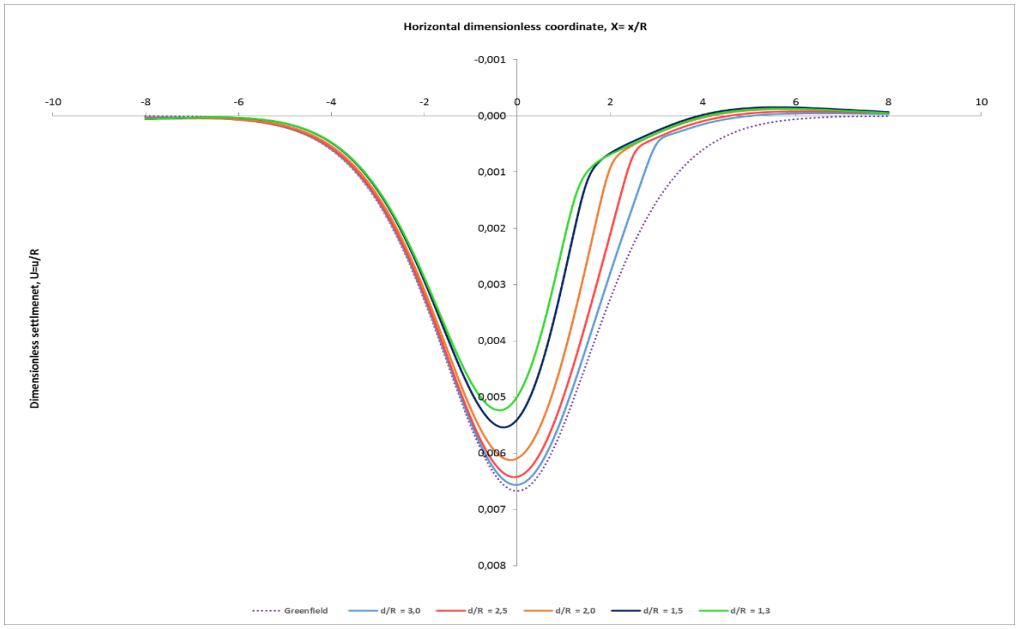

Figure 6. 9.- Effect of the tunnel-wall distance on the settlement trough for a 20-meter lateral wall length

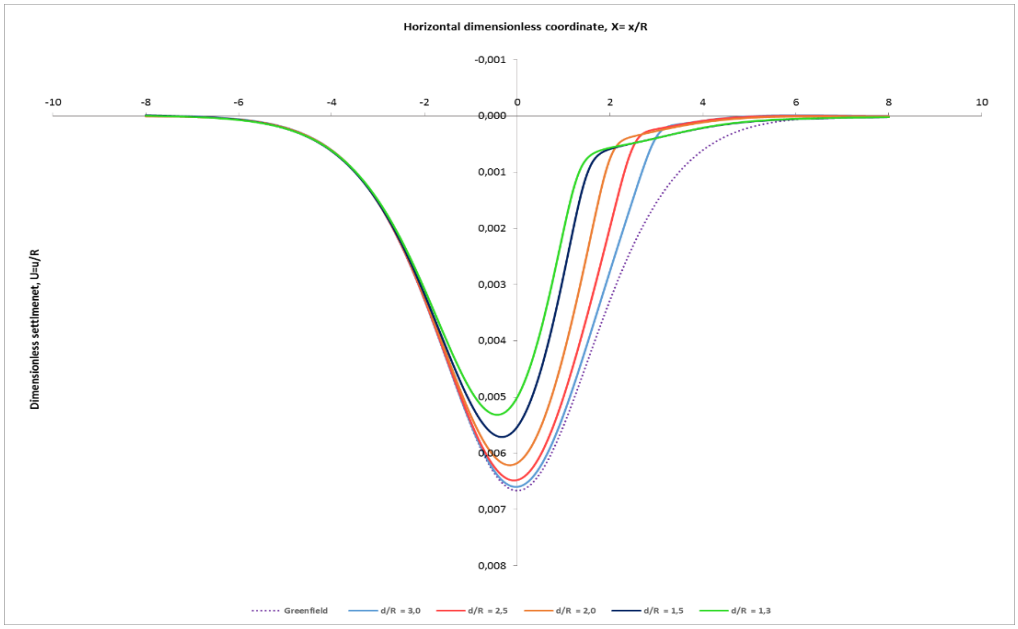

Figure 6. 10.- Effect of the tunnel-wall distance on the settlement trough for a 30-meter lateral wall length

For all the cases presented, as commented in previous results, the symmetry of the vertical displacement trough is lost when the wall is implemented. Furthermore, for the same value of wall length, as the tunnel-wall distance is reduced, the maximum of the vertical displacement trough is drastically reduced. However, in terms of settlement far beyond the wall there are not substantial variations. (Ledesma & Alonso, 2010)

As happens with previus calculations, varying the tunnel-wall distance also affect to the position of the maximum value of the displacement which is moved to the left from respect to the settlement trough axis.

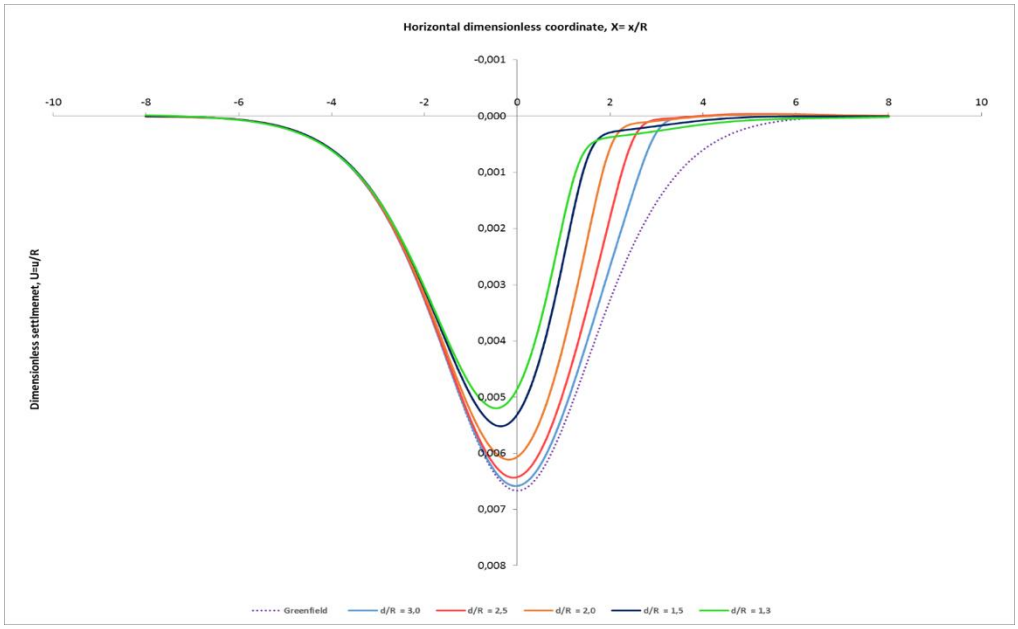

Figure 6. 11.- Effect of the tunnel-wall distance on the settlement trough for a 40-meter lateral wall length

In Figure 6.12, the efficiency is computed and presented. As can be noticed, as higher as the lateral wall is, more efficiency presents. Also it can be seen that, the influence of the tunnel-wall distance do not significantly affect in the wall efficiency as the curves remain almost constant for each wall length. (Bilotta, 2008)

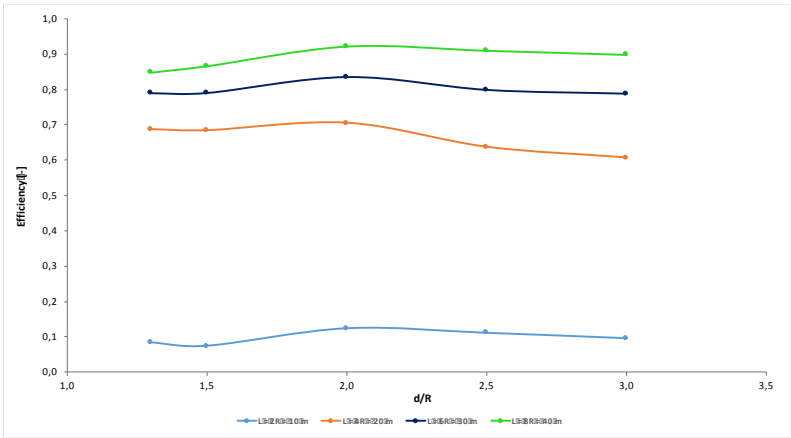

Figure 6. 12.- Efficiency as a function of the of the wall tunnel-distance, d, for all lateral wall length cases

In section 6.3 the sensitivity analysis will be carried out for the results obtained from the analysis of lateral displacements due to both lateral and vertical loads.

6.3. Horizontal displacements

6.3.1. Analytical results (Melan 2D). Lateral displacements due to lateral loads

In the current section of the chapter the lateral displacements due to lateral loads is analysed.

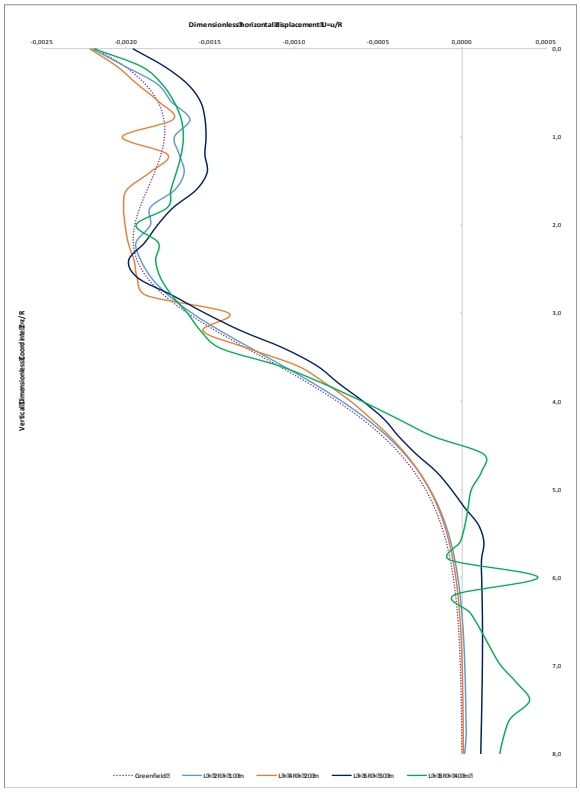

Figure 6. 13.- Effect of the wall length in the lateral displacement trough

In Figure 6.13, the effect of the wall length is computed for different values of it for the case of lateral displacements due to lateral loads. As in the case of vertical displacements due to vertical loads, the purple dashed line belongs to the lateral displacement trough for greenfield conditions.

The blue line belongs to the lateral displacement for the case of the 2R length wall, the orange line belongs belongs to the displacement trough for the case of 4R lateral displacement trough, the dark-blue line belongs to the settlement trough for the case of the 6R length meter wall and finally the green line belongs to the settlement trough for the case of 8R meter length wall.

As was stated for the case of vertical displacement troughs, the symmetry of the displacements field was lost when the lateral wall was implemented while in greenfield conditions the vertical displacement field was symmetric. For the case of lateral displacements, it can be concluded having a deeper look at Figure 6.13, that the symmetry is lost not only when no structural element is built.

In the Table 6.4, the design parameters governing the results provided in Table 6.13 are presented. This results will be assumed as a starting point, and will be compared with the results obtained by changing parameters such as the tunnel-wall distance and the wall stiffness. The goal of carrying out the sensitivity analysis is to determine the parameters governing the ground displacements fields and analyse the limiting values of them.

PARAMETER	UNIT	VALUE
Tunnel radius [R]	meters [m]	5.00
Soil Modulus [E_s]	kilopascals [kPa]	10,000
Tunnel spring line [H]	meters [m]	15.00
Tunnel-wall distance [d]	meters [m]	10.00
Wall Modulus [E_w]	kilopascals [kPa]	20,000,000.00
Wall cross section [A_w]	squared-meter per unit length [m^2/m]	1.00
Wall length / tunnel radius (1)	Dimensionless [-]	2.00
Wall length / tunnel radius (2)	Dimensionless [-]	4.00
Wall length / tunnel radius (3)	Dimensionless [-]	6.00
Wall length / tunnel radius (4)	Dimensionless [-]	8.00
E_sR/E_wA_w [Π_4]	Dimensionless [-]	0.0025

Table 6. 4.- Parameters governing the results presented in Figure 6.13. Case of lateral displacements

In the following sections of this chapter a sensitivity analysis of the results is carried out varying the main parameters that can govern the lateral displacement field in the same way as it has been done for the vertical displacement case. The main parameters controlling the displacement fields are the wall stiffness and the tunnel-wall distance. Hence, by varying this parameters one can analyse how the displacement troughs are affected and modified.

Furthermore, it is important also to quantify the efficiency of the wall as in previous sections. The mathematical expression governing the efficiency of it is presented in Equation 6.4. (Bilotta, 2008)

$$\boldsymbol{\eta}[-] = \frac{[S_{ref} - S_{bw}]}{S_{ref}} \tag{6.4}$$

Where $\mathbf{S_{ref}}$ is defined as the settlement trough in greenfield conditions and $\mathbf{S_{bw}}$ is the settlement of the ground surface immediately beyond the diaphragm wall. When $\boldsymbol{\eta}$ is equal to 1 it means that the solution of a diaphragm wall is totally effective whereas when $\boldsymbol{\eta}$ present a value of 0, means that the wall has no positive effect when reducing the settlement trough. For the following sections the efficiency of the wall will be computed and discussed.

6.3.1.1. Effect of the wall stiffness

In order to compute the effect of the wall stiffness it has been proceed in the same way as for the case of vertical displacements. The dimensionless parameter that controls the stiffness of the lateral wall is defined in Equation 6.5. (Ledesma & Alonso, 2010)

$$\Pi_4[-] = \frac{E_s R}{E_w A_w} \tag{6.5}$$

So modifying the value of the dimensionless parameter presented in Equation 6.5 and keeping constant the remaining parameters, different values for the wall stiffness are obtained leading to compute de lateral displacements for different values of stiffness. The different values used for the calculations are the ones presented in the Table 6.5:

PARAMETER	UNIT	VALUE	WALL MODULUS [kPa]
E_sR/E_wA_w $[\Pi_4]$ (1)	Dimensionless [-]	0.25	200,000.00
E_sR/E_wA_w $[\Pi_4]$ (2)	Dimensionless [-]	0.025	2,000,000.00
E_sR/E_wA_w $[\Pi_4]$ (3)	Dimensionless [-]	0.0025	20,000000.00
E_sR/E_wA_w $[\Pi_4]$ (4)	Dimensionless [-]	0.000025	2,000,000,000.00

Table 6. 5.- Different values of the wall modulus that have been considered for the sensitivity analysis

With all preliminary explanations finished, it is time to present the results. In Figures 6.14 to 6.15, the effect of the soil-wall relative stiffness is computed analysing its effect on the lateral displacement field. The calculations have been carried out for walls of 10, 20 and 30-meter long.

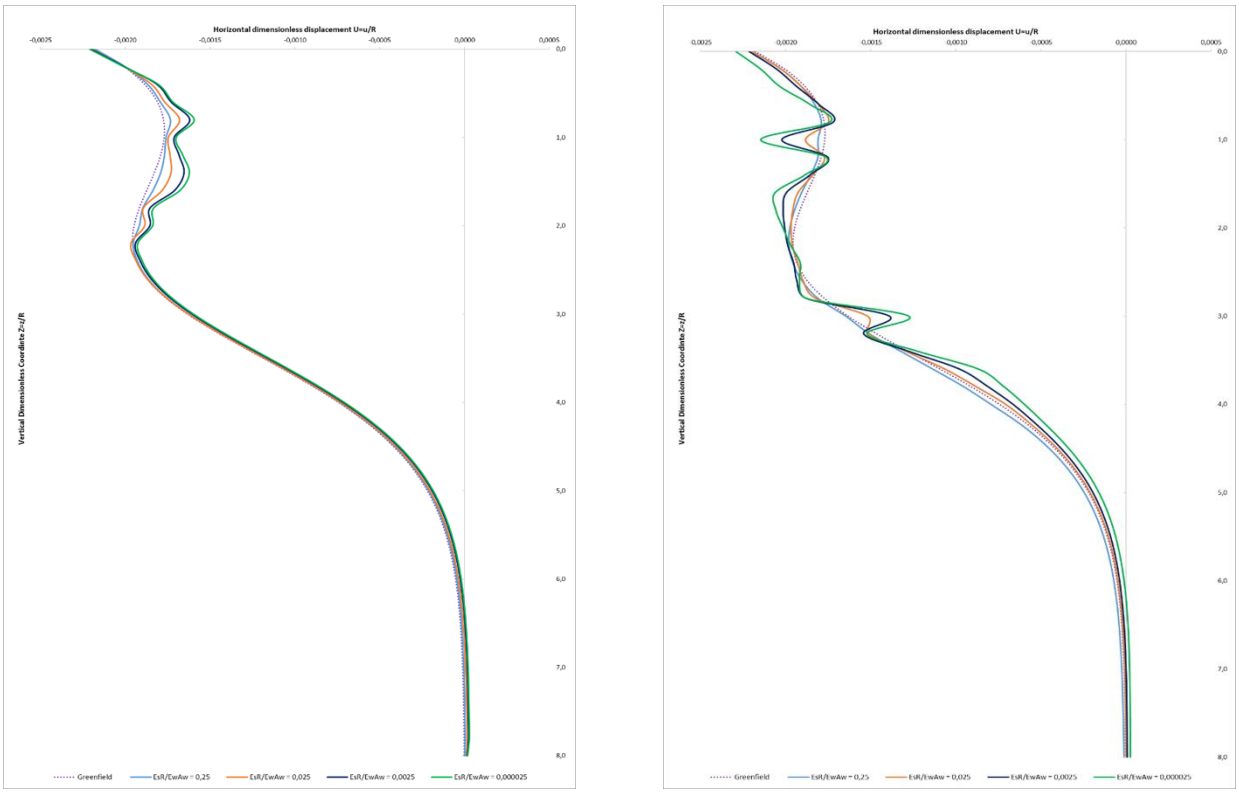

Figure 6. 14.- Influence of the soil wall relative stiffness for a 10 and 20-meter lateral wall

The Figures presented above correspond to the lateral displacements due to a 10 and 20-meter wall length.

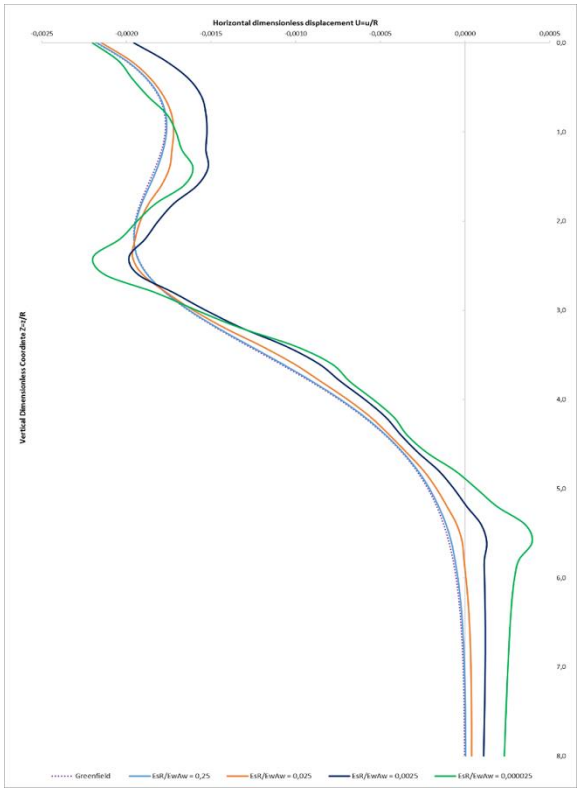

Figure 6. 15.- Influence of the soil wall relative stiffness for a 30-meter lateral wall

In Figure 6.16, the efficiency is computed and presented. As can be noticed, as higher as the lateral wall is, more efficiency presents. Also it can be seen that, in general the efficiencies computed are quite low for lateral displacements and that from a value of Π_4 = 0,0025, the efficiency does not suffer perceptible changes.

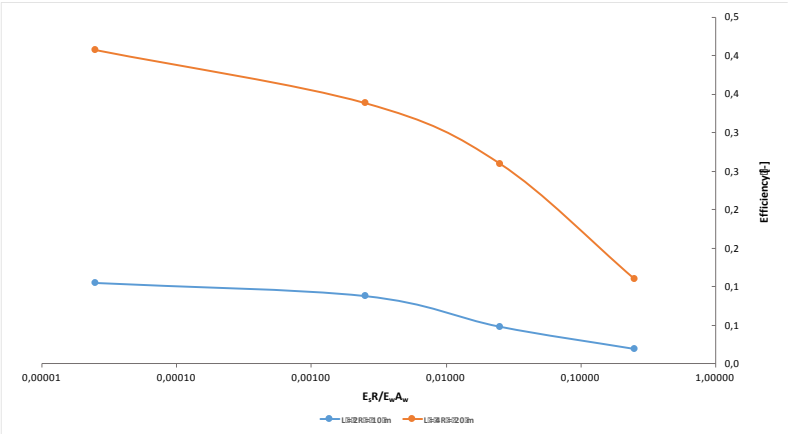

Figure 6. 16.- Efficiency against dimensionless parameter [Π_4] for the 10 and 20-meter wall length

6.3.1.1. Effect of the tunnel-wall distance

In the following section of the current chapter the influence in the lateral displacement trough of the tunnel-wall distance is going to be computed and presented.

The dimensionless parameter that controls the influence of the tunnel-wall distance is governed by the dimensionless ratio presented in Equation 6.6: (Ledesma & Alonso, 2010)

$$\boldsymbol{\Pi_2}[-] = \frac{\mathrm{d}}{\mathrm{R}} \tag{6.6}$$

So modifying the value of the dimensionless parameter presented in Equation 6.6 and keeping constant the remaining parameters, different values for tune tunnel-wall distance are obtained leading to compute de lateral displacements for different values of distance. The different values used for the calculations are the ones presented in the Table 6.6:

PARAMETER	UNIT	VALUE	TUNNEL-WALL DISTANCE [m]
$d/R\ [\Pi_2]$ (1)	Dimensionless [-]	1.25	6.25
$d/R\ [\Pi_2]$ (2)	Dimensionless [-]	1.50	7.50
$d/R\ [\Pi_2]$ (3)	Dimensionless [-]	2.00	10.00
$d/R\ [\Pi_2]$ (4)	Dimensionless [-]	2.50	12.50
$d/R\ [\Pi_2]$ (5)	Dimensionless [-]	3.00	15.00

Table 6. 6.- Different values of the tunnel-wall distance that have been considered for the sensitivity analysis

In Figures 6.17 to 6.18, the effect of the tunnel wall distance in the settlement trough is presented.

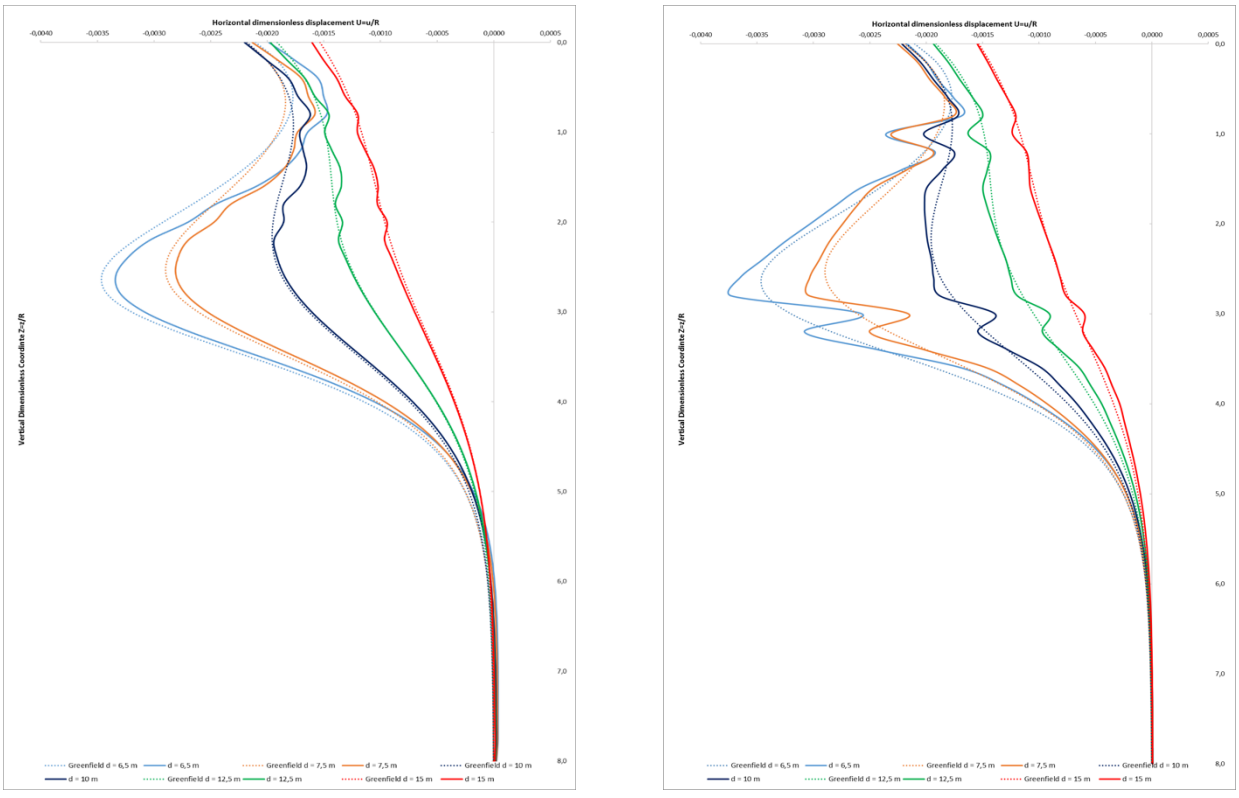

Figure 6. 17.- Influence of the tunnel wall distance for a 10 and 20-meter lateral wall

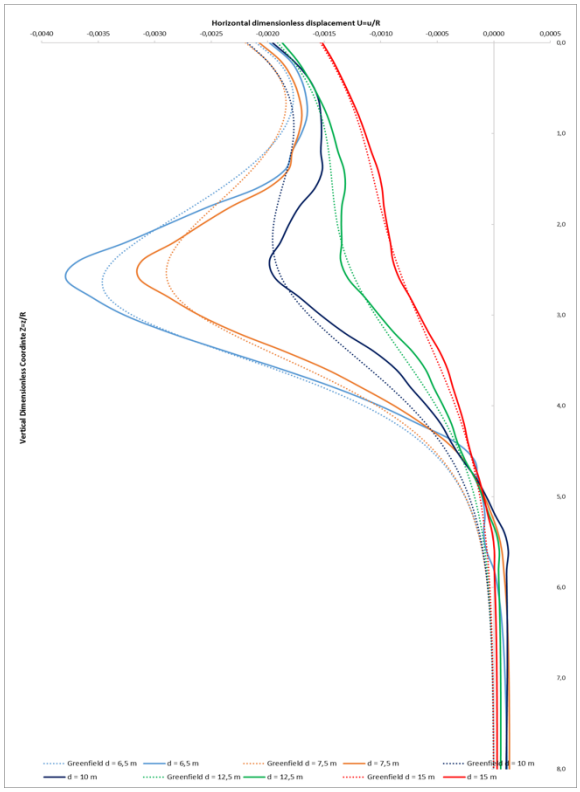

Figure 6. 18.- Influence of the tunnel wall distance for a 30-meter lateral wall

In Figure 6.19, the efficiency is computed and presented. As can be noticed, as higher as the lateral wall is, more efficiency presents. Also it can be seen that, as far from the tunnel axis the wall is located, lower efficiency presents which is consistent with the results obtained.

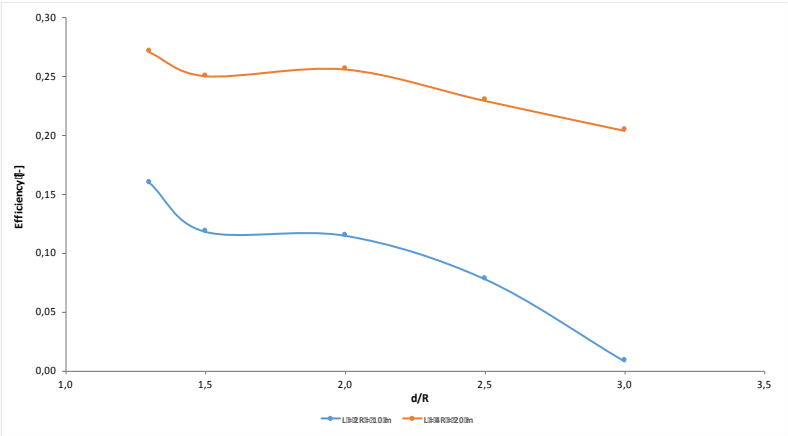

Figure 6. 19.- Efficiency against dimensionless ratio of tunnel-wall distance, d, for 10 and 20-meter wall lenght

6.3.2. Analytical results (Melan 2D). Lateral displacements due to vertical loads

As it can be expected when the soil is deformed by a load acting in the vertical direction, the same force can provide a lateral effect deforming the soil horizontally. The aim of this section is to analyse this phenomenon.

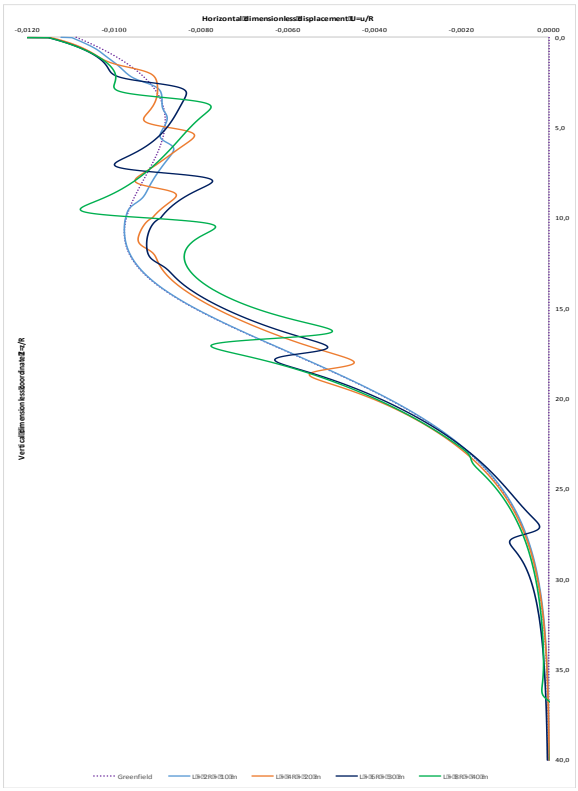

Figure 6. 20.- Effect of vertical loads (from chapter 3) in the horizontal displacement field

Figure 6.20 provides the lateral deformation due to vertical loads. In general terms one can be noticed that the main effect is produced in the tunnel centreline and not in the ground surface. Furthermore, the tip displacement remains almost constant which is not the case of the lateral displacements due to lateral loads.

As it can be seen in the plot and in previous sections, the dashed purple line belongs to the greenfield conditions, the blue line belongs to the wall length of 10 meters, the orange one to the wall length of 20 meters, the dark-blue one to the wall length of 30 meters and finally the green one to the 40-meter lateral wall.

In general comments it is important to highlight again the non-symmetry of the displacement trough and also that as wall the length is increased the lateral displacements suffered at the tunnel centre line are reduced due to the wall effect. As in previous chapters, the sensitivity analysis has been carried out by means of analysing the main parameters governing the displacement troughs which are the wall stiffness and the tunnel-wall distance.

6.3.2.1. Effect of the wall stiffness

In this sections of the chapters the influence of the soil-wall relative stiffness is computed by means of applying the dimensionless ratio controlling this parameter and defined in equation 6.5. By changing this dimensionless ratio one can obtain different values of the wall stiffness and proceed.

The values of the wall Young Modulus are the ones presented in Table 6.7, which at the same time are the same of previous sections. In Figures 6.21 to 6.22, the results for each wall length are provided analysing the impact of the soil-wall relative stiffness in the lateral displacement trough.

PARAMETER	UNIT	VALUE	WALL MODULUS [kPa]
E_sR/E_wA_w $[\Pi_4]$ (1)	Dimensionless [-]	0.25	200,000.00
E_sR/E_wA_w $[\Pi_4]$ (2)	Dimensionless [-]	0.025	2,000,000.00
E_sR/E_wA_w $[\Pi_4]$ (3)	Dimensionless [-]	0.0025	20,000000.00
E_sR/E_wA_w $[\Pi_4]$ (4)	Dimensionless [-]	0.000025	2,000,000,000.00

Table 6. 7.- Different values of the wall modulus that have been considered for the sensitivity analysis

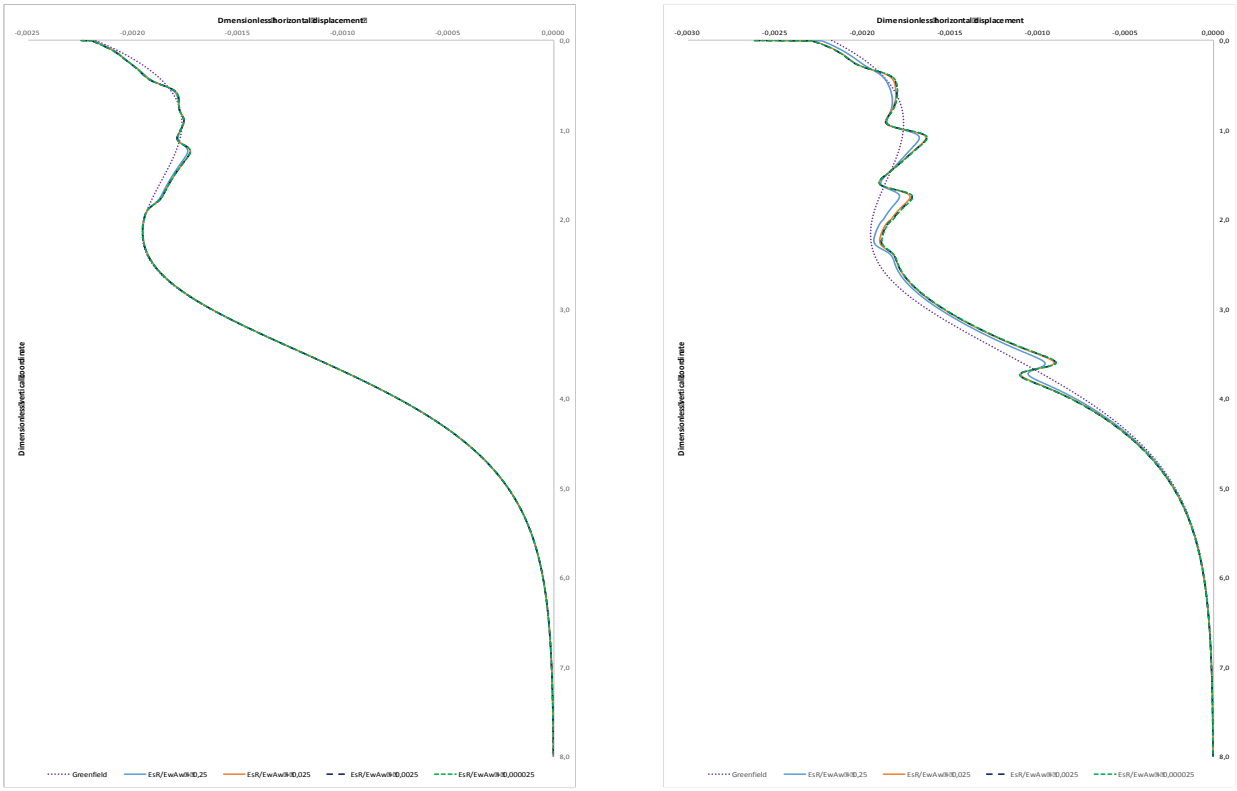

Figure 6. 21.- Effect of the soil-wall relative stiffness for the case of 10 and 20-meter wall length

In Figure 6.21 the influence of the wall length (10 and 20 meter-length) has been provided for the different values of the dimensionless ratio that controls the soil-wall relative stiffness. In Figure 6.22 the influence of a 30 and 40-meter lateral length displacement troughs are presented. In general, it can be observed that there is a limiting value for the wall stiffness from which the lateral displacement trough is not improved hence, the efficiency does not increase. The limiting condition is for the case of **E_w = 20 GPa.**

In addition, it is important to compute the efficiency that the lateral wall has in order to achieve the goal of reducing the ground displacements. The efficiency is computed by means of applying equation 6.4 presented in previous sections of this document.

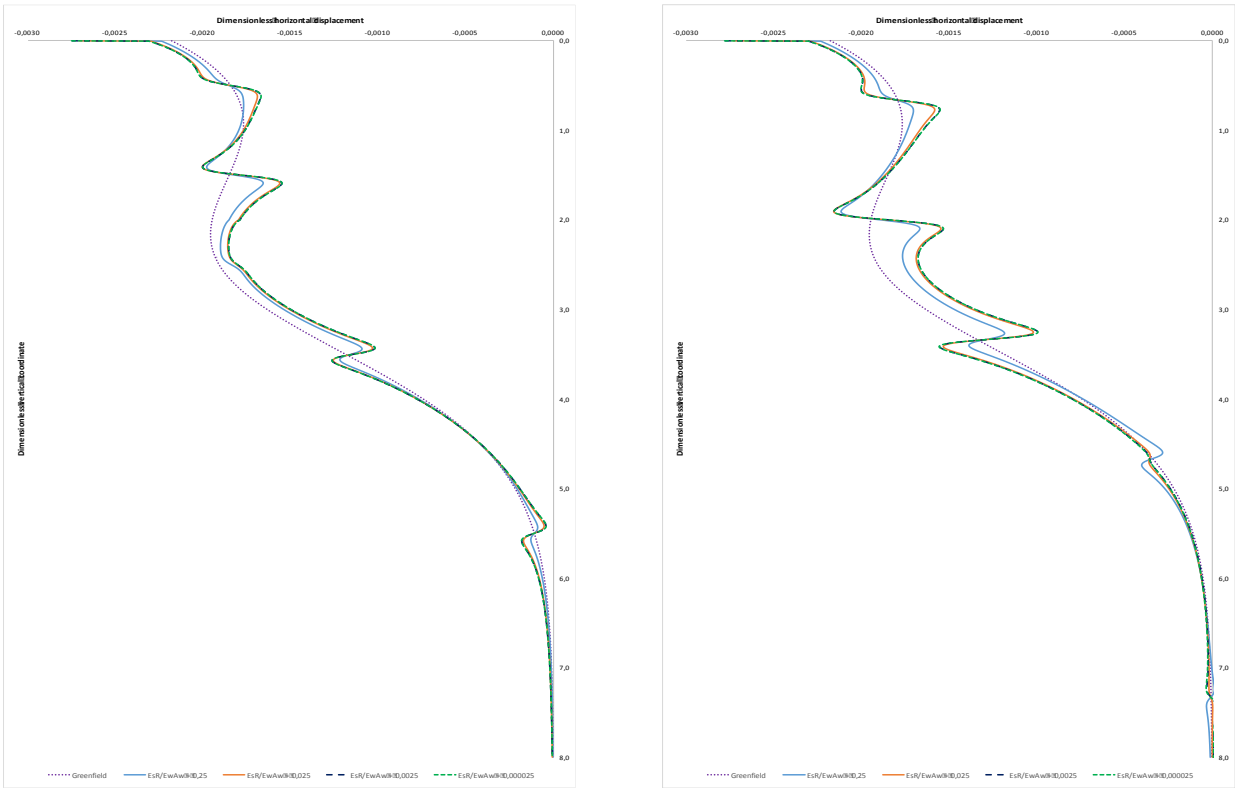

Figure 6. 22.- Effect of the soil-wall relative stiffness for the case of 30 and 40-meter wall length

In Figure 6.23, the efficiency is computed and presented. As can be noticed, as higher as the lateral wall is, more efficiency presents. Also it can be seen that, for values of the dimensionless parameter lower than 0.0025, the effect of the wall modulus in the efficiency is almost imperceptible.

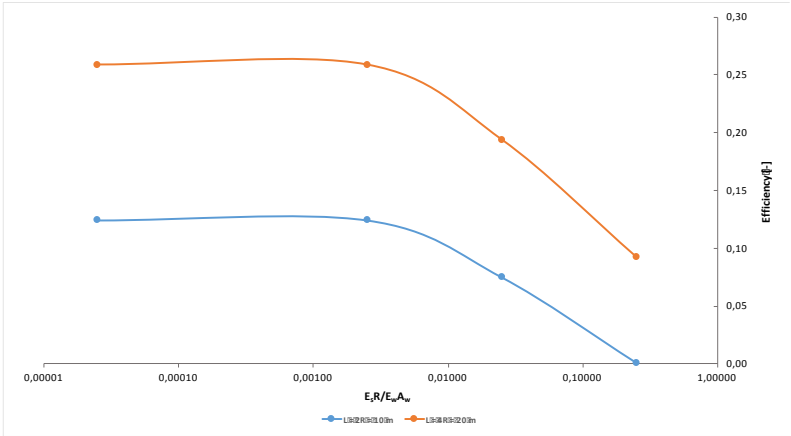

Figure 6. 23.- Efficiency against dimensionless parameter $[\Pi_4]$ for 10 and 20-meter wall length

6.3.2.1. Effect of the tunnel-wall distance

In this section of the document the influence of the tunnel-wall distance is going to be analysed for the case of lateral displacement due to vertical loads.

As explained in previous sections in which the same phenomenon is analysed, the dimensionless ratio that controls the influence of the tunnel-wall distance in the lateral displacement troughs is defined in equation 6.6. The values of the dimensionless ratio adopted in order to compute the analysis are provided in Table 6.8:

PARAMETER	UNIT	VALUE	TUNNEL-WALL DISTANCE [m]
$d/R\ [\Pi_2]$ (1)	Dimensionless [-]	1.25	6.25
$d/R\ [\Pi_2]$ (2)	Dimensionless [-]	1.50	7.50
$d/R\ [\Pi_2]$ (3)	Dimensionless [-]	2.00	10.00
$d/R\ [\Pi_2]$ (4)	Dimensionless [-]	2.50	12.50
$d/R\ [\Pi_2]$ (5)	Dimensionless [-]	3.00	15.00

Table 6. 8.- Different values of the tunnel-wall distance that have been considered for the sensitivity analysis

In Figures 6.24 to 6.25, the effect of the tunnel-distance in the lateral displacement trough is presented. It is important to highlight that as different distance from the tunnel axis have been considered, each of the curves needs to be plotted and compared against its own greenfield curve. For instance, the influence of a 30-meter lateral wall at 6.5 meters from the tunnel axis needs to be compared with the greenfield displacement curve at the same distance from the tunnel axis. That differs from the vertical case because the greenfield settlement curve was the same in all the calculation process.

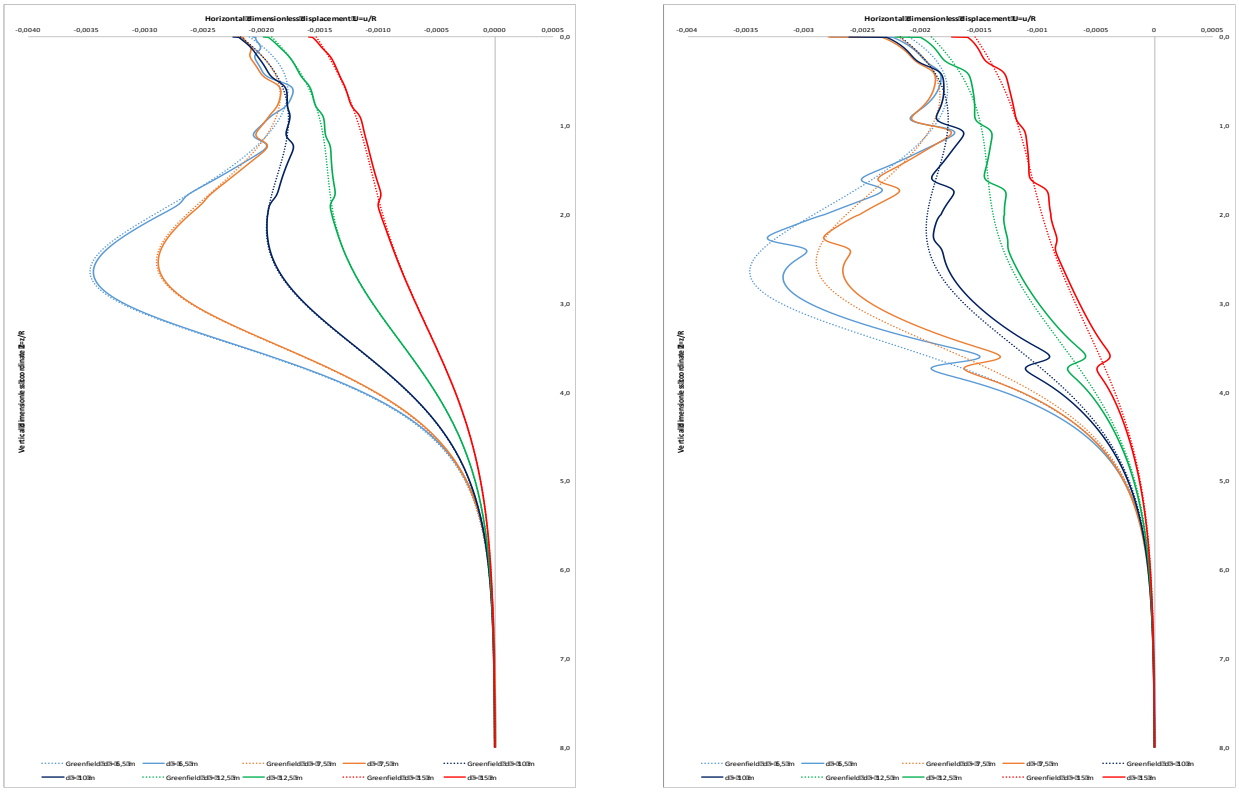

Figure 6. 24.- Effect of the tunnel-wall distance for the case of 10 and 20-meter wall length

In Figure 6.24, the effect of the tunnel-wall distance for a 10 and 20-meter lateral Wall is provided.

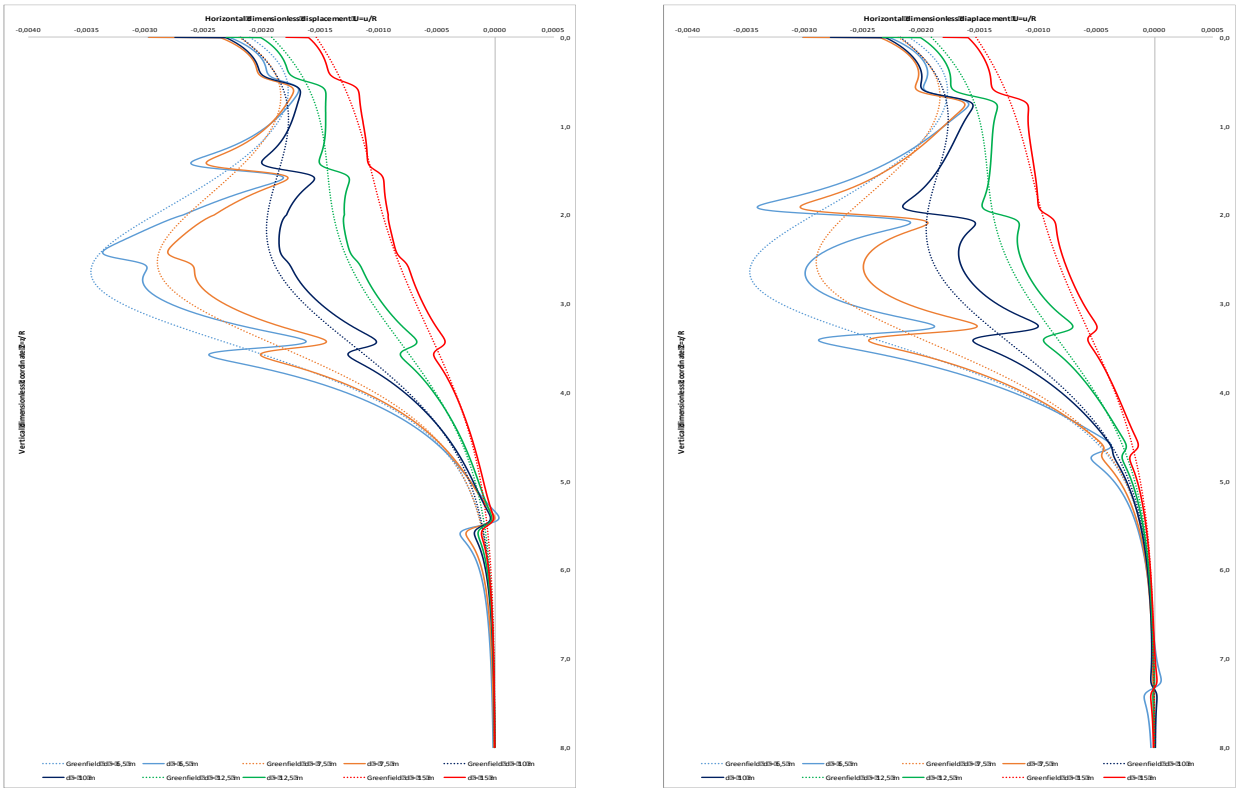

Figure 6. 25.- Effect of the tunnel-wall distance for the case of 30 and 40-meter wall length

In general terms it can be noticed that as near as the wall is to the tunnel axis more effect has on the lateral displacement trough otherwise, the effect is almost imperceptible. It can be noticed also that as far from the tunnel axis the wall is located, the effect of the tunnel excavation is almost insensible which is also consistent with the reality, hence, the wall does not need to provide much resistance.

In Figure 6.26, the efficiency is computed and presented. It is obvious that as higher as the wall is, ore efficiency presents. However, the values of efficiency are lower with respect of the vertical load cases.

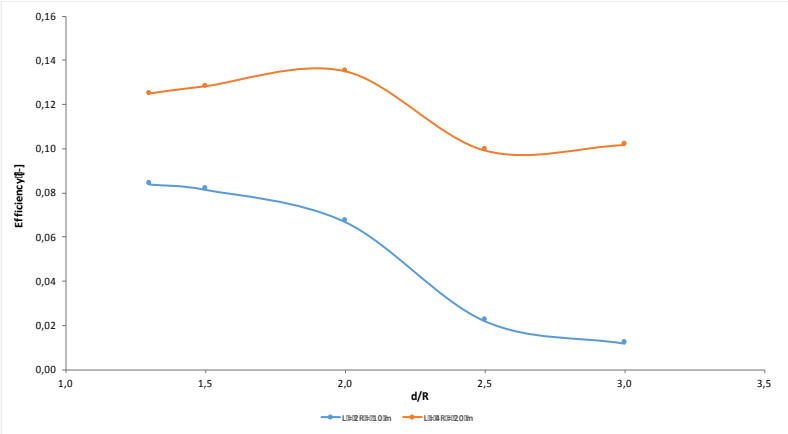

Figure 6. 26.- Efficiency as a function of the of the wall tunnel-distance, d, for the case of 10 and 20-meter wall length

To sum up, it has been revealed that for the case of vertical displacements due to vertical loads the effect of a structural element designed to protect sensitive buildings from tunnelling, presents more efficiency than for the case of lateral displacements. It is important to highlight that the vertical loads are higher than the horizontal loads, hence, the soil deformations concerning lateral deformations are not as high as for the case of vertical deformations.

Another point to remark is the lateral deformations due to vertical loads. Despite the fact that vertical loads are higher than horizontal loads, the effect of those loads in the lateral displacement trough is almost imperceptible presenting lower efficiencies with respect of the case of vertical loads.

6.4. Finite-element simulations

In chapter five, a set of finite-element simulations developed using Plaxis 2D software have been created in order to validate and compare the results obtained from the Melan solutions. When using linear elasticity in finite-element simulations one need to be aware that the boundaries may strongly influence the displacement troughs.

In Figure 6.27 the vertical settlement troughs computed by means of solving the Melan 2D vertical problem are presented as well as the settlements obtained when running the 2D Plaxis model. (Brinkgreve, Kumarswamy, & Swolfs et al., 2019)

The model geometry is made of a rectangle 160 m width and 100 m deep. The tunnel spring line is located at 15-meter depth and a radius of 5 meters. As stated in chapter five, the constitutive models adopted is Linear Elasticity with a soil Young Modulus of 10 MPa and a Poisson coefficient of 0.5.

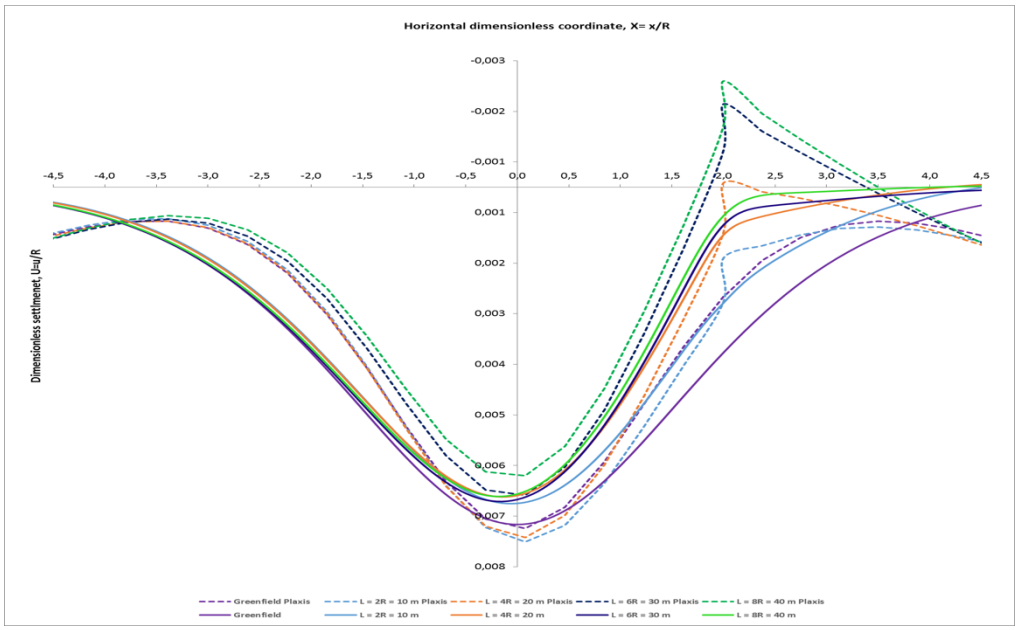

Figure 6. 27.- Effect of wall length in the vertical settlement trough when using finite-element simulations

In the plot presented Figure 6.23, the dashed curves represent the linear elastic results from Plaxis software while the continuous ones represent the Melan analytical solution. Despite the evident differences in the vertical displacement troughs between the dashed and continuous curves, the trends are similar. Having a deeper look at the Plaxis results, in the point where the lateral wall is located, the soil seems to swell which is not consistent with the results obtained from the analytical solutions and also it is not consistent with the field and experience observations. These problem may be solved by means of applying a more sophisticated constitutive model such as a Hardening Soil Model which is a more advanced model for the simulation of soil behaviour. However, this is far away from the goals of this thesis and only Linear elasticity has been considered.

CHAPTER 7

Conclusions

FINAL MASTER THESIS

7.1. Introduction

In the current document the efficiency of lateral walls as a measure to mitigate ground displacements induced by tunnelling works has been presented and developed. Furthermore, as stated in previous chapters, these displacements, in case of being excessive may generate a potential damage to neighbour structures. This thesis has presented a simplified methodology based on linear elasticity to estimate and quantify the settlement troughs in the case of a tunnel excavation with a lateral wall built at a certain distance of its axis.

In the state of the art, an analysis of the most relevant documents presented by important Geotechnicians has been carried out, presenting different case studies with both physical and numerical methods in which the efficiency of lateral walls is computed. Analysing these previous documents, it can be concluded that in general, the main approach to solve this type of problems is by means of empirical methods. This is manly due to the lack of field data and observations that can allow to develop, validate and calibrate different models to analyse the problems. It has to be pointed out that the technique of building a lateral wall has been applied in different real cases and it has performed well mitigating the impact of tunnelling works in surrounding buildings.

In the following points of this chapters, the main conclusions are going to be presented and discussed. As the analysis has been developed for both vertical and horizontal displacements, the conclusions are going to be divided in two main sections. In point 7.2, the comments concerning vertical displacements are going to be presented while in 7.3 the horizontal displacements will be analysed.

7.2. Vertical displacements

Concerning vertical displacements, throughout chapter three, the Melan vertical two-dimensional problem has been solved by means of applying the different elastic equations governing that problem. In the same chapter the influence of the vertical wall length has been provided analysing its effect in the vertical settlement trough.

As stated in the basic theory presented, based on experience and field observations, Peck stablished that the vertical settlement trough in greenfield condition can be related to a Gaussian distribution. It is trivial to know that this type of distribution presents a symmetric shape with respect to its axis. The first thing one notice when a lateral wall is implemented between the tunnel axis and a building is that this symmetry is lost with respect to the tunnel axis. This happens because the wall is constructed and because of the interaction forces between the soil and the wall which lead the settlement trough become non-symmetric.

When the sensibility analysis has been carried out, three factors have been analysed. The first one is the effect of the wall length on the vertical settlement trough. It has been revealed with the diagrams presented that as long as the wall is, more reduced are the settlements far beyond the wall.

This is validated with the efficiency diagram which clearly shows what is stated in the previous paragraph. Another aspect to take into account is the influence of the wall stiffness. It has been proved with the analysis presented in chapter 6, that there is a value of stiffness from which the efficiency of the lateral wall does not increase anymore. The limiting value is for the condition of E_w = 20 GPa. (Ledesma & Alonso, 2010)

The final parameter analysed is the influence of the tunnel-wall distance in the vertical settlement trough. From the results obtained in the analysis it can be concluded that the distance between the tunnel axis and the lateral wall does not have an important influence in the settlement troughs. That has been noticed analysing the efficiency diagrams presented for each wall length. It is important to highlight that the efficiency curves remain almost constant when analysing the effect of the tunnel-wall distance. (Ledesma & Alonso, 2010)

7.3. Horizontal displacements

The analysis of lateral displacements has been divided in two main blocks. In one hand, the analysis of the lateral displacements due to lateral loads and in the other hand, the analysis of lateral displacements due to vertical loads. For both cases, the Melan 2D lateral problem has been solved. As it has been explained in the corresponding chapters of the document for the case of lateral displacements some previous work has been carried out in order to analyse and understand the mathematical procedure to develop the problem.

It was not trivial to develop the methodology necessary to obtain the results presented previously. The Melan 2D lateral problem is divided firstly, in the Kelvin solution which gives the solution for the displacement field in an infinite space and secondly, the addition to the Kelvin solution what is called the Complementary solution. The goal of that is to obtain an elastic solution which gives the displacement fields in an elastic half-space. So, for lateral displacements due to both lateral and vertical loads, the same methodology has been applied but, obviously, with different mathematical approaches due to the different load directions.

The first thing one notice when analysing the displacement troughs is that the greenfield curve is non-symmetric in comparison with the vertical displacement greenfield curve. Concerning the sensitivity analysis of the results presented in chapter 6, the main factors analysed have been the effect of the sol-wall relative stiffness and also the tunnel-wall distance, both parameters governed by a dimensionless ratio presented in the corresponding section.

For both displacements due to lateral loads and vertical loads it has been noticed in general that the influence of the lateral wall does not provide a substantial increase in the efficiency. Furthermore, the ratios of efficiency obtained, for the cases in which it has been computed, are quite far from the results obtained for the case of vertical loads. In addition to that, it is a true fact that the displacements due to vertical loads were almost three times higher than the lateral ones. As it is trivial to understand, the efficiency increases as the wall length increases too.

When analysing the influence of the tunnel-wall distance in the lateral settlement trough for both vertical and lateral loads the results are quite similar. The efficiency computed for both cases are again, quite far from the results obtained from the case of vertical displacements but in general it has been revealed that as far from the tunnel axis the wall is located, less efficiency the wall presents which is consistent with the results.

In general terms it has been proved that lateral walls constructed between the tunnel axis and the neighbouring buildings sensitive to ground displacements perform well firstly, because of some case studies and experience and secondly because of the analysis developed throughout this Final Master Thesis. It has been provided a simplified empirical methodology to estimate and quantify the ground displacements and, due to the sensitivity analysis carried out it, has been proved the efficiency of the measure and the main parameters controlling displacement troughs.

7.4. Finite-Element (FE) analysis

As stated before, the methodology developed throughout this thesis is a simplified procedure to assess and quantify the effect of a lateral wall in the settlement troughs. This does not exclude the need of a full Finite-Element analysis when analysing a real case study. Despite that, dealing with the simplified procedure helps to understand the main parameters governing the tunnel-wall interaction problem and also helps to understand the real case. Plaxis software is going to be applied as is widely used in terms of analysing soil-structure interaction problems.

The empirical method presented, deals with linear elasticity. That means that only the Young Modulus of the soil and wall are implemented as an input parameter as well as the main geometric features and the Poisson coefficient. If one wants to validate the results of the simplified procedure will need to apply linear elasticity also in the finite-element simulations. However, in case of dealing with a real project, more sophisticated constitutive models need to be applied such as Hardening Soil model or Hardening Soil model with small strains.

When carrying out a comparison between the results obtained by means of the Melan problem and Plaxis software one needs to be aware that the Finite-Element results are quite sensitive to the model boundaries leading to unrealistic results in some cases. It is important to notice that for the Linear Elastic constitutive model, the differences in the greenfield curves between the model results and the Loganathan & Poulos (1998) are quite obvious.

It is not provided any calculation of the efficiency of the lateral wall for the case of the Finite-Element simulations. That is due to the fact that the results obtained by means of Plaxis software are not comparable to those obtained by means of the Melan 2D empirical problem. However, it has been a good opportunity to analyse the trend of the results and conclude that despite the fact that due to the model boundaries of the constitutive model is not the most accurate one, the trend of both displacement troughs is similar and the simplified empirical procedure presented in this Final Master Thesis is consistent. (Ledesma & Alonso, 2010)

To sum up, it has been analysed and proved the efficiency of lateral walls as a measure to protect sensitive constructions from tunnelling in order to reduce the settlement troughs far beyond the wall. At the same time, it has been computed the efficiency of the system analysing the main parameters that govern the tunnel-wall interaction problem by means of both empirical and finite-element methods.

CHAPTER 8

References

FINAL MASTER THESIS

8.1. References

[1] Bilotta, E. (2008). Use of diaphragm walls to mitigate ground movements induced by tunnelling.

[2] Bilotta, E., & Russo, G. (2011). Use of a line of piles to prevent damages induced by tunnel excavation .

[3] Bilotta, E., & Stallebrass, S. (2009). Prediction of stresses and strains around model tunnels with adjacent embedded walls in overconsolidated clays.

[4] Bilotta, E., & Taylor, R. (2005). Centrifuge modelling of tunnelling close to a diaphragm wall. International journal of physical modelling in Geotechnics .

[5] Brinkgreve, R., Kumarswamy, S., & Swolfs et al., W. (2019). Plaxis 2D - Tutorial Manual .

[6] Gens, A., Di Mariano, A., & Gesto et al., J. (2006). Ground movement control in the construction of a new metro line in Barcelona . Geotechnical aspects of Unferground Construction in soft ground

[7] Hirokazu, A. (2006). Mitigating measures for underground construction in soft ground . General report for the 3rd edition: Mitigating measures .

[8] Kupussamy, T., Zarco, M., & Ebeling, R. (1992). Solution of Soil-Structure Interaction Problems by Coupled Boundary Element-Finite Element Method. 58 .

[9] Leca, E., & New, B. (2007). Settlements induced by tunnelling in soft ground . Tunnelling and underground Space technology 22 .

[10] Ledesma, A., & Alonso, E. E. (2010). Protecting sensitive constructions from tunnelling: the case of world heritage buildings in barcelona . Géotechnique .

[11] Loganathan, N., & Poulos, H. (1998). Analytical prediction for tunnelling-induced ground movements in clays .

[12] Perez-Garcia, A., & Guardiola-Víllora, A. (2012). Formulario para vigas y pórticos. Prontuario y Herramientas Informáticas para el Cálculo de Estructuras .

[13] Podio-Guidugli, P., & Favata, A. (2014). Elasticity for Geotechnicians .

[14] Telles, J., & Brebbia, C. (1981). Boundary element solution for half-plane problems . International Journal of Solids and Structures .

[15] Verruijt, A. (2014). Surface settlements due to deformation of a tunnel in an elastic half plane . Géotechnique .

[16] Verruijt, A., & Booker, J. (2000). Complex variable analysis of Mindlin's tunnel problem .

Barcelona, September 30th 2019